

UNIVERSITY OF NAPLES “FEDERICO II”
PhD Program
Molecular Pathology and Physiopathology



School of Molecular Medicine

XXVII Cycle

Survival in glioblastoma patients is predicted by miR-340, that regulates key cancer hallmarks by inhibiting NRAS

Supervisor

Prof. Gerolama Condorelli

CANDIDATE

Danilo Fiore

PhD COORDINATOR
Prof. Vittorio Enrico Avvedimento

Academic Year 2013-2014

“Survival in glioblastoma patients is predicted by miR-340, that regulates key cancer hallmarks by inhibiting NRAS”

TABLE OF CONTENTS

	Page
LIST OF ABBREVIATIONS	4
ABSTRACT	7
1. BACKGROUND	8
1.1 Central nervous system tumors	8
1.2 Pathology and risk factors	8
1.3 Pathogenic pathways involved in gliomagenesis	11
1.3.1 RTK/RAS/PI3K pathway	11
1.3.2 p53 and Rb pathways	12
1.3.3 Proangiogenic pathways	13
1.3.4 Glioma stem cell (GSCs)	14
1.3.5 Invasion and cell motility	14
1.4 Therapeutic approaches for glioblastoma	15
1.4.1 Conventional therapy: temozolomide	15
1.4.2 Novel therapeutic approaches	16
1.5 Long term survivors (LTS) glioblastoma patients	19
1.6 N-RAS and glioblastoma	20
1.7 MicroRNAs	22
1.7.1 Evolution and Physiological function	24
1.7.2 miRNAs and cancer	24
1.7.3 miRNAs and glioblastomas	25
2. AIM OF THE STUDY	28
3. MATERIALS AND METHODS	29
3.1 Cells and tissue specimens	29
3.2 TCGA data analysis	29
3.3 Cell transfection	29
3.4 RNA extraction and real-time PCR	30
3.5 miRNAs expression microarray and data analysis	30
3.6 Establishment of miR-340 stable expressing glioblastoma cells	31
3.7 Protein isolation and western blotting	31
3.8 Cell proliferation assay	31
3.9 Cell cycle analysis	32
3.10 Soft-Agar assay	32
3.11 Cell death quantification and apoptosis detection	32
3.12 Rescue experiments	32

3.13 In vivo tumor formation	33
3.14 Luciferase assay	33
3.15 Statistical analysis	33
4. RESULTS	35
4.1 miR-340 expression is correlated with survival of glioblastoma patients	35
4.2 N-RAS is a direct target of miR-340	39
4.3 Effects of miR-340 in glioblastoma cells	42
4.4 N-RAS is the key target molecule for miR-340 effects	46
4.5 miR-340 blocks cell cycle and cell proliferation via inhibition of signaling pathways downstream N-RAS	49
4.6 Overexpression of miR-340 inhibits glioblastoma growth in vivo	51
5. DISCUSSION	53
6. CONCLUSIONS	58
7. REFERENCES	59
8. LIST OF PUBLICATIONS	69

LIST OF ABBREVIATIONS

AGO: Argonaute

ALL: Acute Lymphatic Leukemia

ANG: Angiopoietin

ATCC: American Type Culture Collection

CDK: Cyclin Dependent Kinase

CLL: Chronic

CNS: Central Nervous System

CT: Computed Tomography

EGF: Epidermal Growth Factor

EGFR: Epidermal Growth Factor Receptor

EXP5: Exportin 5

FACS: Fluorescent Activated Cell Sorting

FBS: Fetal Bovine Serum

FDA: Food and Drug Administration

FFPE: Formalin Fixed Paraffin Embedded

FGF: Fibroblast Growth Factor

GBM: Glioblastoma Multiforme

GFAP: Glial Fibrillary Acidic Protein

GFP: Green Fluorescent Protein

GSC: Glioma Stem Cell

HDAC: Histone Deacetylase

HFUS: High Frequency Ultra Sound

HIF-1: Hypoxia Inducible Factor 1

LTS: Long Term Survivors

miR: Micro Rna

MOI: Multiplicity Of Infection

MRI: Magnetic Resonance Imaging

NF1: Neurofibrimin 1

PDGF: Platelet Derived Growth Factor

PDGFR: Platelet Derived Growth Factor Receptor

PI3K: Phosphoinositide 3 Kinase

PTEN: Phosphatase and Tensin Homolog

RB: Retinoblastoma

RISC: RNA Induced Silencing Complex

RTK: Receptor Tyrosine Kinase

SCR: Scrambled

SD: Standard Deviation

SHH: Sonic Hedgehog

STS: Short Term Survivors

TKI: Tyrosine Kinase Inhibitor

TMZ: Temozolomide

TV: Tumor Volume

UTR: Untranslated

VEGF: Vascular Endothelial Growth Factor

VEGFR: Vascular Endothelial Growth Factor Receptor

WHO: World Health Organization

ABSTRACT

Glioblastoma (GBM) is the most common primary brain tumor in adults, with a poor prognosis and a survival rate of only 12 months after diagnosis. Long-term survivors (LTS) are a small subgroup of glioblastoma patients characterized by a survival rate longer than 12-14 months. There is an increasing interest in the identification of molecular signatures to predict patient prognosis in GBM and delineate the best therapeutic approach. In this work, we reported miR-340 as a novel prognostic tumor-suppressor miRNA in glioblastoma. We analyzed miRNAs expression in two different cohorts of glioblastoma patients accounting for >500 patients, demonstrating that miR-340 is strongly down-regulated in glioblastoma, while is over-expressed in LTS patients compared to short term survivors (STS). Further, we demonstrated that miR-340 expression predicts a better prognosis of GBM patients. miR-340 overexpression in glioblastoma cells had a strong tumor-suppressive activity in vitro and in vivo in nude mice. Finally, we identified N-RAS as a direct critical target of miR-340, and demonstrated that, through N-RAS, miR-340 negatively influence multiple aspects of glioblastoma tumorigenesis, regulating AKT and ERKs pathways. Taken together, our data suggest that miR-340 is down-regulated in glioblastoma, where it exerts a strong tumor-suppressive effect by regulating N-RAS. Thus, miR-340 may represent a novel potential marker for the diagnosis, prognosis and treatment of GBM.

1. BACKGROUND

1.1 Central nervous system tumors.

Central nervous system (CNS) tumors or gliomas are a large collection of primary brain tumors that present features similar to glia, astrocytes and oligodendrocytes (and their precursors) which together support the function of neurons in the brain (Tran B and Rosenthal MA 2010). Gliomas are the most frequently occurring types of primary brain tumors in in USA (Porter KR et al. 2010), accounting for 80% of patients and with an annual incidence of 5,26 per 100000 population, or 17000 new cases diagnosed per year (Dolecek TA et al. 2012). Prevalence studies estimate that 138054 patients had a diagnosis of a primary malignant brain tumor in the United States in 2010 (Porter KR et al. 2010). Because these tumors arise in the central nervous system and affect the surrounding brain structure, patients commonly develop symptoms that include headaches, local neurologic alterations or languages disturbance (Tran B and Rosenthal MA 2010). So, brain tumors are among the most feared kinds of cancer, not only for their poor prognosis, but also because of the direct repercussion on quality of life and cognitive functions.

1.2 Pathology and risk factors.

Classification of CNS tumors is essentially based on histology and prognosis. The most recent classification of brain tumors is the World Health Organization (WHO) classification, which was first formalized in 1979 and updated in 2007 (Louis DN et al. 2007). The WHO classification divides gliomas into 4 histological grades, defined by increasing degrees of undifferentiation, anaplasia and aggressiveness (Louis DN et al. 2007). So, in addition to a morphological grouping of brain tumors on the basis of presumed histogenesis, the WHO scheme has been notable for grading individual tumor classes (I, II, III and IV) as a mean of biological behaviors. In this way, higher grade tumors are expected to show a more aggressive clinical course than their lower grade counterparts (Huse JT and Holland EC 2010). The WHO scheme divides the brain tumors into astrocytic, oligodendroglial and mixed categories. Additionally, the presence of histological features such as nuclear atypia, increased proliferation, microvascular proliferation and necrosis typically results in higher grade classification, as either anaplastic glioma or glioblastoma (Figure 1).

Glioblastoma multiforme (GBM) accounts for 82% of cases of malignant gliomas (Dolecek TA et al. 2012). GBMs are heterogeneous intraparenchymal masses that display evidence of necrosis and haemorrhage. Histologically, they are characterized by considerable cellularity and mitotic activity, and vascular proliferation. Glioblastoma consists of several cell types:

the glioma cells, hyper-proliferative endothelial cells, macrophages, and trapped cells of the normal brain structures that are overrun by the invading neoplastic mass. The blood vessels both within and adjacent to the tumor are hypertrophied. Furthermore, the nuclei of tumor cells are extremely variable in size and shape, a characteristic called nuclear pleomorphism. Tumor cells characteristically invade the surrounding normal brain parenchyma, migrating through the white matter tracts to collect around blood vessels and neurons. The extent to which these tumors invade adjacent structures is variable; at its extreme, large portions of the brain are diffusely infiltrated by individual tumor cells with no clear focus of tumor. GBM cells are typically confined to the central nervous system and do not metastasize. Glioblastoma may develop from diffuse low grade or anaplastic astrocytomas (secondary glioblastoma), but more frequently, they manifest de novo, without a less malignant precursor lesion (primary glioblastoma).

Low grade gliomas are divided into two histological variants: astrocytomas and oligodendrogliomas.

Anaplastic astrocytoma arises from low grade astrocytomas, but are diagnosed at first biopsy without a less malignant precursor lesion. This kind of tumor consists of a cell with large amounts of cytoplasm which expresses the astrocyte-specific marker gene GFAP (GLIAL FIBRILLARY ACIDIC PROTEIN). These tumors tend to progress to glioblastoma.

Anaplastic oligodendroglioma is a diffusely infiltrating tumor composed of oligodendroglia-like tumor cells which have small rounded nuclei, a minimal cytoplasm and do not express GFAP, with focal or diffuse histological features of malignancy (Huse JT and Holland EC 2010).

CNS tumors are usually detected by computed tomography (CT) and magnetic resonance imaging (MRI) scans (Tran B and Rosenthal MA 2010).

Malignant gliomas arise in a multistep process involving sequential and cumulative genetic alterations resulting from intrinsic and environmental factors (Gu J et al. 2009). Malignant gliomas may manifest at any age including congenital and childhood cases. Peak incidence is, however, in adults older than 40 years. Males are more frequently affected than females (Ohgaki H and Kleihues P 2005).

Excepted for inherited tumor syndromes (10% of all brain tumors) the etiology is still largely unknown. A number of rare hereditary syndromes are associated with an increased risk of glioma, including Cowden, Turcot, Li-Fraumeni, neurofibromatosis type 1 and type 2, tuberous sclerosis, and familial schwannomatosis (Gu J et al. 2009; Ohgaki H and Kleihues P 2005; Hottinger AF and Khakoo Y 2007). A family history of glioma is rarely observed but, when present, is associated with a 2-fold increase in the risk of developing glioma. Genome-wide association studies have identified a few susceptibility variants such as 20q13.33 (RTEL), 5p15.33 (TERT), 9p21.3 (CDKN2BAS), 7p11.2 (EGFR), 8q24.21 (CCDC26), and 11q23.3 (PHLDB1), but these genes are only weakly associated with glioma, possibly reflecting multiple molecular subsets (Shete S et al. 2009; Rajaraman P et al. 2012). Preventive measures,

such as lifestyle changes, are ineffective in averting gliomas. Early diagnosis and treatment unfortunately do not improve outcomes, precluding the utility of screening for this disease.

The only unequivocal risk factor for glioma development is therapeutic ionizing irradiation. This association was demonstrated in children receiving prophylactic CNS irradiation for acute lymphatic leukemia (ALL) and in individual exposed to atomic bomb and nuclear weapon testing. No association of exposure to radiation used in diagnostic procedures, electromagnetic fields, viral infections or diet and glioma has been proven so far (Ohgaki H and Kleihues P 2005).

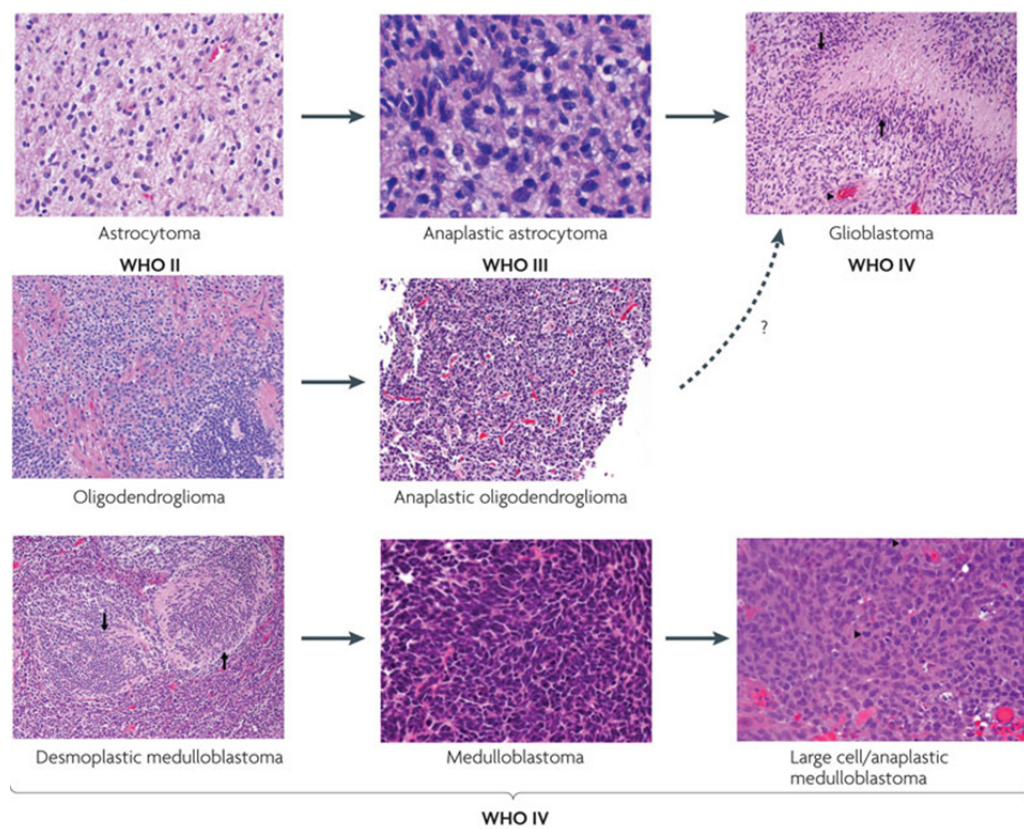


Figure 1. Current World Health Organization classification for diffuse glioma and medulloblastoma. Adapted from Huse and Holland 2010.

1.3 Pathogenic pathways involved in gliomagenesis.

In general, neoplastic disorders are genetic diseases. The genetic alterations are associated with alteration of cell proliferation, apoptosis, senescence, migration, and cell-to-cell communication. Genetic alterations in malignant gliomas are extremely complex and diverse. Clarifying the mechanisms of tumorigenesis, proliferation and treatment resistance in malignant gliomas are critical for the development and application of molecular-targeted therapies. As in other tumors, also in glioblastoma have been identified multiple alterations in the expression levels of genes and/or proteins, including both activation of oncogenes and/or silencing of tumor-suppressor genes. Three signaling pathways are commonly de-regulated in GBM, including alterations in pathways related to receptor tyrosine kinase (RTK)/Ras/PI3K, p53 and Rb signaling (Cancer Genome Atlas Research Network 2008). Alterations in these three pathways play a central role for the development of glioblastoma, but it remains possible that other pathways will be uncovered to be essential in glioblastoma tumorigenesis.

1.3.1 RTK/RAS/PI3K pathway.

Different RTKs are frequently involved in GBM tumorigenesis. EGFR amplification is the most common oncogenic alteration, identified in approximately 40% of GBM patients (Cancer Genome Atlas Research Network 2008). In approximately 50% of tumors with amplified EGFR, a unique EGFR variant is present (EGFRvIII), resulting in ligand-independent constitutive activation of downstream signaling pathways (Huang HS et al. 1997). It has been found also a co-amplification of multiple RTKs (such as PDGFR or MET), and it has been suggested that co-activation of redundant RTKs reduces tumor responsiveness to therapies (Stommel JM et al. 2007; Snuderl M et al. 2011; Szerlip NJ et al. 2012). In glioma these growth factor receptors activate several common signaling pathways, mainly RAS and AKT pathways.

PI3K family initiates activation of Akt and other downstream effectors which affects tumor cell growth, proliferation, and survival (Engelman JA et al. 2006; Engelman JA 2009). The phosphatase and tensin homolog (*PTEN*) tumor suppressor gene, located on chromosome 10q, encodes a protein that dephosphorylates phosphatidylinositol (3,4,5)-trisphosphate, which counteracts PI3K activity (Engelman JA 2009). *PTEN* mutations and homozygous deletions are found in 36% of glioblastomas, and result in an increased tumorigenesis (Cancer Genome Atlas Research Network 2008) (Figure 2a).

The Ras/MAPK pathway has been implicated in a wide variety of cellular processes, such as growth, differentiation, and apoptosis (Downward J 2003). Different reports also identified inactivating mutations or deletions of the neurofibromin (*NFI*) gene (Cancer Genome Atlas Research Network 2008), a negative regulator of Ras, underlining the critical role of Ras/MAPK signaling pathway in glioblastoma (Figure 2a).

1.3.2 p53 and Rb pathways.

Cell-cycle pathways alterations are also frequently identified in malignant gliomas, including disruption of the p53 and Rb pathways (Cancer Genome Atlas Research Network 2008). The *TP53* tumor-suppressor gene, located on the short arm of chromosome 17, encodes a protein that determines cell-cycle arrest in the G1 and/or G2 phase of the cell cycle, and also promotes apoptosis upon DNA damage (Vousden KH and Lane DP 2007). Loss of its function due to *TP53* mutation or deletion confers a growth advantage, resulting in clonal expansion of glioma cells (Sidransky D et al. 1993). Impairment of DNA repair as a result of *TP53* mutations induces genetic instability (Bogler O et al. 1995). Moreover, inactivation of the p53 protein may be also determined by *MDM2* amplification, which is found in high-grade gliomas in the absence *TP53* mutation (Reifenberger G et al. 1993). Other frequent genetic alterations include loss of p14ARF through homozygous deletion of the cyclin-dependent kinase (CDK) inhibitor 2A (*CDKN2A*) gene, resulting in *MDM2* overexpression and functional p53 loss (Ohgaki H and Kleihues P 2009) (Figure 2b).

The Rb pathway has been found to be defective in a significant number of high grade gliomas. Normally, Rb protein keeps the cell cycle in check until phosphorylated by cyclin D, CDK4 and CDK6. Rb mutations and *CDK4* amplification lead to dysregulation of the Rb signaling pathway (Cancer Genome Atlas Research Network 2008). Moreover, amplification of Rb negative regulators cyclin-dependent kinase 4 (CDK4) and, less frequently, CDK6 can be found in GBM, leading to dysregulation of Rb signaling. p14ARF and p16INK4a are translated from the same gene, *CDKN2A*, underscoring the cooperative function of these two pathways (Stott FJ et al. 1995) (Figure 2c).

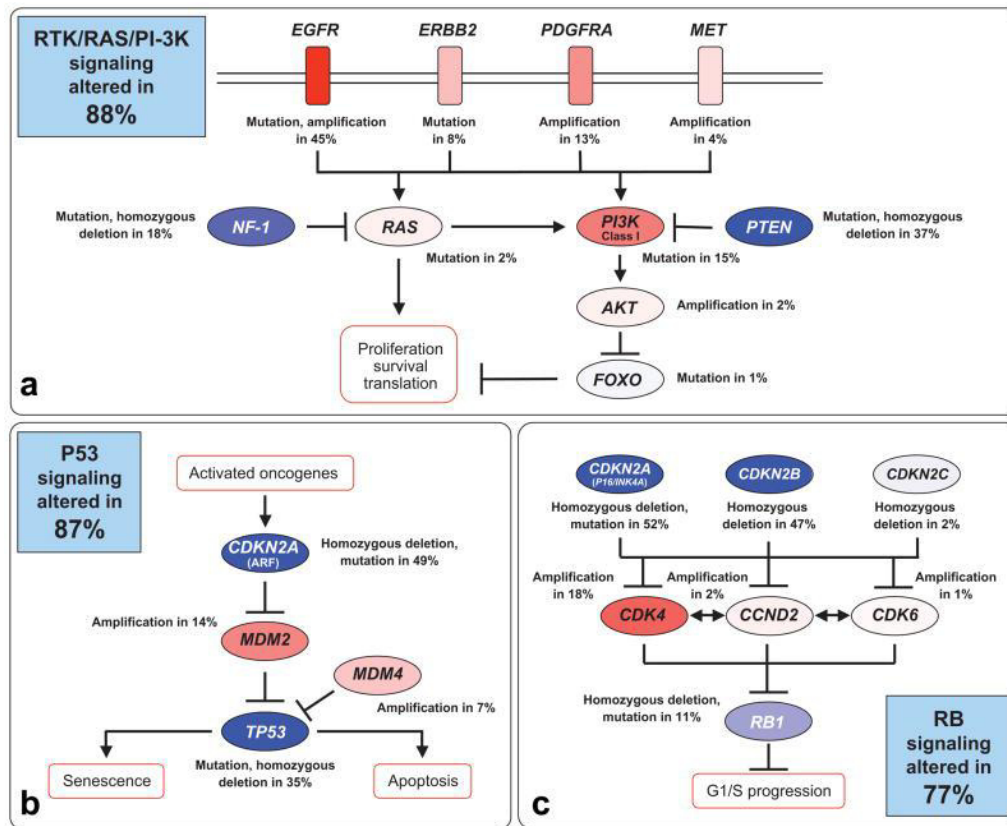


Figure 2. Schematic representation of genetic alterations occurring in glioblastoma in RAS/PI3K, p53 and RB signaling pathway. Adapted from Tanaka et al. 2013.

1.3.3 Proangiogenic pathways.

Microvascular proliferation is one of the diagnostic hallmarks in glioblastoma (Norden AD 2009). Activation of several proangiogenic pathways contributes to this tumorigenic feature. VEGF and its receptor (VEGFR) have a central role in this process. VEGF binding to VEGFR on endothelial cells and tumor cells results in dimerization of VEGFR, which activates an intracellular signaling cascade through stimulation of the PI3K/Ras/MAPK pathway. All this process determines an enhanced endothelial cell proliferation, migration, and survival (Gomez-Manzano C et al 2003; Yoshino Y et al. 2006; Kerbel RS 2009). Moreover, angiopoietin-2 destabilizes the tumor vessels and promotes angiogenesis upon binding to its receptor Tie-2 located on endothelial cells, whereas angiopoietin-1 exerts opposing effects by stabilizing the tumor vasculature (Kerbel RS 2009). Other proangiogenic factors include bFGF, HIF-1 α and HGF (Gomez-Manzano C et al 2003; Yoshino Y et al. 2006; Kerbel RS 2009; Jain RK et al. 2007). The Notch signaling pathway is another

important contributor to tumor angiogenesis (Kerbel RS 2009; Jain RK et al. 2007). Under physiological conditions, the effects of proangiogenic factors are balanced by endogenous antiangiogenic factors such as angiostatin, endostatin, and thrombospondins (Jain RK 2005). All these mechanisms are altered in tumor, including in malignant gliomas.

1.3.4 Glioma stem cells (GSCs).

Glioma stem-like cells (GSCs) are characterized by their ability of self-renewal, multilineage differentiation and tumorigenicity. Identification of GSCs has increased our understanding of signaling pathways involved in the development of treatment resistance in malignant gliomas (Dietrich J et al. 2008; Dietrich J et al. 2010). For instance, Sonic Hedgehog (SHH) and Notch are fundamental regulators of GSCs. Notch signaling contributes to maintenance and proliferation of GSCs. Binding of SHH to the transmembrane receptor protein Patched Homolog 1, determines the releasing of the membrane protein Smoothed homolog, resulting in activation of the Gli proteins (Dietrich J et al. 2010). Gli proteins are zinc-finger transcription factors that, upon translocation to the nucleus, promote the expression of target genes, such as *MYC* and *CCND1* (Dietrich J et al. 2010). Different reports suggest that activated Notch signaling within the vascular niche propagates GSCs and facilitates their self-renewal (Hovinga KE et al. 2010; Shen Q et al. 2004). Other signaling pathways critical for GSCs are Wnt/ β -catenin, Polycomb complex protein BMI-1, and the RTK-mediated pathways, including VEGF, EGF, bFGF and PDGF (Dietrich J et al. 2010; Hovinga KE et al. 2010; Shen Q et al. 2004; Vescovi AL et al. 2006).

1.3.5 Invasion and cell motility.

The vast majority of glial tumors are invasive and, typically, the degree of invasiveness does not necessarily correlate with the grade of malignancy. The invasion of high-grade gliomas often shows extensive infiltration of normal brain. After surgical removal of a malignant glioma, in more than 95% of the cases a recurrent tumor will manifest, frequently immediately adjacent to the resection cavity. However, distant lesions far away from the site of the initial tumor may also be found (Giese A et al. 2003). Invasion is a complex multistep process (Dear TN and Kefford RF 1990). The initial step requires receptor-mediated adhesion of tumor cells to matrix proteins, followed by the degradation of matrix by tumor-secreted proteases and accompanied by biochemical processes supportive of active cell movement (Gressens P 2000). The proteolytic activity of matrix-metalloproteinases has been correlated with invasiveness in tumors of various tissue types and may be an important mediator of glioma invasion. Protease degradation of extracellular matrix creates an intercellular space into which invading cells can migrate (Mariani L et al. 2001).

1.4 Therapeutic approaches for glioblastoma.

Primary brain tumors are widely regarded as being particularly resistant to the most commonly used antineoplastic strategies. Although surgery plays a central role in removing some brain tumors, often the tumor cannot be effectively removed. Both radiation and chemotherapy are often not well effective because many glial-derived tumors seem to be particularly resistant to apoptosis following DNA damage, and are very difficult to reach by the drugs because they should be able to pass the hematoencephalic barrier. However, the strategies used to fight primary brain tumors are based on the use of alkylating agent. Recently, the increased understanding of signaling pathways involved in the initiation of malignant gliomas has stimulated the development of targeted therapies, such as anti-EGFR molecules, antiangiogenic therapy and novel treatment strategies, such as targeting glioma stem cells and the use of immunotherapies.

1.4.1 Conventional therapy: temozolomide.

A new alkylating agent, Temozolomide (TMZ), has been recently introduced for the treatment of primary or recurrent high grade gliomas (Plowman J et al.1994; Stupp R et al. 2005). TMZ has several advantages over other existing alkylating agents because of its features: TMZ is a small lipophilic molecule that can be administered orally and crosses the blood brain barrier. Moreover, temozolomide is less toxic to the hematopoietic progenitor cells than conventional chemotherapeutic agent, because it doesn't result in chemical cross-linking of the DNA strands. For all this characteristics, temozolomide is a promising agent for the treatment of malignant gliomas (Agarwala SS and Kirkwood JM 2000).

There are different evidence which demonstrate how temozolomide is able to improve survival and increase the likelihood of long-term survivors when given currently with radiotherapy and then following surgery, instead of radiotherapy alone following by surgical resection (Stupp R et al. 2005).

O6-methylguanine DNA methyltransferase (MGMT) is a key enzyme in the DNA repair network that remove mutagenic, cytotoxic adducts from O6-guanine in DNA, the preferred point of attack of alkylating agents as temozolomide. This transfer irreversibly inactivates MGMT. Accordingly, MGMT knockout mice are hypersensitive against alkylating drugs, including TMZ, and depletion of the enzyme by the substrate analog O8-benzylguanine increased the sensitivity of glioma cells against alkylating drugs (Bobola MS et al 2004; Liu L and Gerson SL 2006; Friedman HS et al.2002). A direct relationship between MGMT activity and resistance to alkylating agents has also been proved in cell lines and xenografts derived from a variety of human tumors, including gliomas (Esteller et al. 2001). Therefore, adjuvant chemotherapy based on temozolomide is limited by the action of this enzyme, contributing to the very poor survival of glioblastoma patients.

The loss of MGMT expression is commonly attributable to deletion, mutation, or rearrangement of MGMT gene or messenger MGMT instability. MGMT activity is frequently lost in the presence of CpG island hypermethylation in the promoter region of certain types of human primary neoplasm, including gliomas. Therefore, the methylation status of the MGMT promoter was considered to be indicative of a good outcome in patients with malignant gliomas treated with an alkylating agent. The most complete data were provided by Hegi et al., who investigated the MGMT methylation status in a large cohort of glioblastoma by comparing patients receiving either radiotherapy alone or radiotherapy combined with concomitant and adjuvant TMZ (Hegi ME et al. 2005). Patients with methylated MGMT tumors benefited the most from the addition of TMZ, while those with unmethylated MGMT tumors showed only a non-significant improvement in survival with TMZ.

1.4.2 Novel therapeutic approaches.

Recently, a variety of cancer-specific molecular alterations have been identified and explored as potential targets for glioblastoma treatment.

a) EGFR-targeted therapies: The EGFR tyrosine kinase inhibitors (TKIs) erlotinib and gefitinib were the first generation of targeted agents to be investigated in newly diagnosed and recurrent malignant gliomas, either as monotherapy, or in combination with other cytotoxic drugs. These agents were not associated with any significant treatment benefit (Brown PD et al. 2008; van den Bent MJ et al. 2009; Lassman AB et al. 2005), and limited activity was also evaluated with cetuximab, a monoclonal antibody directed against EGFR (et al. 2009). With the development of next-generation TKIs that determine irreversible EGFR inhibition and are currently in clinical testing, such as afatinib, dacomitinib, and nimotuzumab (a humanized monoclonal antibody against EGFR), there is hope that future therapies designed to target EGFR signaling will be more beneficial.

b) Inhibitors of other signaling pathways: mTOR antagonists such as temsirolimus and everolimus have long been used to treat various solid cancers, and also have been tested in a phase II clinical trial (Galanis E et al. 2005; Kreisl TN et al. 2009). However, these agents were only associated with minimal activity and no overall survival benefit in gliomas.

Inhibition of PDGFR signaling, another important RTK pathway in glioma development, was considered to be a promising strategy. However, clinical trials with imatinib, which in addition to Bcr-Abl and c-Kit also inhibits PDGFR, displayed only a minimal activity (Wen PY et al. 2006; Reardon DA et al. 2009; Dresemann G et al. 2010).

Because of the minimal activity of existing RTK signaling inhibitors in glioblastoma, novel agents designed to interfere with downstream molecules have increasingly gained attention. For instance, PD-0332991, an inhibitor of CDK4 and CDK6, is currently being tested in a phase II study of recurrent glioblastoma with known Rb-pathway alterations (Michaud K et al. 2010).

Another treatment approach involves inhibition of histone deacetylases (HDAC), regulators of chromatin structure and gene expression.

c) Targeting glioma stem cells: a growing body of evidence implicates GSCs in the mechanism of resistance to cytotoxic therapies, such as radiotherapy and chemotherapy, and indicates that GSCs are critical in the insurgence of tumor recurrence (Liu G et al. 2006). Thus, GSCs and GSC-associated signaling pathways have been proposed as new attractive treatment strategy. For instance, RO4929097, an inhibitor of γ -secretase that has a critical role in Notch signaling, is currently being evaluated in phase II clinical trials in patients with recurrent glioblastoma, and in a phase I clinical trial in combination with standard chemo-radiation in newly diagnosed glioblastoma. Vismodegib, a small molecule designed to target sonic hedgehog signaling, received FDA approval in 2012 for the treatment of metastatic basal-cell carcinoma (Sekulic A et al. 2012). A phase II surgical trial is currently recruiting patients with recurrent glioblastoma.

d) Antiangiogenic therapies: One of the most important features of malignant gliomas is extensive neovascularisation, which is thought to provide oxygen and nutrients to rapidly growing tumor cells in hypoxic tumor environments. This process is known as angiogenesis. Angiogenesis is regulated by several proteins that promote or prevent this process. During tumor progression, growth is sustained by nutrients and oxygen through passive diffusion. Once new blood vessels form, the tumor start to grow and spread faster. In gliomas, angiogenesis is typically associated with an increase in vascular endothelial growth factor (VEGF), a protein that stimulates new blood vessel formation (Hanahan D and Folkman J 1996). The majority of the anti-angiogenic drugs that have been evaluated in clinical trials to date interfere with the VEGF pathway by directly blocking ligand or VEGF-receptor. However, there is increasing interest in targeting proangiogenic molecules that function by alternative mechanisms. For example, the neuropilins are non-tyrosine kinase receptors that are activated by VEGF binding and potentiate VEGFR signaling. Neuropilin-1 also facilitates HGF/SF signaling (Hu B et al. 2007). The angiopoietins (Ang-1 and Ang-2) are involved in the stability and maintenance of the tumor vasculature. Binding of Ang-2 to its cognate receptor, Tie-2, serves to destabilize vessels, which is a requirement for angiogenesis to proceed. Ang-2 inhibitors are therefore of interest as therapeutic agents (Oliner J et al. 2004). After bevacizumab was approved by the FDA for colon cancer, several neuro-oncology centers began to use it to treat patients with recurrent malignant glioma, often in combination with irinotecan. Different reports demonstrated that bevacizumab therapy leads to rapid reductions in peritumoral edema, often permitting a decrease in dose or even cessation of corticosteroid use. These studies also indicated that bevacizumab treatment is well tolerated in most cases. The risk of intracranial haemorrhage is low. Common toxicities related to bevacizumab therapy in the malignant glioma population include hypertension, proteinuria, fatigue, thromboembolic events, and wound-healing complications (Pope WB et al. 2006; Poulsen HS et al.

2009). In addition to VEGF inhibitors, small molecule inhibitors of VEGFR have been tested in recurrent malignant gliomas. Cediranib (AZD2171) inhibits all known subtypes of VEGFR and was evaluated in a phase 2 trial of patients with recurrent GBM. Cediranib therapy reduced blood vessel size and permeability. In addition to VEGF or VEGFR inhibition, a variety of other approaches may have antiangiogenic activity. Because of its role in pericyte recruitment, inhibition of PDGFR may prove useful. Several trials of PDGFR and dually targeted VEGFR/PDGFR inhibitors are ongoing. Although antiangiogenic therapies prolong progression-free survival, further progression of disease is inevitable. Combining antiangiogenic therapy with anti-invasion therapy may therefore delay disease progression.

1.5 Long term survivors (LTS) glioblastoma patients.

Glioblastoma multiforme is the most common and most malignant primary tumor of the brain and is associated with one of the worst 5-year survival rates among all human cancers (Louis DN et al. 2004). Despite multimodal aggressive treatment, comprising surgical resection, local radiotherapy and systemic chemotherapy, the median survival time after diagnosis is still in the range of just 12 months, with population-based studies indicating even shorter median survival (Krex D et al. 2007; Stupp R et al. 2009). Nevertheless, a small fraction of glioblastoma patients survives for more than 36 months. These patients are referred to as long-term survivors (Krex D et al. 2007). Despite the progress in the understanding of the genetic alterations in glioblastomas, clinically useful molecular markers that help to predict response to therapy and prognosis are still rare. To date, only IDH1/2 mutation status and the methylation status of the O-6-methylguanine methyltransferase (MGMT) gene have become molecular markers of clinical significance (Reifenberger G et al. 2014). MGMT encodes a DNA repair protein that causes resistance to DNA alkylating agents, such as nitrosoureas and temozolomide. Transcriptional silencing of the MGMT gene by promoter hypermethylation is seen in 50% of glioblastomas and has been linked to prolonged progression-free and overall survival in glioblastoma patients treated with alkylating agents (Hegi ME et al. 2005; Esteller M et al. 2000). Combined deletions of the chromosomal arms 1p and 19q have been shown to be associated with a favorable prognosis in oligodendroglial tumors. In glioblastoma, however, this aberration is rare and its prognostic significance is less clear (Krex D et al. 2007). The investigation of glioblastoma long-term survivors could help to identify yet unknown clinical, environmental and/or molecular factors that are associated with favorable prognosis.

1.6 N-RAS and glioblastoma.

The three cellular Ras genes encode four highly homologous 21 kD proteins: HRAS, NRAS, KRAS4A and KRAS4B. KRAS4A and KRAS4B result from alternative splicing at the C terminus. The N-terminal portion (residues 1–165) of HRAS, KRAS and NRAS comprises a highly conserved G domain that has a common structure. Ras proteins diverge essentially at the C-terminal end, which is known as the hypervariable region. This region contains residues that specify post-translational protein modifications that are essential for targeting Ras proteins to the cytosolic leaflet of cellular membranes. All Ras proteins are farnesylated at a terminal CAAX motif, in which C is cysteine, A is usually an aliphatic amino acid and X is any amino acid. NRAS, HRAS and KRAS4A are additionally modified by one or two palmitic acids upstream of the CAAX motif. The addition of the hydrophobic farnesyl moiety is complemented by the hydrophobic palmitates (the so-called ‘second signal’) to firmly anchor these Ras proteins in the membrane. By contrast, KRAS4B, the predominant splice variant referred to from now on as KRAS, contains an alternative second signal that is composed of a poly-basic stretch of lysine residues. In this case, membrane anchoring is mediated by the electropositive lysines that form ionic bonds to the predominantly electronegative lipid head groups of the inner leaflet of the plasma membrane (Schubert S et al. 2007) (Figure 3).

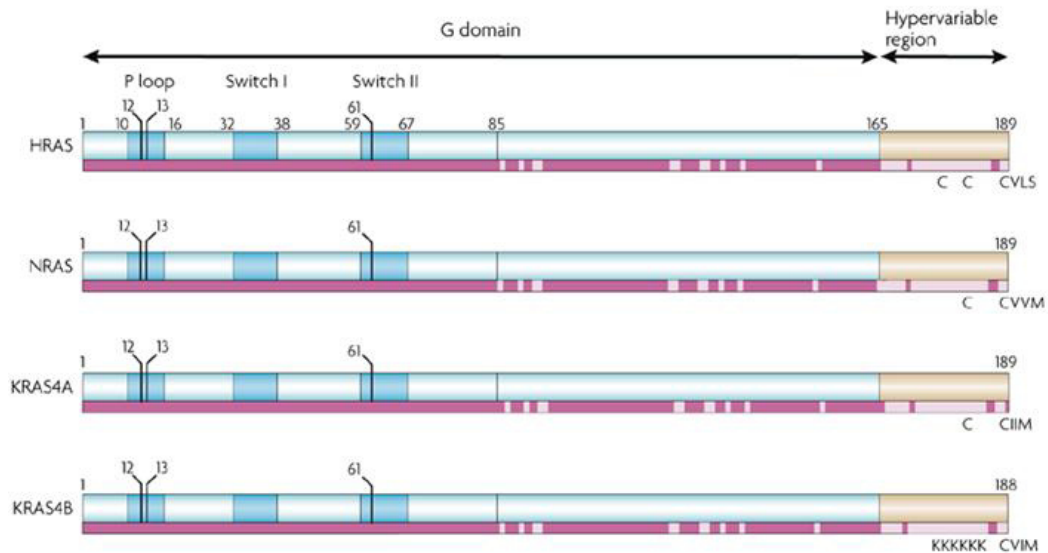


Figure 3. The four isoforms of Ras. Adapted from Scubbert et al. 2007.

N-RAS is a member of Ras oncogene family (comprising K-Ras, H-Ras and N-Ras), that encodes small GTPases involved in cellular signal transduction. Ras is activated by a complex signal cascade and in turn triggers downstream signaling pathways, including the mitogen-activate protein kinases (MAPKs) pathway and the phosphatidylinositol 3-kinase (PI3K)/AKT pathway to modulate cell growth and survival (Scubbert and al. 2007) (Figure 4).

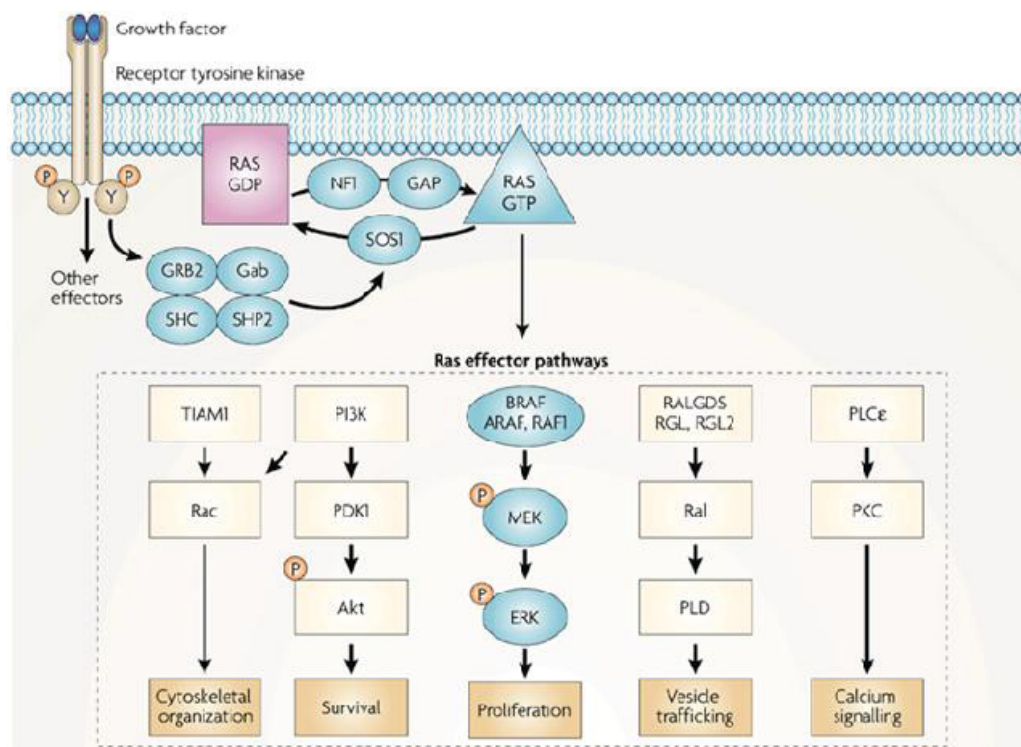


Figure 4. The Ras signaling pathway. Adapted from Scubbert et al. 2007.

Various studies have demonstrated a recurrent aberrant N-RAS activation in glioblastoma. Mutation in N-RAS gene contributes to the aberrant activation of RAS signaling only in approximately 5% of glioblastomas. In most glioblastomas, however, RAS activation must be due to other alterations, such as amplification and/or overexpression of growth factor receptor genes, or aberrations in yet other RAS pathway genes (Knobbe CB et al 2004). Moreover, recently several miRNAs –miR-181d, let-7, miR143- have been reported to suppress RAS expression, thus acting as tumor-suppressors, suggesting that miRNAs targeting RAS may have an important role in carcinogenesis (Johnson SM et al. 2005; Lee ST et al. 2011; Wang L et al. 2014).

1.7 MicroRNAs.

In the last decade, many non-coding RNAs were found to regulate a wide variety of biological processes. Among these, microRNAs (miRNAs) are the best characterized. miRNAs are a class of endogenous non-coding RNA of 19-24 nucleotides in length that play a central role in the negative regulation of gene expression, blocking translation or directly cleaving the targeted mRNA. The biogenesis of miRNAs is a complex and coordinate process in which are involved different enzymes and proteins (Bartel DP 2004).

miRNAs genes encoded in the genome are transcribed into long primary miRNAs (pri-miRNAs) by polymerase II or in little rare case, by polymerase III. Typically, pri-miRNAs display a 33bp stem and a terminal loop structure with flanking segments. Primary miRNA processing begins in the nucleus where an RNaseIII enzyme, Drosha, removes the flanking segments and 11 bp of the stem region, inducing the conversion of pri-miR into precursor miRNAs (pre-miRs). Pre-miRs are 60-70 nt long hairpin RNAs with 2-nt overhangs at the 3' end. Pre-miRNAs are transported into the cytoplasm for further processing to become mature miRNAs. The transport occurs through nuclear pore complexes and is mediated by the RanGTP-dependent nuclear transport receptor exportin-5 (EXP5). EXP5 exports the pre-miRNA out of the nucleus, where hydrolysis of the GTP results in the release of pre-miRNA. In the cytoplasm the pre-miRNA is subsequently processed by Dicer, an endonuclease cytoplasmic RNase III enzyme, to create a mature miRNA. Dicer is a highly specific enzyme that cleaves pre-miRNAs into 21-25 nt long miRNA duplex, of which each strand shows 5' monophosphate, 3' hydroxyl group and 3' 2-nt overhang. Of a miRNA duplex, only one strand, designed the miRNA strand, is selected as the guide of the effector RNA-induced silencing complex (RISC). The core component of RISC is a member of Argonaute (Ago) subfamily proteins. During RISC loading, the miRNA duplexes are incorporated into Ago proteins. RISC loading is not a simple binding of the duplexes and Ago proteins, but also an ATP-dependent active process. After RISC loading, the duplex is unwound and in the complex is maintained only the miRNA strand (Bartel DP 2004; Lee Y et al.2002; Gregory RI and Shiekhattar R 2005).

miRNAs target sites in the 3' untranslated region (UTR), because the movement of ribosome (the translation), counteracts RISC binding. Typically, a target mRNA contains multiple binding sites of the same miRNA and/or several different miRNAs. Not all nucleotides of a miRNA contribute equally to RISC target recognition. The recognition of the target is largely determined by base pairing of nucleotides in the seed region and is enhanced by additional base-pairing in the middle of the 3'UTR region. The binding of RISC to 3' UTR of mRNA, through the action of Ago protein, is capable of RNA cleavage, but this reaction requires extensive base-pairing between the miRNA strand and mRNA target. This is the same mechanisms used by siRNAs. If the complementarity between the miRNA strand and the mRNA is limited, RISC is

unable to cleave the target. In such case, Ago protein can recruit other factors required for translation repression and subsequently mRNA deadenylation/degradation (Lewis BP et al. 2003). To date, the exact mechanisms used by RISC to repress translation are subjects of debate. Between the mechanisms proposed at least six seems to be possible: RISC could induce deadenylation of mRNA which cause decrease the efficiency of translation by blocking mRNA circularization, RISC could block the cap at 5' or the recruitment of ribosomal subunit 60S; RISC could block the initial step of elongation or could induce proteolysis of nascent peptides; RISC could recruits mRNA to processing bodies, in which mRNA is degraded or temporary stored in an inactive form. These models do not necessarily exclude each other (Kwak PB et al. 2010).

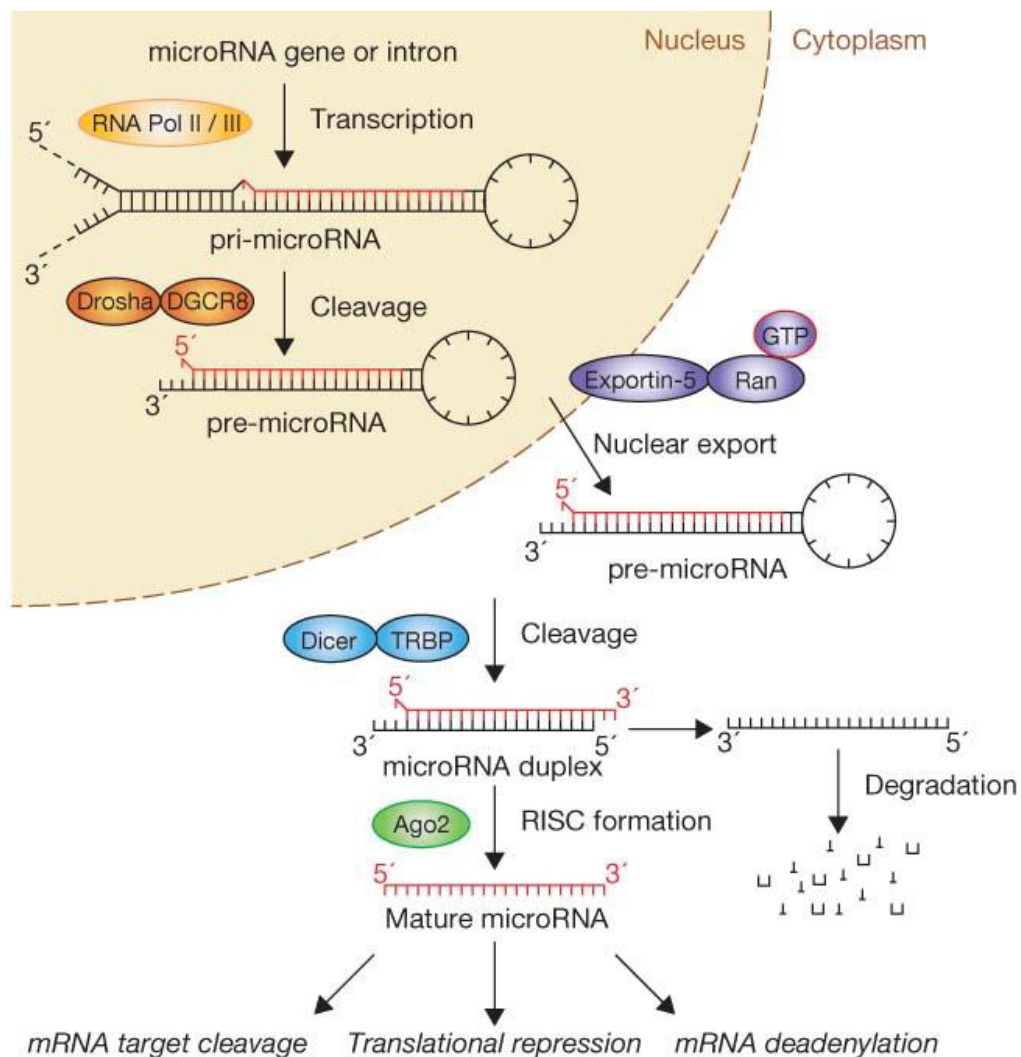


Figure 5. miRNAs biogenesis. Adapted from Winter et al. 2009.

1.7.1 Evolution and Physiological function.

miRNAs play key role in the regulation of many processes in mammals. For example, miRNAs have an evolutionarily conserved role in the development and in the physiological functions in animals. Knockout gene strategies have been used in different mammals to study the role of miRNAs in developmental processes. A dicer knockout was made in zebrafish and this revealed a role of the family of miR-140, which plays a fundamental role in neurogenesis. miRNAs can also control late-stage mouse development by miR-196 which acts upstream Hox B8 and Sonic hedgehog in limb development. miR-1 and miR-133 are important for muscle generation and differentiation of cardiomyocytes and myoblast (Chen JF et al. 2003). miR-181 is preferentially expressed in B-lymphocytes and regulates mouse hematopoietic lineage differentiation (Chen CZ et al. 2004). miR-181 is also able to regulate homeobox proteins involved in myoblast differentiation. miR-122a is highly expressed in adult livers, and its expression is upregulated during mammalian liver development. miR-143 is strongly expressed in adipose fat tissue and is upregulated during the differentiation of human pre-adipocytes into adipocytes (Esau C et al. 2004). miRNAs are also involved in skin morphogenesis; for example, miR-134 acts in dendritic spine development (Schratt GM et al. 2006).

Some miRNAs regulate multiple physiological processes, for example miR-375 is expressed in pancreatic islets and inhibits glucose-induced insulin secretion, or miR-16 which controls the ARE-containing mRNAs. Recently, it has been found that some endogenous miRNAs participate in adenoviral defense mechanisms; for example miR-32 protects human cells from retrovirus type 1.

Others studies have established a role of miRNAs in cellular processes including apoptosis, proliferation, stress resistance, metabolism, and cancer.

1.7.2 miRNAs and cancer.

Cancer is characterized by abnormally proliferative cells that undergo rapid and uncoordinated cell growth. Malignant cancers are able to invade adjacent tissues and/or metastasize to more distant, and sometimes specific, tissues. Genes involved in cancer are generally classified into oncogenes or tumor suppressor genes.

The first evidence for miRNAs involvement in human cancer came from a study by Calin et al., examining a recurring deletion at chromosome 13q14 in the search for a tumor suppressor gene involved in chronic lymphocytic leukemia (CLL). They found that the region of deletion encodes two miRNAs, miR-15a and miR-16-1. Subsequent investigations have confirmed the involvement of these two miRNAs in the pathogenesis of CLL (Calin GA et al. 2002). To date, a lot of miRs have been characterized for their function in human cancers. Let-7 family contains miRNAs that have been shown to regulate the RAS family of oncogenes (Johnson SM et al. 2005). Constinean et al reported, for the first time, that a miRNA by itself could induce a neoplastic

disease. In fact, by using a transgenic mouse model, they demonstrated that overexpression of miR-155 in B cells was able to induce a pre-B leukemia (Costinean S et al. 2006). Petrocca et al have demonstrated that the miR-106b-25 cluster plays a key role in gastric cancer, regulating both cell cycle and apoptosis (Petrocca F et al. 2008). miRNAs have an important role also in tumor metastasis. miR10-b was found to be highly expressed in metastatic breast cancer cells, and Tavazoi et al found that miR-26 and miR-335, whose expression is lost in human breast cancer cells, modulate metastatic potential (Tavazoie SF et al. 2008). Deregulation of miRNA expression levels emerges as the main mechanism that triggers their loss or gain of function in cancer cells. The activation of oncogenic transcription factors such as MYC, represents an important mechanism for altering miRNA expression. Genomic aberrations such amplification, chromosomal deletions, point mutations or aberrant promoter methylation might alter miRNA expressions. Chromosomal abnormalities can trigger oncogenic actions of miRNAs by modulating miRNA expression in the wrong cell type or at wrong time.

Several examples of miRNAs whose expression is deregulated in human cancer have been reported. miR-155 is overexpressed in Hodgkin lymphoma, in pediatric Burkitt lymphoma and in diffuse large B-cell Lymphoma (Eis PS et al. 2005; Kluiver J et al. 2005; Metzler M et al. 2004). miR-21 is upregulated in breast cancer and in glioblastoma, while miR-143 and miR-145 genes are significantly down-regulated in colon cancer tissue compared with colonic mucosa. Evidence now indicates that the involvement of miRNAs in cancer is much more extensive than initially expected. Studies that investigated the expression of the entire microRNAome in various human solid tumors and hematologic malignancies have revealed differences in miRNAs expression between neoplastic and normal tissues (Calin GA et al. 2005; Ciafre SA et al. 2005; Pallante P et al. 2006; Weber F et al. 2006). These studies show that each neoplasia has a distinct miRNAs signature that differs from that of other neoplasms and that of the normal tissue counterpart. Moreover, it has become clear that some miRNAs are recurrently deregulated in human cancer. In most case, miRNAs are upregulated or down-regulated in all tumors, suggesting a crucial role for these miRNAs in tumorigenesis. However, there are some unusual situation: for example members of the miR-181 family are up-regulated in some cancers, such as thyroid (Pallante P et al. 2006), pancreatic (He L et al. 2005), and prostate carcinomas (Volinia S et al. 2006) but downregulated in others, such as pituitary adenomas (Bottoni A et al. 2007).

1.7.3 miRNAs and glioblastomas.

The first report on altered miRNA expression in glioblastomas came in 2005. In this report, miR-21 was shown to be highly upregulated and to have anti-apoptotic capabilities in both early-passage glioblastoma cultures and commercial cell lines (Chan JA et al.2005). Almost simultaneously, Ciafre et al. confirmed miR-21 up-regulation in glioblastomas using global expression profiling of both glioblastoma cell lines and patient biopsies (Ciafre SA et al.

2005). Since then, miRNA expression in glioblastomas has been evaluated by several profiling studies, while other studies have focused on specific promising miRNAs. These studies were based on a comparison to normal brain tissue, which is difficult to acquire. Consequently, normal brain tissues comprise of tissue adjacent to tumor and non-neoplastic brain. Furthermore, “non-neoplastic brain” is a broad category covering tissue recovered from autopsy as well as tissue from patients with gliosis, epilepsy, severe head trauma or arteriovenous malformations.

The most consistently upregulated miRNAs in glioblastomas or glioblastoma cell lines, when compared to normal brain tissue, were miR-21, miR-10b, miR-155, miR-210 and miR-221. The most consistently down-regulated were miR-128(-1,a), miR-330, miR-124, miR-149, miR-153, miR-154*, miR-181(a, b, c), miR-323 and miR-328 (Table1). These prominent miRNAs hold great potential as new biomarkers and/or therapeutic targets as they are oncomiRs, or tumor suppressor-miRs, which are directly involved in regulation of apoptosis, proliferation, tumor growth, angiogenesis, invasion, migration, cell cycle, chemosensitivity, tumorigenesis and differentiation. All of these are key factors in the development and growth of glioblastoma (Hermansen SK and Kristensen BW 2008).

Upregulation	Downregulation
Profiling studies (n = 10)	
miR-21	miR-128(-1,a)
miR-10b	miR-323
miR-155	miR-330(-3p)
miR-210	miR-124(a)
miR-221	miR-149
	miR-153
	miR-154*
	miR-181a
	miR-181b
	miR-181c
	miR-328
Studies using selected assays (n = 18)	
miR-21	miR-124(a)
miR-10b	miR-7

Table 1. Up- and down-regulated miRNAs in GBM or GBM cell lines compared to non-neoplastic controls. Adapted from Hermansen et al. 2008.

In the last years, many miRNAs have been associated with survival and prognosis of GBM, and proposed as new promising biomarkers. Overexpression of miR-196 family has been shown to indicate poor prognosis in GBM (Guan Y et al. 2010). Zhi et al showed that high expression levels of miR-21 and low of miR-181b also was able to predict glioblastoma prognosis (Zhi F et al. 2010). Moreover, Jiang et al. demonstrated that miR182 expression is associated with poor overall survival of malignant gliomas (Jiang L et al. 2012). High levels of miR-195 and miR-196b were later associated with longer overall survival (Lakomy R et al. 2011). These results contradict the findings of Guan et al. that reported miR-196 associated with shorter survival (Guan Y et al. 2010). Recently, Wu et al. found an association between low levels of miR-328 and worse overall survival in primary glioblastomas, using frozen samples (Wu Z et al. 2012). Until now, up-regulation of miR-21, miR-182, combined up-regulation of miR-196a and miR-196b and down-regulation of miR-181b, miR-195, miR 196b and miR-328 have been associated with poor prognosis in glioma (Hermansen SK and Kristensen BW 2013). However, miRNA biomarkers do not rely necessarily on a single highly up- or down-regulated miRNA. Future miRNA biomarkers are expected to consist of disease-specific miRNA signatures. Niyazi et al. found a specific 30-miRNA signature in glioblastomas that effectively distinguished short-term survivors from long-term survivors (Niyazi M et al. 2011). Srinivasan et al. found a 10-miRNA signature that independently predicted survival collecting a large number of glioblastoma patients from the Cancer Genome Atlas Database (TCGA) (Srinivasan S et al. 2011). Surprisingly, none of the identified miRNAs overlapped in these two studies. Moreover, recently Hayes et al. reported a panel of nine microRNAs able to predicts the clinical outcome of GBM patients (Hayes J et al. 2015), and Huang et al. performed an analysis of miRs, mRNA and survival of glioblastoma multiforme (Huang YT et al. 2014).

2. AIM OF THE STUDY

Glioblastoma is the most aggressive and lethal malignant brain tumor, with an average survival rate of only 12 months. However, a small subgroup of patients survives longer, and is defined as LTS. Therefore, the study of the molecular features typical of LTS is really attractive. The aim of this work is to individuate the microRNAs de-regulated in LTS subgroup of glioblastoma patients and their role in patients survival. The results achieved by this project may represent a good starting point to develop novel markers for the diagnosis, prognosis and treatment of this tumor.

3. MATERIALS AND METHODS

3.1 Cells and tissue specimens.

Glioblastoma cell lines T98G, U87MG, LN229 and LN18 were obtained from American Type Culture Collection (ATCC), (LG Standards, Milan Italy), U251MG, LN428, LN308, SF767, and A172 were kindly donated by Frank Furnari (La Jolla University, San Diego, CA, USA). U87, U251, T98G, AM38, A172, LN319, LN308, LN428 and SF767 were grown in Dulbecco's modified eagle's Medium, while LN18 and LN229 in Advanced Dulbecco's modified eagle's Medium. Media were supplemented with 10% heat-inactivated fetal bovine serum (FBS) -5% FBS for LN229 and LN18, -2 mM L-glutamine, and 100 U/ml penicillin/streptomycin. All media and supplements were from Sigma Aldrich (Milan, Italy). Glioblastoma surgical specimens (n=61) were obtained from patients undergoing surgery at the Cancer Center of Eastern Finland (University of Eastern Finland, Kuopio, Finland). A total of 61 formalin-fixed, paraffin-embedded (FFPE) tissue samples were collected from the archives of the Department of Pathology, University Hospital of Kuopio, Finland. Among the 61 samples, survival information for 43 cases was available. Permission to use the material was obtained from the National Supervisory Authority for Welfare and Health of Finland, and the study was accepted by the ethical committee of the Northern Savo Hospital District, Kuopio, Finland.

3.2 TCGA data analysis.

The collection of the data from TCGA platform was compliant with laws and regulation for the protection of human subjects, and necessary ethical approvals were obtained. Analysis of all data was done using GraphPad Prism 6 (San Diego, CA, USA). For different expression analysis and determination of the effect of miR-340 and N-RAS on patient's survival, we downloaded Agilent 8x15 miRNA expression (level 2) and HT_HG-U133A (level 3) along with clinical information from TCGA database in April 2014.

3.3 Cell transfection.

For miRs and siRNAs transient overexpression, cells at 50% confluence were transfected using Oligofectamine (Invitrogen, Milan, Italy) and 100nM of pre-miR-340, scrambled miR, anti-miR-340, scrambled anti-miR (Ambion®, Life Technologies), siN-RAS or a siRNA Control (Santa Cruz Biotechnologies, MA, USA). For transient overexpression of 4 µg of pcDNA3-N-RAS, pcDNA3-AKT⁺, pcDNA3-ERK⁺ or pcDNA3, cells were transfected using XtremeGENE 9 DNA Transfection Reagent (Roche, Milan, Italy).

Temozolomide for cell treatment was purchased from Sigma Aldrich (Milan, Italy).

3.4 RNA extraction and real-time PCR.

Cell culture: Total RNA (microRNA and mRNA) was extracted using Trizol (Invitrogen, Milan, Italy) according to the manufacturer's protocol. *Tissue specimens:* total RNA (miRNA and mRNA) from FFPE tissue specimens was extracted using RecoverAll Total Nucleic Acid isolation Kit (Ambion, Life Technologies, Milan, Italy) according to the manufacturer's protocol. Reverse transcription of total RNA was performed starting from equal amounts of total RNA/sample (500ng) using miScript reverse Transcription Kit (Qiagen, Milan, Italy) for miR analysis, and using SuperScript® III Reverse Transcriptase (Invitrogen, Milan, Italy) for mRNA analysis. Quantitative analysis of miR-340 and RNU6A (as an internal reference) were performed by Real-Time PCR using specific primers (Qiagen, Milan, Italy) and miScript SYBR Green PCR Kit (Qiagen, Milan, Italy). Real-Time PCR was also used to assess the mRNA of N-RAS and β -actin (as an internal reference), using iQTM SYBR Green Supermix (Bio-Rad, Milan, Italy). The primer sequences were:

N-RAS-Fw: 3'-CGCACTGACAATCCAGCTAA-5',

N-RAS-Rv: 3'-TCGCCTGTCCTCATGTATTG-5',

Act-FW: 5'-TGCGTGACATTAAGGAGAAG-3',

Act-Rv: 5'-GCTCGTAGCTCTTCTCCA-3'.

The reaction for detection of mRNAs was performed in this manner: 95 °C for 5', 40 cycles of 95 °C for 30'', 60 °C for 30'' and 72 °C for 30''. The reaction for detection of miRs was performed in this manner: 95 °C for 15', 40 cycles of 94 °C for 15'', 55 °C for 30'' and 70 °C for 30''. All reactions were run in triplicate. The threshold cycle (CT) is defined as the fractional cycle number at which the fluorescence passes the fixed threshold. For relative quantization, the $2^{(-\Delta\Delta CT)}$ method was used. Experiments were carried out in triplicate for each data point, and data analysis was performed by using Applied Biosystems StepOne Plus™ Real-Time PCR Systems.

3.5 miRNAs expression microarray and data analysis.

From each sample, 5 μ g of total RNA (from 6 long- and 6 short- glioblastoma survivor's patients) was reverse transcribed using biotin-end-labelled random octamer oligonucleotide primer. Hybridization of biotin-labelled cDNA was performed on an Ohio State University custom miRNA microarray chip (OSU_CCC version 3.0), which contains 1150 miRNA probes, including 326 human and 249 mouse miRNA genes, spotted in duplicates. The hybridized chips were washed and processed to detect biotin-containing transcripts by streptavidin-Alexa647 conjugate and scanned on an Axon 4000B microarray scanner (Axon Instruments, Sunnyvale, CA, USA). Raw data were normalized

and analyzed with GENESPRING 7.2 software (zcom Silicon Genetics, Redwood City, CA, USA). Expression data were median-centered by using both the GENESPRING normalization option and the global median normalization of the BIOCONDUCTOR package (www.bioconductor.org) with similar results. Statistical comparisons were done by using the GENESPRING ANOVA tool, predictive analysis of microarray and the significance analysis of microarray software (<http://www.stat.stanford.edu/Btibs/SAM/index.html>).

3.6 Establishment of miR-340 stable expressing glioblastoma cells.

Lentivirus encoding an expression cassette containing a puromycin resistance gene, the green fluorescent protein (GFP) gene and the miR-340 sequence under the hCMV promoter were purchased from GE Healthcare Dharmacon (Milan, Italy). U251MG cells were infected with the lentivirus or control Empty virus (lacking the miR-340 sequence) at a final concentration of 20 MOI. After culturing in selection media supplemented with puromycin, GFP was detected by fluorescence microscopy. Finally, puromycin resistant and GFP positive clones were picked.

3.7 Protein isolation and western blotting.

Cells were lysed in JS buffer (50 mM HEPES pH 7.5 containing 150 mM NaCl, 1% Glycerol, 1% Triton X100, 1.5mM MgCl₂, 5mM EGTA, 1 mM Na₃VO₄, and 1X protease inhibitor cocktail). Protein concentration was determined by the Bradford assay (BioRad, Milan Italy) using bovine serum albumin as the standard, and equal amounts of proteins were analyzed by SDS-PAGE (12% acrylamide). Gels were electroblotted into nitrocellulose membranes (G&E Healthcare, Milan Italy). Membranes were blocked for 1 hr with 5% non-fat dry milk in Tris Buffered Saline (TBS) containing 0.1% Tween-20, and incubated at 4°C over night with the primary antibody. Detection was performed by peroxidase-conjugated secondary antibodies using the enhanced chemiluminescence system (Thermo, Euroclone Milan Italy). Primary antibodies used were: anti-N-RAS (Santa Cruz Biotechnologies, MA, USA), anti-pP42/44, anti-pAKT (Cell Signaling, Danvers, MA, USA), and anti-βActin (Sigma Aldrich, Milan Italy).

3.8 Cell proliferation assay.

Cell vitality was evaluated with the CellTiter 96® AQueous One Solution Cell Proliferation Assay (Promega, Madison, WI), according to the manufacturer's protocol. The assay is based on reduction of 3-(4,5-dimethylthiazol-2-yl)-5-(3-carboxymethoxyphenyl)-2-(4-sulfophenyl)-2H-tetrazolium, inner salt (MTS) to a colored product that is measured spectrophotometrically. After 24 hrs from the miRs or siRNAs transfection as described, cells (1×10^3) were plated in 96-

well plates in triplicate, and incubated at 37°C in a 5% CO₂ incubator. Metabolically active cells were detected by adding 20 µl of MTS to each well. After 30 min of incubation, the plates were analyzed on a Multilabel Counter (Bio-Rad, Richmond, VA, USA).

3.9 Cell cycle analysis.

Cell cycle was analyzed via propidium iodide incorporation in permeabilized cells by flow cytometry. The cells (5×10^4) were washed in PBS and resuspended in 200 µl of a solution containing 0.1% sodium citrate, 0.1% Triton X-100 and 50 µg/ml propidium 6 iodide (Sigma Aldrich, Milan, Italy). Following incubation at 4°C for 30 min in the dark, nuclei were analyzed with a Becton Dickinson FACScan flow cytometer. Cellular debris was excluded from analyses by raising the forward scatter threshold, and the DNA content of the nuclei was registered on a logarithmic scale. The percentage of elements in the hypodiploid region was calculated.

3.10 Soft-Agar assay.

10^4 cells were plated in 60mm dishes in a solution containing Dulbecco's modified Eagle's medium 2× (Sigma, St Louis, MO, USA), TPB Buffer (Difco, BD, Franklin Lakes, NJ, USA), and 1.25% of Noble Agar (Difco, BD, Franklin Lakes, NJ, USA). Briefly, cells were harvested and counted then a layer of 7ml with the solution containing Noble Agar were left to polymerize on the bottom of the dishes. Then cells were resuspended in 2ml of same solution and plated. Cells were left grown for 2 weeks in the incubator.

3.11 Cell death quantification and apoptosis detection.

Cells were transfected with miRNAs as described and were plated in 96-well plates in triplicate, treated and incubated at 37°C in a 5% CO₂ incubator. Temozolomide was used at final concentration of 300µM for 24 h. Cell viability was assessed using the CellTiter 96® AQueous One Solution Cell Proliferation Assay (Promega, Madison, WI), as described above. Apoptosis was analyzed with Caspase-Glo® 3/7 Assay Systems (Promega, Madison, WI), as reported by instruction manual. Briefly, cells were incubated with medium supplemented with caspase 3/7 reagent. Following incubation for 30 minutes at room temperature, luminescence was measured.

3.12 Rescue experiments.

To determine whether N-RAS mediate the effects of miR-340, rescue experiments were performed in which the effects of miR-340 were measured in the setting of overexpression of a deletion mutant of N-RAS lacking the 3'UTR. Cells were transfected with miR-340 and with the mutant N-RAS

lacking the 3'UTR using X-tremeGENE 9 DNA Transfection Reagent (Roche, Milan, Italy), as described. Growth and cell cycle were assessed as above.

3.13 In vivo tumor formation.

Female 5 week-old CD1 nude mice (Charles River, Milan, Italy) were maintained in special pathogen free condition for one week. Animal handling and experimental procedures were in accordance with the guidelines and approved by the Animal Experimental Ethics Committee of University of Naples. U251MG cells stably expressing miR-340 or miR-Empty were injected subcutaneously into the left flank of nude mice (2×10^6 cells in 100 μ l). Tumor size was weekly examined by HFUS (Vevo 2100) with a 40 MHz probe after one, two, and three weeks from injection. The procedures were performed under general anesthesia with 2% isoflurane in 100% oxygen at 0.8 L/min. For each tumor, mediolateral, anteroposterior and craniocaudal diameters were measured. Tumor volumes (TV) were calculated according to the formula $V = (\text{height} \times \text{width} \times \text{length} \times 3.16)/6$.

3.14 Luciferase assay.

The two predicted region on the 3' UTR of the human N-RAS gene (R1 and R2) containing the putative miR-340 binding site were PCR amplified using the following primers:

N-RAS-R1-FW 3'-GCTCTAGATGGCATCTGCTCTAGATTCATAAA-5',
N-RAS-R1-Rv 3'-GCTCTAGATTTCATACATGTACAAAATGGCATC-5',
N-RAS-R2-FW 3'-GCTCTAGACTATTTTAGTGGGCCCATGTT-5',
N-RAS-R2-Rv 3'-GCTCTAGACAAGAAGCAGAACGCACC-5',

and cloned downstream of the Renilla luciferase stop codon in pGL3 control vector (Promega, Milan Italy). An inverted sequence of the miRNA-binding sites was used as negative control. A549 cells were transfected with miR-340 or Scrambled miR for 6 hours. Then, the cells were co-transfected with 1.2 μ g of 3'UTR N-RAS -R1 or -R2 plasmids or relative mutant constructs and 400 μ g of a Renilla luciferase expression construct, pRL-TK (Promega, Milan, Italy), with Lipofectamine 2000 (Life Technologies, Milan, Italy). Cells were harvested 24 hrs post-transfection and the luciferase activity was assayed with Dual Luciferase Assay (Promega, Milan, Italy), according to the manufacturer's instructions. Three independent experiments were performed in triplicate.

3.15 Statistical analysis.

All experiments were repeated at least three times. Continuous variables are given as mean \pm 1 standard deviation. For two groups comparison, the Student's t test was used to determine differences between mean values for normally distributed. Survival was illustrated by Kaplan-Meier curves; survival

differences between groups were examined with log-rank test. All data were analyzed for significance using GraphPadPrism 6 (San Diego, CA, USA) software, where probability level <0.05 was considered significant throughout the analysis.

4. RESULTS

4.1 miR-340 expression is correlated with survival of glioblastoma patients.

In order to identify the potential miRNAs de-regulated in long vs short glioblastoma survivors, we performed a miRNA profile in primary glioblastoma tissues obtained from 6 long and 6 short survivors patients. The analysis was performed with a microarray chip containing 1150 miR probes, including 326 human and 249 mouse miRs, spotted in duplicates. Data obtained indicated that seven miRs (miR-193b, -340, -19b, -20a-b, -219-5p, -137 and -129-3p) were significantly de-regulated in long vs short glioblastoma survivors, with at least >1.5-fold change (Table 2).

	Unique id	Ratio of geom means Long vs Short survivors
1	hsa-mir-193b	0.491352201
2	hsa-mir-340	1.505219391
3	hsa-mir-19b	1.537663509
4	hsa-mir-20a - b	1.880932671
5	hsa-mir-219-5p	1.905150526
6	hsa-mir-137	2.235717499
7	hsa-mir-129-3p	2.644557823

Table 2. miRNAs differentially expressed between long and short glioblastoma survivors patients. Note: only the most significant are listed. Fold change values were generated from the median expression of the miRNAs in the groups compared.

Among these differentially expressed miRNAs, we focused our attention on miR-340, since we and others have already demonstrated its oncosuppressive role in different human tumors. Accordingly with microarray data, miR-340 levels resulted up-regulated in LTS patients, as assessed by Real-Time PCR (figure 6).

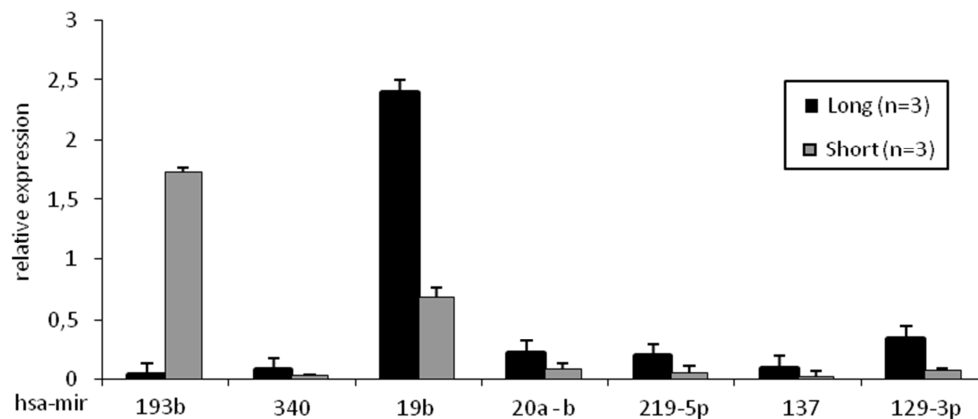


Figure 6. Array validation. Real-time PCR of the miRNAs resulted deregulated in LTS vs STS. Representative of three independent experiments.

Then, we analyzed miR-340 expression in a larger cohort of glioblastoma patients (n=61), as well as in data collected from the TCGA database (493 glioblastomas and 10 normal brain samples). As expected, the expression level of miR-340 was significantly decreased in the short survivors compared to the LTS ($p < 0.05$; figure 7a-b), and in glioblastoma compared to normal brain ($P < 0.0001$; figure 7c). Furthermore, Log-Rank analyses of two different cohorts of glioblastoma patients (43 glioblastoma patients from our lab and 327 from TCGA) showed that the patients with higher levels of miR-340 had a longer overall survival, indicating a prognostic role of miR-340 ($P < 0.05$; $P < 0.01$). The Kaplan-Meier curves of the patient cohorts are shown in fig.7d-e. These data show a strong down-regulation of miR-340 in glioblastoma, and reveal the potential role of this miRNA as a biomarker for glioblastoma prognosis.

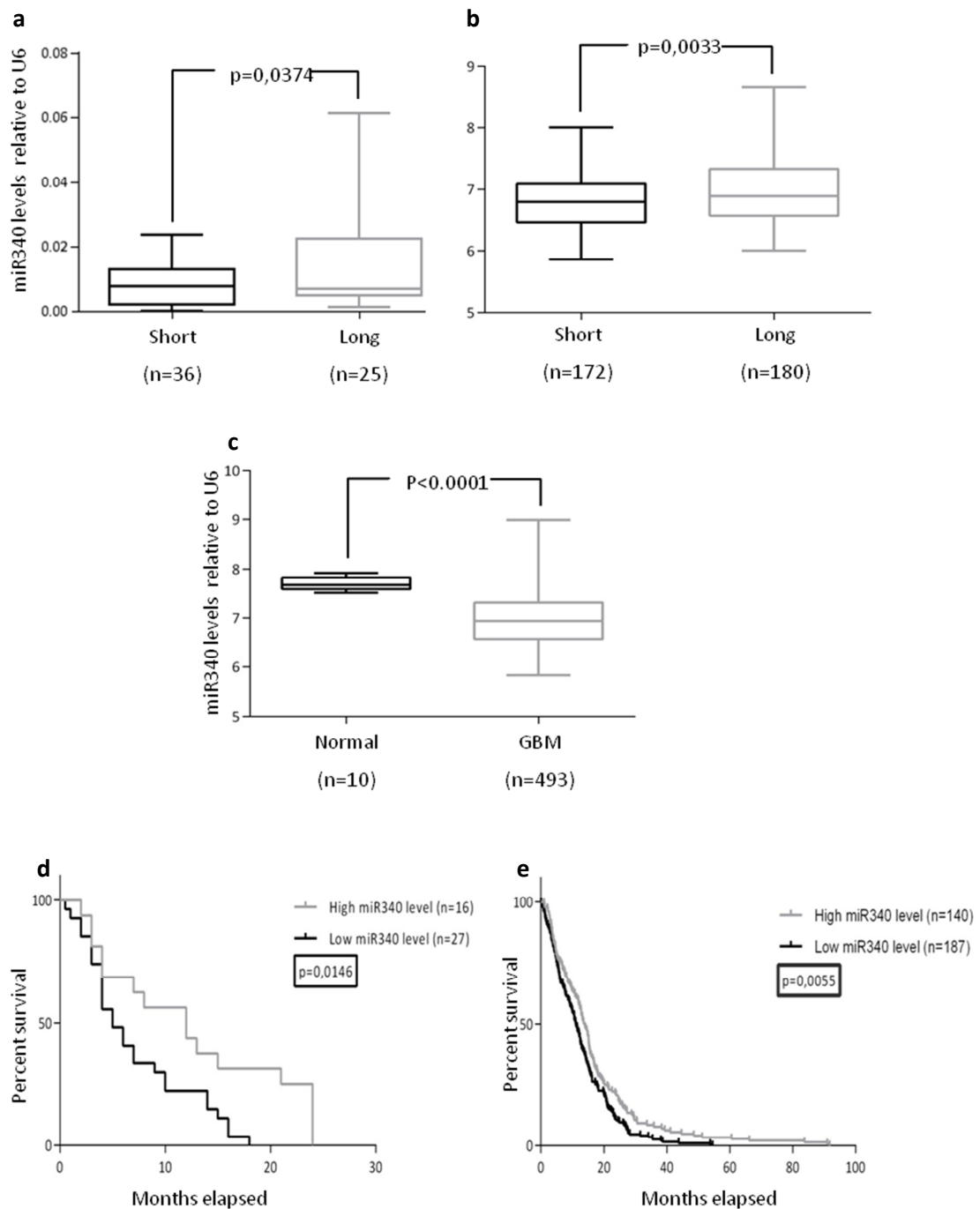


Figure 7. miR-340 is down-regulated in GBM and correlated with prognosis of GBM patients. The analysis was performed on two independent patient cohorts from our lab and from TCGA database. **a, b, and c,** miR-340 expression in: **a,** the FFPE tissues from 36 LTS and 25 STS glioblastoma patients; **b,** 180 LTS and 172 STS glioblastoma patients from TCGA; **c,** 10 normal brain and 493 glioblastomas collected from TCGA. Significant increase of miR-340 expression was identified between LTS vs STS in both cohorts and in normal brain vs glioblastoma. miR-340 expression level was assessed by Real-Time PCR. The transcript level was normalized against U6. An

arbitrary cut-off of 12 months was used to divide patients. P was calculated using Student's t test. $P < 0.05$ was considered significant. **d** and **e**, Kaplan-Meier survival curve analysis of the correlation between miR-340 and overall survival of: **d**, the FFPE tissues from 16 high and 27 low miR-340 expressing glioblastoma patients; **e**, 140 high and 187 low miR-340 expressing glioblastoma patients collected from TCGA. High miR-340 expression predicted a better prognosis in both cohorts. The patients were assigned to the high- or low-miR-340 expression group using the media as a threshold. P was calculated using log-rank test test. $P < 0.05$ was considered significant.

4.2 N-RAS is a direct target of miR-340.

To identify possible miR-340 targets involved in the long survival phenotype, we used bioinformatic databases (Targetscan, Miranda, Pictar), that revealed the presence in the 3'UTR of N-RAS of two distinct putative miR-340 binding sites (fig.8a). To analyze if the miR-340 directly binds the two putative regions in the 3'UTR of N-RAS, we cloned these regions downstream of a luciferase reporter gene in the pGL3 vector. A549 cells were co-transfected with the reporter plasmids singularly or in combination, in the presence of the control miR (Scrambled miR) or miR-340. As shown in Figure 8b, both the N-RAS 3'UTR luciferase reporters activity were repressed by the addition of miR-340. Moreover, the effect was higher in cells co-transfected with both the reporters, indicating that both the regions of N-RAS 3'UTR are direct targets of miR-340. Luciferase activity was not affected by miR-340 overexpression in the presence of mutant constructs, in which the seed sequences were inversely cloned (Fig.8a-b).

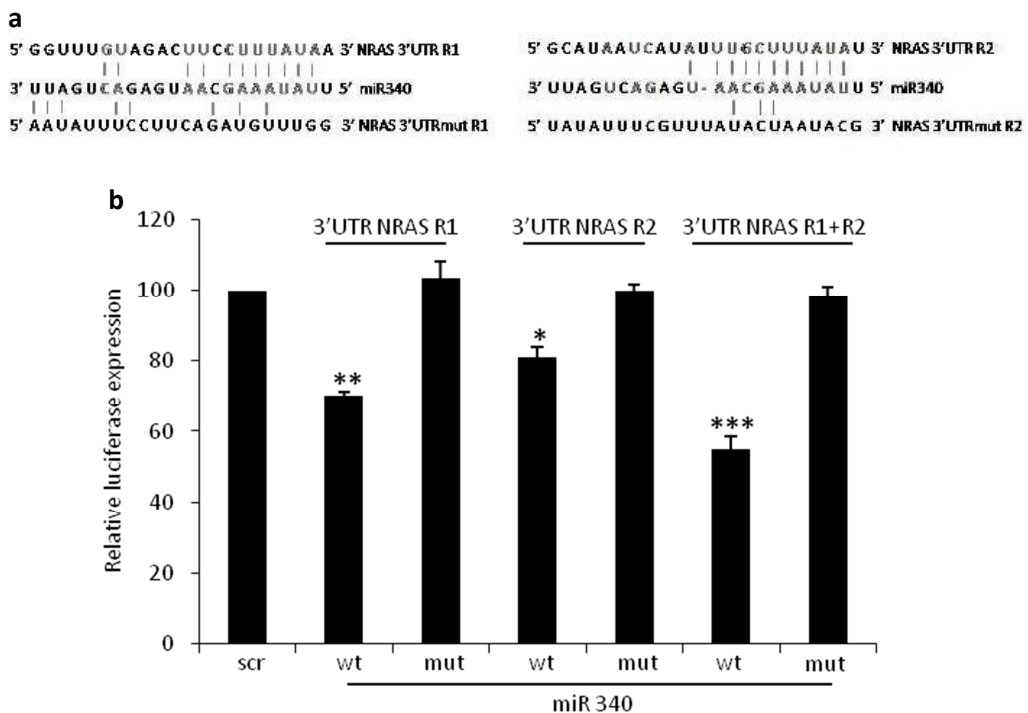
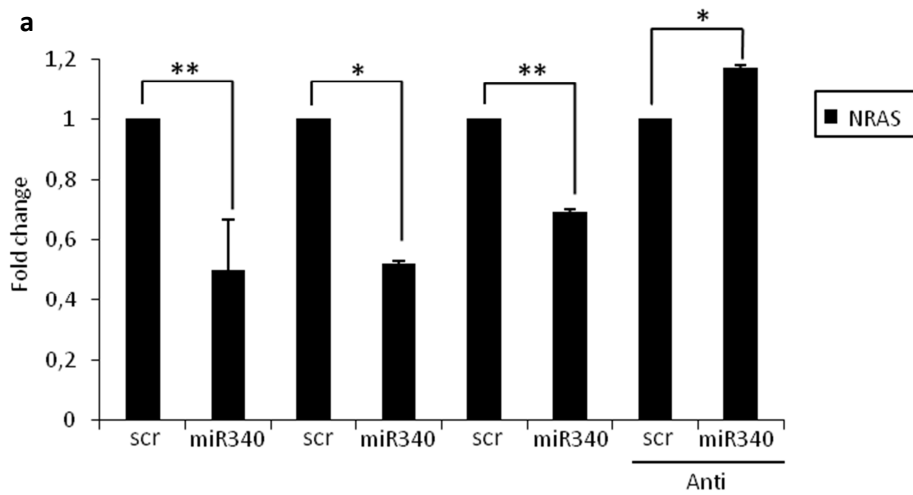


Figure 8. miR-340 directly targets N-RAS. **a**, the predicted miR-340 binding sites in the N-RAS-3'UTR region 1 and 2 (3'UTR NRAS R1 and 3'UTR NRAS R2) by MIRANDA and the designed mutant sequences (3'UTR NRAS R1mut and 3'UTR NRAS R2mut). **b**, N-RAS luciferase constructs containing a wild-type or mutated N-RAS-3'UTR R1 or R2, were co-transfected alone or in combination with miR-340 or scrambled miR in A549 cells. Luciferase activity was measured 24 hrs after transfection. Reporter activities of cells co-transfected with Scrambled miR sequence are arbitrary set as 100. The results were obtained from three independent experiments

and are presented as mean +/- SD. P was calculated using Student's t test. *,p<0.05; **, p<0.01; ***, p<0.001.

To establish a causative effect between miR-340 and N-RAS, we transfected different glioblastoma cell lines with miR-340 and analyzed N-RAS levels by Real-Time PCR and Western Blot. We revealed a strong decrease of both N-RAS mRNA and protein levels consistently in all cell lines transfected (Figures 9a and 9b). On the contrary, AntimiR-340 induced an increase of N-RAS levels in T98G cells (Figures 9a and 9b).



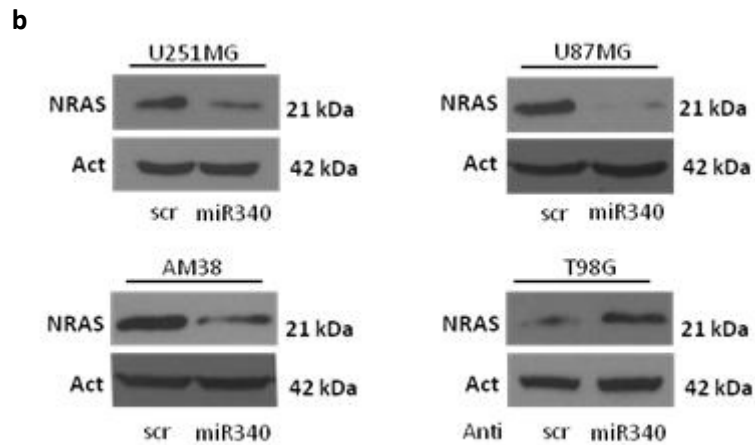


Figure 9. miR-340 overexpression decreased N-RAS levels. Glioblastoma cell lines (U251MG, U87MG and AM38) were transfected with a Scrambled miR sequence and miR-340, or with Scrambled AntimiR sequence and AntimiR-340 in T98G cells for 72 hrs. Real-time PCR (**a**) and Western blot (**b**) were performed to analyze N-RAS mRNA and protein levels. Western blot analyses are from representative experiments. Actin was used as loading control. The experiments were repeated at least three times. In **a**, the results are presented as mean \pm SD. P was calculated using Student's t test. *, $p < 0.05$; **, $p < 0.01$.

4.3 Effects of miR-340 in glioblastoma cells.

We investigated the tumor suppressive role of miR-340 in different GBM cell lines (U251MG, U87MG and AM38) transfected with miR-340 or with Scrambled miR. We chose these three cell lines since they expressed low levels of miR-340, as assessed by Real-Time PCR on a panel of 11 different glioblastoma cells (figure 10).

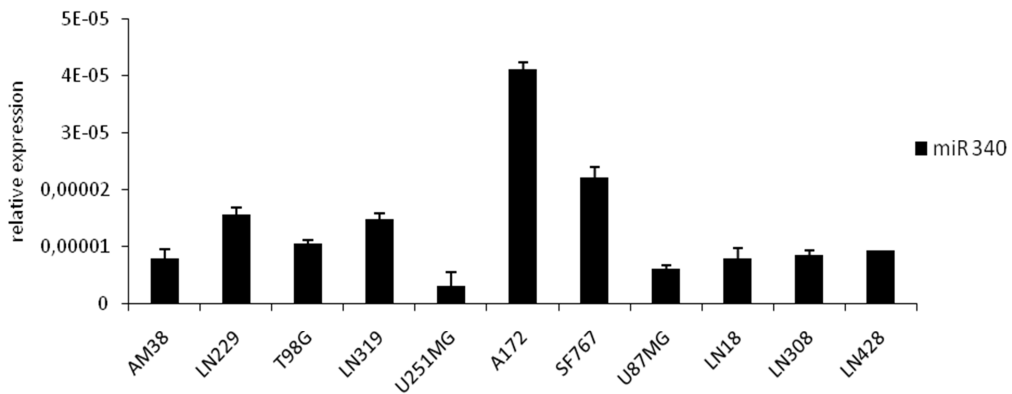


Figure 10. miR-340 expression in glioblastoma cell lines.

We analyzed the effects of miR-340 on cell cycle, cell proliferation and sensitivity to therapy. miR-340 transfection induced a significant block of the S-phase of the cell cycle, as assessed by FACS analysis after propidium iodide staining (figure 11), and a significant decrease in cells proliferation, as assessed by MTT assay (figure 12a). On the contrary, expression of Anti-miR340 in T98G was able to increase cell proliferation (figure 12b). We next investigated whether miR-340 expression had an impact on anchorage independent cell growth by a soft agar assay. As showed in fig.13, miR-340 induced a reduction of the colony formation in U251MG, U87MG and AM38 cells. Finally, we investigated a possible role of miR-340 in Temozolomide (TMZ) sensitivity. MTT and Caspase 3/7 assays showed that miR-340 induced an increase of TMZ sensitivity in all the cells analyzed (figure 14a-b). These results clearly demonstrate that miR-340 acts as tumor-suppressor in glioblastoma cells by regulating cell cycle, proliferation, anchorage independent cell growth and TMZ-sensitivity.

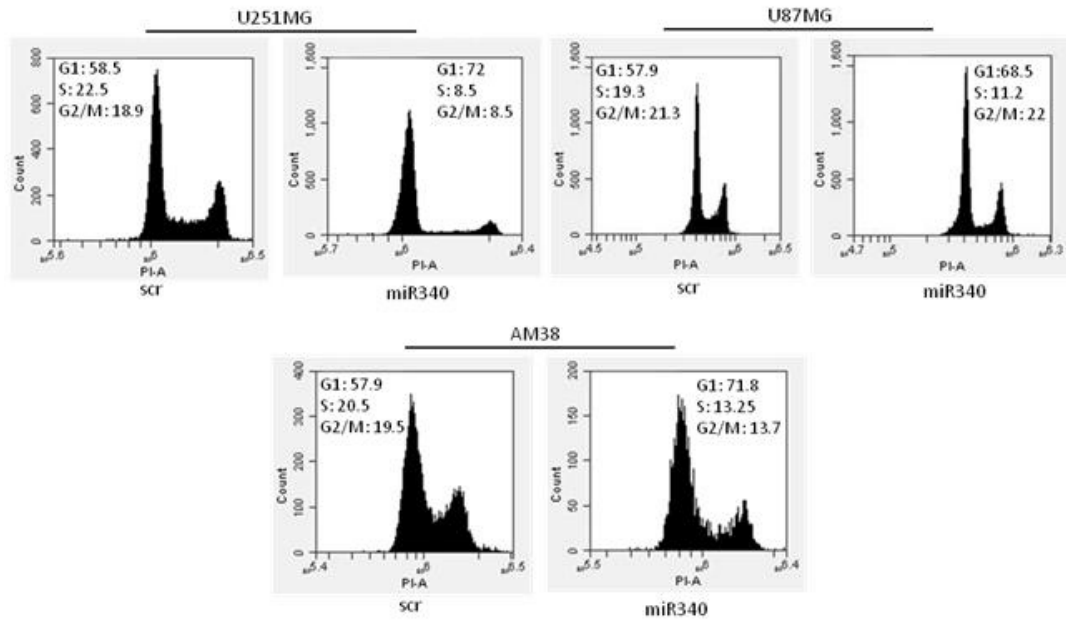


Figure 11. miR-340 blocks cell cycle in glioblastoma cells. Glioblastoma cell lines (U251MG, U87MG and AM38) were transfected with a Scrambled miR sequence and miR-340 and cell cycle was analyzed by flow cytometry after propidium iodide staining 72 hrs after transfection. The data show that miR-340 overexpression blocks cell cycle. The data are representative of three independent experiments.

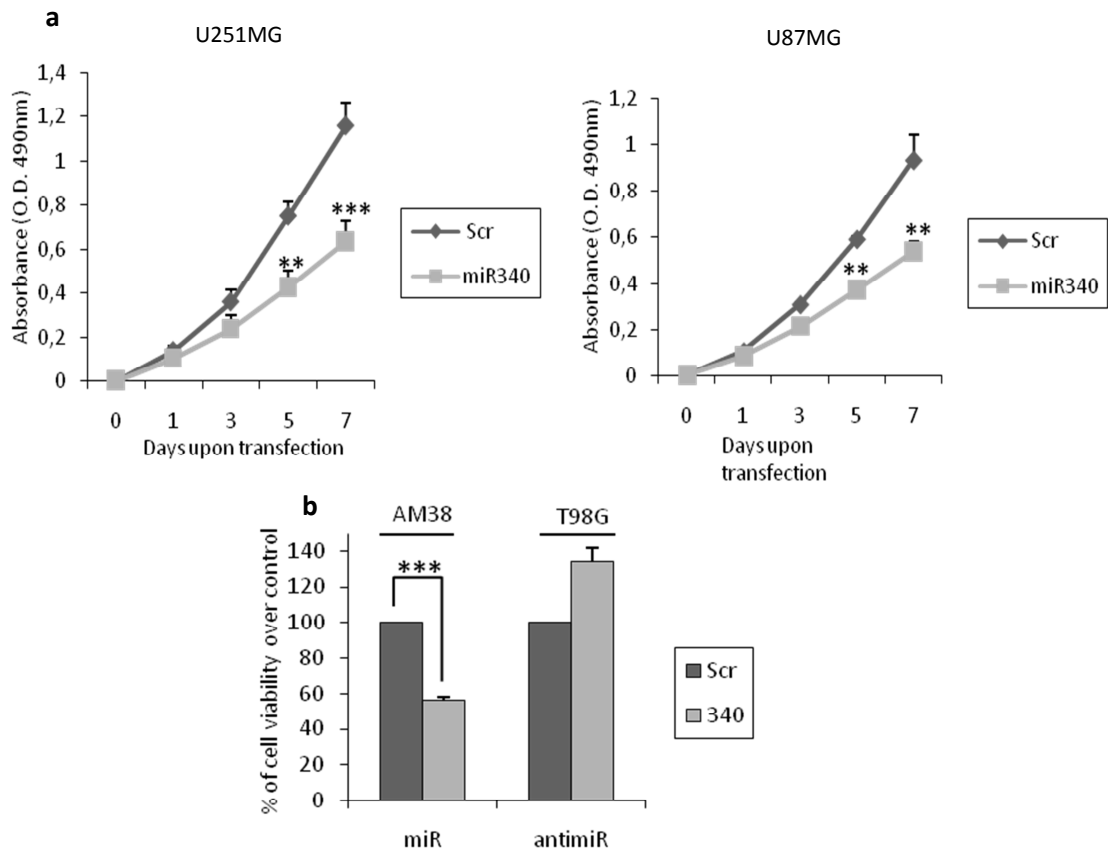


Figure 12. miR-340 decreases proliferation in glioblastoma cells. Glioblastoma cell lines (U251MG, U87MG and AM38) (**a**, **b**) were transfected with a Scrambled miR sequence and miR-340, or with Scrambled AntimiR sequence and AntimiR-340 in T98G (**b**) cells. Cell proliferation was analyzed by MTT assay 1, 3, 5 and 7 days after transfection. The data show that miR-340 overexpression decreases cell proliferation. Data are mean values \pm SD from three independent experiments. P was calculated using Student's t test. *, $p < 0.05$; **, $p < 0.01$; ***, $p < 0.001$.

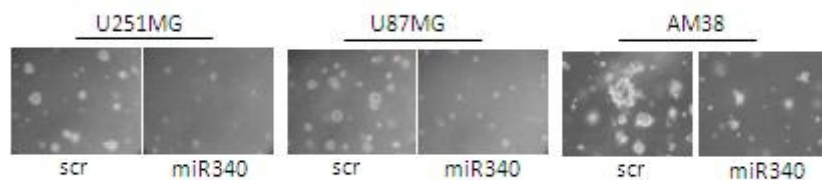


Figure 13. miR-340 decreases anchorage independent cell growth in glioblastoma cells. Glioblastoma cell lines (U251MG, U87MG and AM38) were transfected with a Scrambled miR sequence and miR-340 for 24 hrs. Anchorage independent cell growth was analyzed by Soft Agar cell growth 14 days after transfection. The data show that miR-340 overexpression decreased anchorage independent cell growth. The experiment was repeated three times.

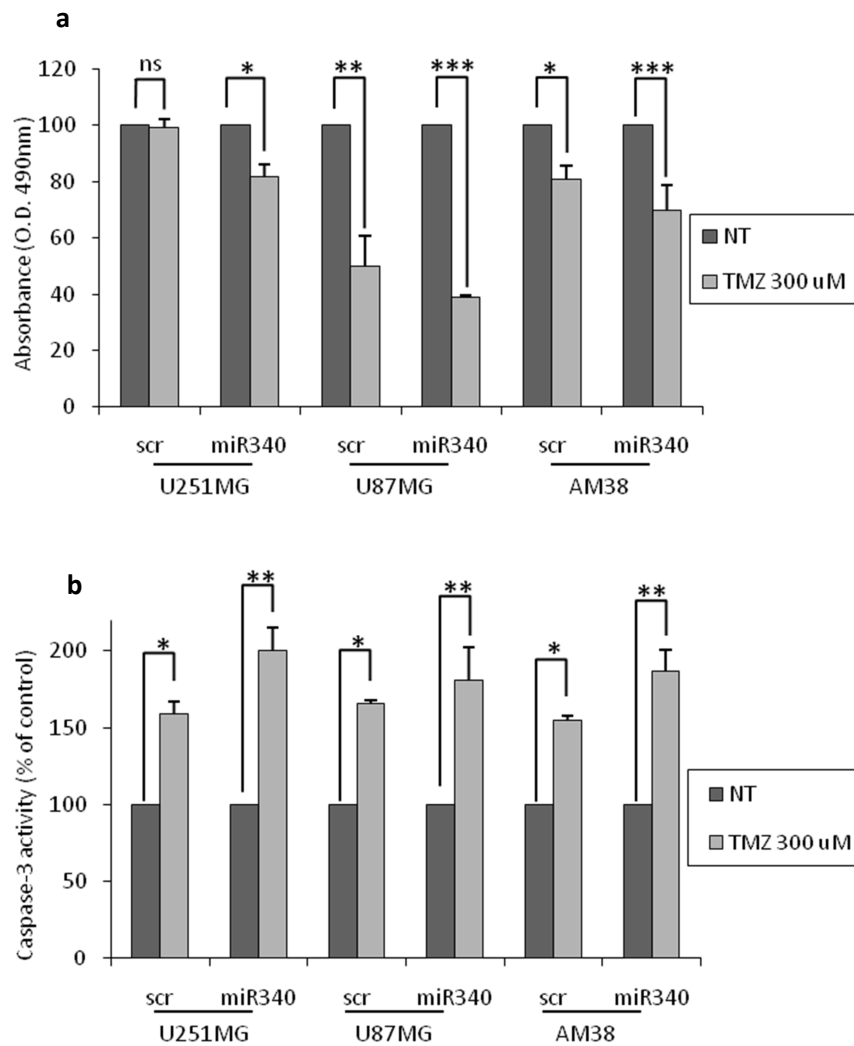


Figure 14. miR-340 increases TMZ sensitivity of glioblastoma cells. Glioblastoma cell lines (U251MG, U87MG and AM38) were transfected with a Scrambled miR sequence and miR-340 for 24 hrs, and then treated with TMZ 300 μ M for 24 hrs. Cell death and apoptosis activation were analyzed respectively by MTT assay (a) and caspase assay (b). The data show that miR-340 overexpression promotes the TMZ induced apoptosis. Presented data are mean values \pm SD from three independent experiments. P was calculated using Student's t test. *, $p < 0.05$; **, $p < 0.01$; ***, $p < 0.001$.

4.4 N-RAS is the key target molecule for miR-340 effects.

N-RAS is a key oncogene, deregulated in many different human cancers. In order to demonstrate a causative link between miR-340 and N-RAS, we performed rescue experiments transfecting U251MG with miR-340 and with a construct expressing N-RAS lacking the 3'UTR. Levels of transfected N-RAS were detected by western blot. Interestingly, the re-expression of N-RAS was able to rescue the effects of miR-340 on cell cycle, proliferation and anchorage independent cell growth (figure 15a-b-c).

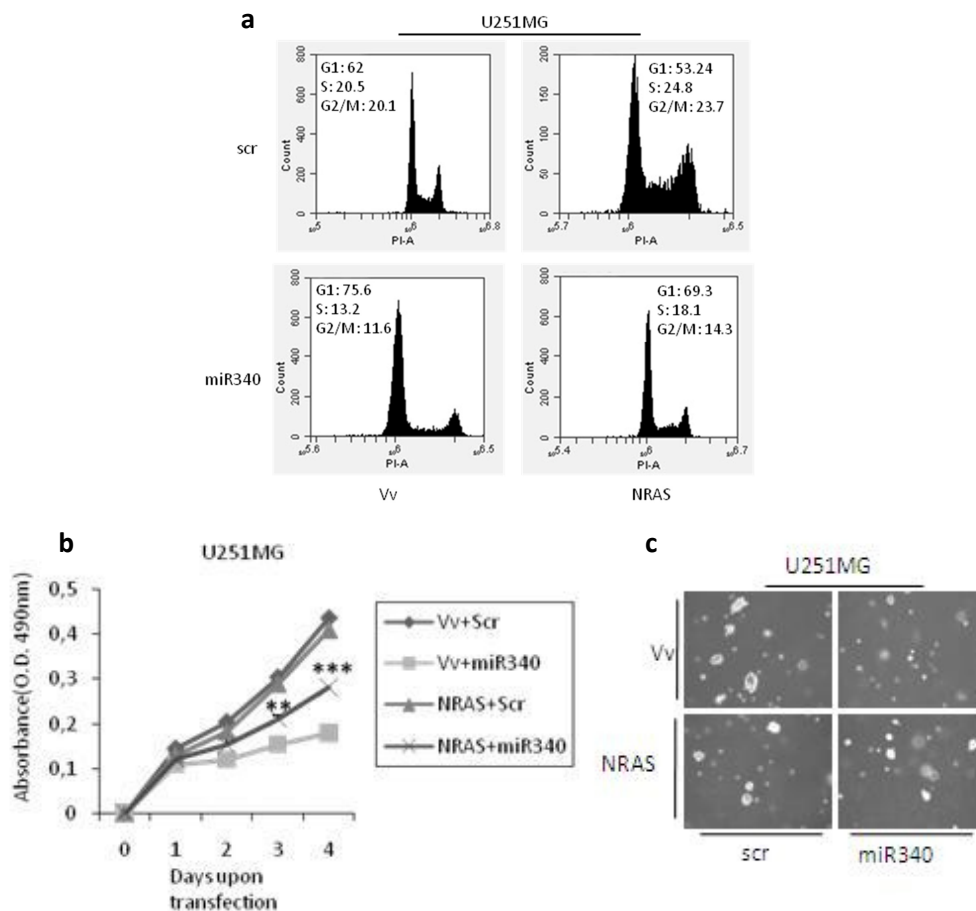


Figure 15. N-RAS mediates the effects of miR-340 on cell cycle, proliferation and anchorage independent cell growth. U251MG glioblastoma cells were co-transfected with miR-340 and N-RAS vector lacking 3'UTR or control vector. Exogenous N-RAS expression was able to partially rescue the effects of miR-340 on cell cycle (a), proliferation (b) and anchorage independent growth (c). Presented data are mean values +/- SD from three independent experiments. P was calculated using Student's t test. *, $p < 0.05$; **, $p < 0.01$; ***, $p < 0.001$.

Similarly, the N-RAS knock-down by a specific N-RAS siRNA blocked cell cycle and reduced proliferation (figure 16a-b), and was effectively able to decrease N-RAS and phosphorylated forms of ERK and AKT kinases (figure 16c). Then, we analyzed N-RAS expression in a cohort of 39 glioblastoma patients and we found that N-RAS was down-regulated in long vs short survivors ($p < 0.05$, figure 17a). Moreover, N-RAS expression resulted higher in 542 glioblastoma tissues compared to 10 normal brain (data collected from oncomine database, $p < 0.0001$, figure 17b). Further, Log-Rank analysis of 28 glioblastoma patients showed that patients with higher levels of N-RAS had a shorter overall survival (figure 17c). This result was also confirmed collecting the data from the R2.aml database (504 tissues, $p < 0.05$, figure 17d). In conclusion, our results suggest that the anti-tumoral effects of miR-340 are, at least in part, mediated by N-RAS targeting.

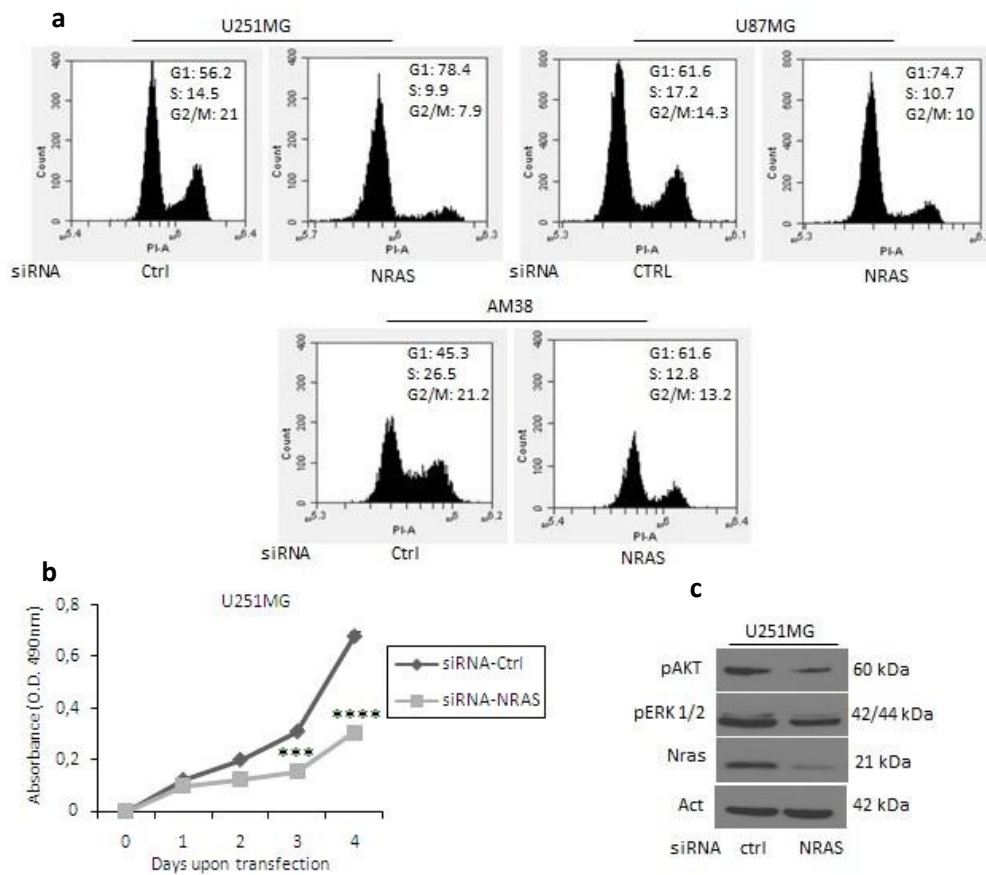


Figure 16. N-RAS Knock-Down reproduces the effects of miR-340 transfection in GBM cells. U251MG cells were transfected with a siRNA Control or with a siNRAS sequence. N-RAS silencing was able to mimic the effects of miR-340 on cell cycle (a) and proliferation (b), and to decrease the molecular pathways downstream N-RAS mediated by AKT and ERKs kinases (c). Presented data are mean values \pm SD from three independent experiments. Western blot analyses are from representative

experiments. Actin was used as loading control. P was calculated using Student's t test. *, $p < 0.05$; **, $p < 0.01$; ***, $p < 0.001$; ****, $p < 0.0001$.

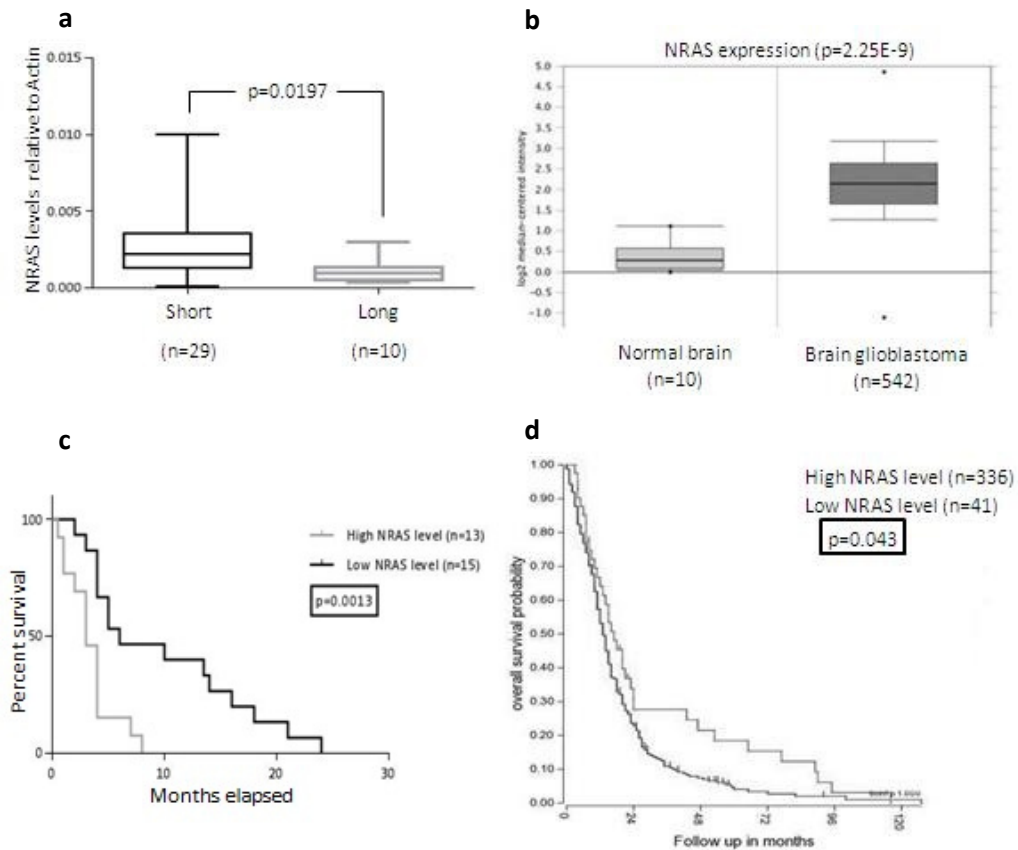


Figure 17. N-RAS is down-regulated in GBM and correlated with prognosis of GBM patients. The analysis was performed on three independent patient cohorts from our lab (a), from ONCOMINE database (b), and from R2.aml database (c). miR-340 expression in: a, the FFPE tissues from 10 LTS and 29 STS glioblastoma patients; b, 10 normal brain and 542 glioblastoma patients from ONCOMINE. Significant increase of N-RAS expression was identified between STS vs LTS (a) and in glioblastoma vs normal brain (b). miR-340 expression level was assessed by Real-Time PCR. The transcript level was normalized against U6. An arbitrary cut-off of 12 months was used to divide patients. P was calculated using Student's t test. $P < 0.05$ was considered significant. c, d, Kaplan-Meier survival curve analysis of the correlation between N-RAS and overall survival of 13 high and 15 low N-RAS expressing glioblastoma patients from our lab (c), and of 336 high and 41 low N-RAS expressing glioblastoma patients collected from R2.aml database (d). Low N-RAS expression predicted a better prognosis in GBM patients. The patients were assigned to the high- or low-N-RAS expression group according to R2.aml database. P was calculated using log-rank test. $P < 0.05$ was considered significant.

4.5 miR-340 blocks cell cycle and cell proliferation via inhibition of signaling pathways downstream N-RAS.

AKT and ERK1/2 pathways act as major downstream of RAS signaling, promoting multiple RAS oncogenic features, such as cell proliferation and apoptosis resistance. We investigated by western blot the levels of phosphorylated (activated) forms of AKT and ERK1/2 (p-AKT and p-ERK1/2) in glioblastoma cells transfected with miR-340 or Scrambled miR sequence. As shown in fig.18, miR-340 drastically reduced p-AKT and p-ERK1/2 levels in U251MG, U87MG and AM38 cells. On the contrary, transfection of AntimiR-340 induced an increase of p-AKT and p-ERK1/2 in T98G cells (fig.18).

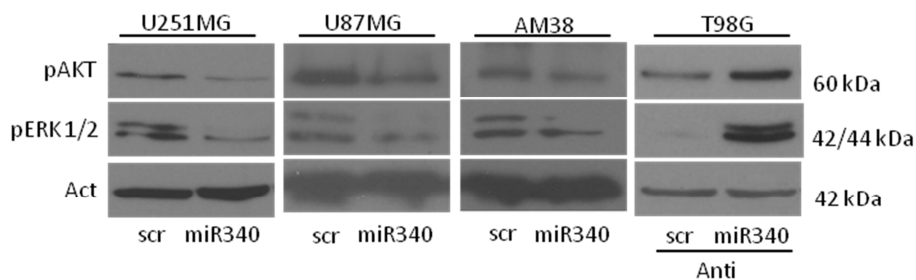


Figure 18. miR-340 inhibits molecular pathways downstream N-RAS. Glioblastoma cell lines (U251MG, U87MG and AM38) were transfected with a Scrambled miR sequence and miR-340, or with a Scrambled Anti miR sequence and AntimiR-340 in T98G cells for 72 hrs. Western blot was performed to analyze pAKT and pERK1/2 protein levels. Western blot analyses are representative experiments. Actin was used as loading control. The experiments were repeated at least three times.

Next, we wondered whether the block of cell cycle and cell proliferation observed upon miR-340 transfection were mediated by the inhibition of AKT and ERK1/2 signaling pathways downstream of N-RAS. To this aim, we transfected U251MG with miR-340 and with two constructs expressing the constitutively active forms of AKT (AKT⁺) and ERK1 (ERK⁺) for 48 hrs, alone or in combination. Levels of transfected AKT⁺ and ERK⁺ were detected by western blot (data not shown). Interestingly, AKT⁺ and ERK⁺ were able to partially rescue the effects of miR-340 both on cell cycle and proliferation (fig.19a-b). Importantly, these effects were higher in cells co-transfected with both AKT⁺ and ERK⁺ compared with cells transfected with AKT⁺ or ERK⁺ alone (fig.19a-b). These results further support the notion that miR-340 acts as tumor-suppressor in glioblastoma targeting N-RAS, and thus inhibiting AKT and ERK1/2 downstream pathways.

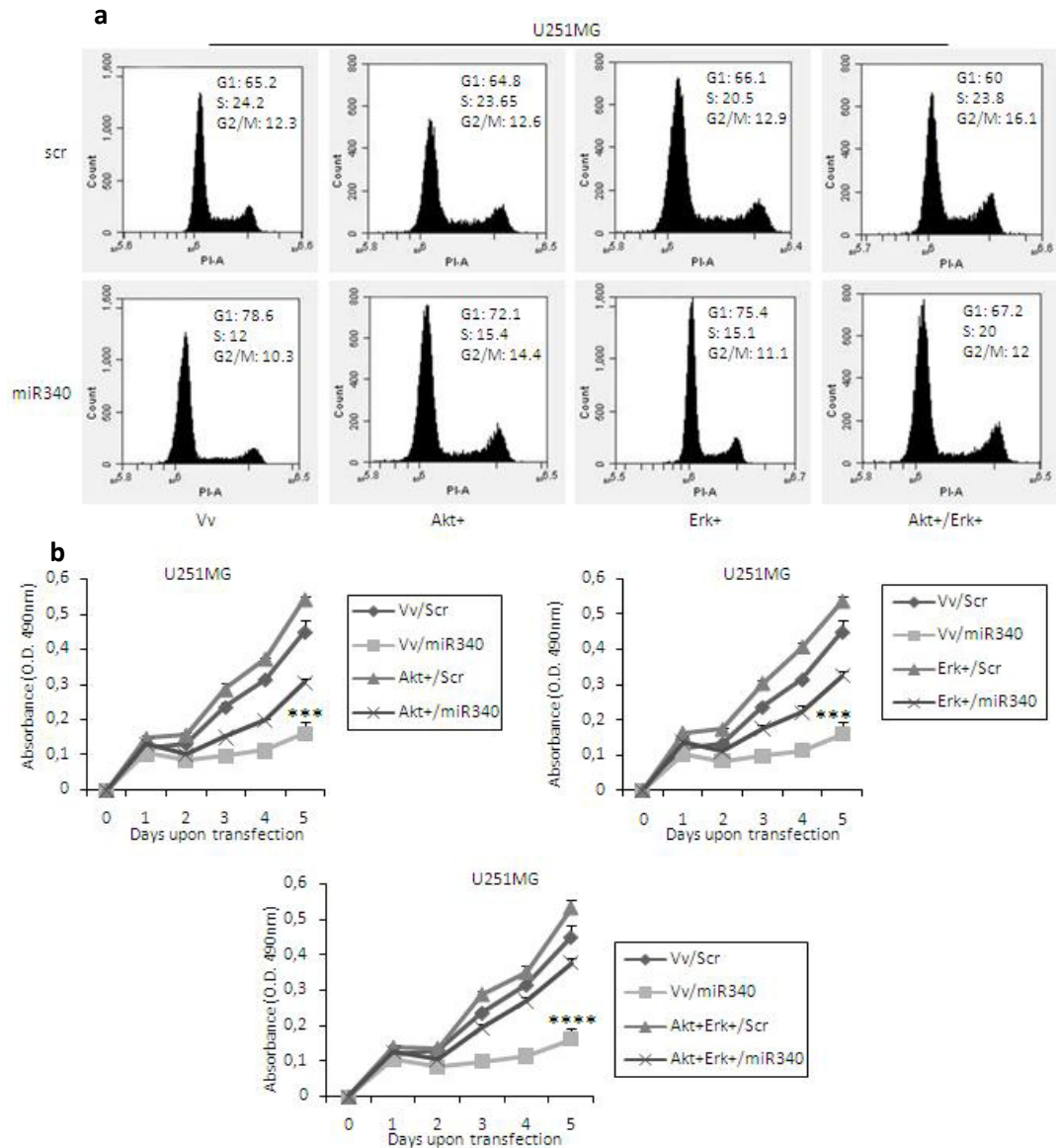


Figure 19. Molecular pathways downstream N-RAS mediates the effects of miR-340 on cell cycle and proliferation. U251MG glioblastoma cells was co-transfected with miR-340 and dominant positive mutants constructs of ERK and AKT kinases alone or in combination, or with control vector. Exogenous dominant positive expression of both ERKs and AKT expression was able to partially rescue the effects of miR-340 on cell cycle (a) and proliferation (b). Presented data are mean values +/-SD from three independent experiments. P was calculated using Student's t test. **, p<0.001; ***, p<0.0001.

4.6 Overexpression of miR-340 inhibits glioblastoma growth in vivo.

To analyze a possible role of miR-340 in glioblastoma tumorigenesis, we assessed the effects of miR-340 overexpression on tumor growth in vivo. To this aim, U251MG cells stably over-expressing miR-340 and their respective control cells (figure 20a-b) were subcutaneously injected in the left flank (2×10^6 cells per flank) of CD1 nude mice. Tumors volume and vessel formation were measured weekly by HFUS (Vevo 2100) and color-doppler HFUS (Vevo 2100) with a 40MHz probe for three weeks. Xenograft tumor volumes and vessels formation from miR-340-U251MG cells resulted significantly smaller compared to miR-Control-U251MG cells xenografts (n=6 animals per group, figure 20c-d).

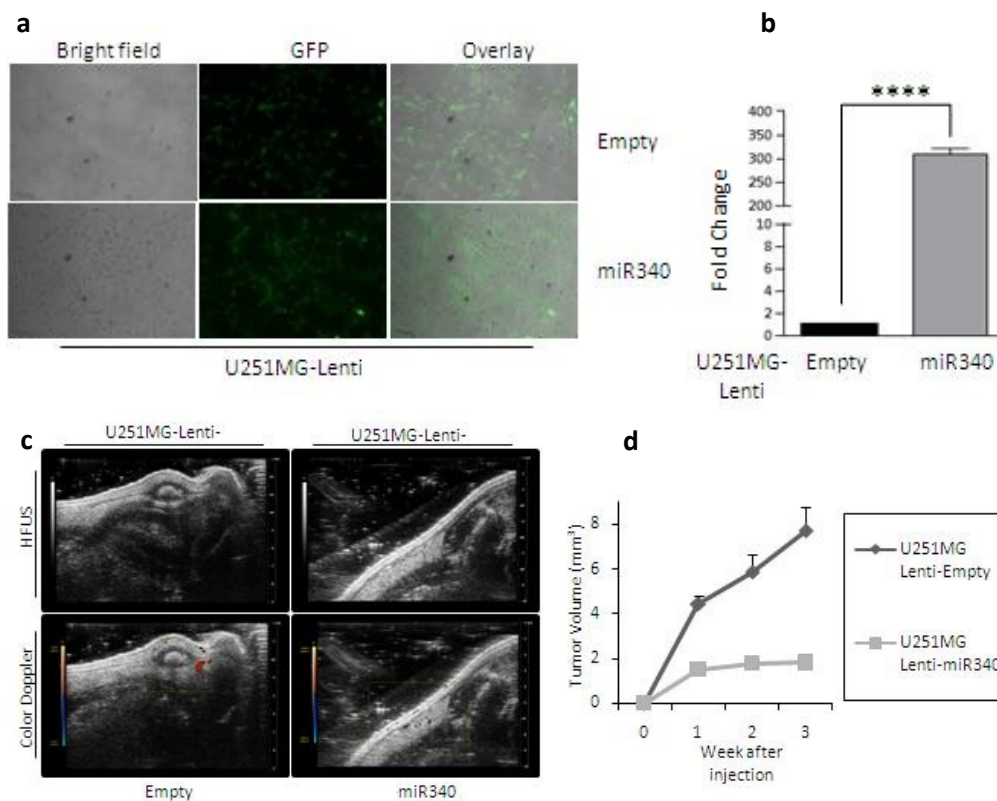


Figure 20. miR-340 inhibits the growth of glioblastoma xenograft in vivo. **a**, U251MG cells were stably infected with a lentivirus encoding mature miR-340 or Control sequence, together with GFP and puromycin-resistance gene (MOI=20). Stably infected clones were isolated by GFP expression in a medium supplemented with puromycin. Expression levels of miR-340 were checked by Real-Time PCR. The transcript level was normalized against U6 (**b**). U251MG stably infected with a lentivirus encoding miR-340 or Control particles were subcutaneously injected in the left flank of CD1 nude mice (n=6 for each group). Tumors volume and vessels formation were measured weekly by HFUS (Vevo 2100) and color-doppler HFUS

(Vevo 2100) with a 40MHz probe for three weeks. Data from **c** and **d** showed that miR-340 was able to reduce glioblastoma cell-derived xenograft growth and vessels formation. ^{****}, $p < 0.0001$.

5. DISCUSSION

GBM is one of the most aggressive types of human tumors, and is the most lethal form of brain cancer. It is characterized by an extremely bad prognosis, with a median survival rate of only 12 months after diagnosis (Tran B and Rosenthal MA 2010). Interestingly, a small subgroup of patients survives longer, and is defined as long term survivors (LTS) (Krex D et al. 2007; Stupp R et al. 2009). The understanding of the specific molecular features typical of LTS may represent an excellent chance to improve diagnosis, prognosis, treatment and lastly survival of GBM patients. At present, several molecular markers have been correlated to glioblastoma prognosis, and many need further validation before their use in clinical settings. The most important and well established marker of glioblastoma prognosis is MGMT promoter methylation, which is associated with a favorable outcome after Temozolomide chemotherapy in patients with new diagnosed glioblastoma (Hegi ME et al. 2005). However, despite the deep efforts of the last years, the cellular and molecular features of LTS are not been elucidated yet.

In the last decade, microRNAs have been frequently indicated to be deregulated in different human cancers, acting both as oncogenes or tumor-suppressors. It is well reported that microRNAs are involved in basic cellular functions, including proliferation, cell death, differentiation, metabolism and, importantly, tumorigenesis. In addition, these noncoding RNAs have the capacity to target tens to hundreds of genes simultaneously. Thus, they are attractive candidates as prognostic biomarkers and therapeutic targets in cancer. Since their discovery more than a decade ago, microRNAs are emerging as new key players in the scenario of tumor biology. Several recent studies have demonstrated that the expression of miRNAs is deregulated in gliomas. Ciafre` et al. examined the alterations of 245 miRNAs in World Health Organization grade IV GBMs, in which miR-221 was up-regulated, whereas miR-128, miR-181a, miR-181b, and miR-181c were down-regulated (Ciafre SA et al. 2005). Chan et al. showed that expression of miR-21 was markedly up-regulated in primary GBMs and glioma cell lines compared with normal brain tissues and non-tumor glial cells. In contrast, miR-124 and miR-137 were found to be significantly decreased in grade III anaplastic gliomas and grade IV GBMs compared with adjacent non-tumor brain tissues. Additionally, miR-128, miR-181a, miR-181b, and miR-451 were found to be down-regulated in glioblastoma tissues and cell lines compared with normal brain tissues (Chan JA et al.2005). These findings suggest that miRNAs are involved in glioma development and progression.

In addition, our previous studies reported an active role of three distinct miRNAs in different features important for glioblastoma tumorigenesis. Firstly, we identified a new molecular mechanism of PTP μ down-regulation in

human glioblastoma by two miRs, miR-221 and -222, that directly target this phosphatase, decreasing glioblastoma cells motility (Quintavalle C et al. 2010). Moreover, we found that miRs-30c and -21 were able to sensitize glioblastoma cells to TRAIL induced apoptosis by targeting, respectively, caspase 3 and Tap63 (Quintavalle C et al. 2012). Finally, we demonstrated that overexpression of miRs-221 and -222 produced an increase of Temozolomide sensitivity, via a reduction of MGMT expression levels (Quintavalle C et al. 2013).

Moreover, in the last years different reports established direct connections between different microRNAs and glioblastoma patients prognosis. Jiang et al. found that expression levels of miR-182 is strongly correlated with histological grades and overall survival times of glioblastoma patients, providing evidence in support of the possibility that up-regulation of miR-182 might play an important role in the progression and aggressiveness of glioblastoma (Jiang L et al. 2012).

It has been shown recently that GBMs display a distinct miRNA expression signature and a number of recent studies have linked these microRNAs alterations to key hallmarks of GBM including proliferation, survival, invasion, angiogenesis, and stem-cell like behavior. Among these studies, some of them reported panels of microRNAs associated with prognosis in glioblastoma. For example, the study from Niyazi et al. resulted of a strong interest. They defined two complementary miRNAs patterns able to predict early death compared to long term survival (split at 450 days) in a significant way ($p < 0.01$), and this prediction was independent of MGMT status. Their findings indicated that complex alterations of the regulatory network involved in tumor gene expression are at least as important as a single disturbance of a single DNA repair enzyme. Among the miRNAs reported as deregulated, there are some with relatively unknown cell cycle function, such as miR-3163, miR-1305, and miR-1260. The most deregulated miRNA resulted let-7a. It was found to be associated with several cancers, such as lung, colon, and glioblastoma, by inhibiting cell growth, inducing apoptosis and decreasing survival. For example, in Hep-2 cells, let-7a induced apoptosis down-regulating RAS and c-MYC oncogenes (Niyazi M et al. 2011). Another interesting study about miRNAs expression pattern and glioblastoma survival was performed recently by Srinivasan et al. They reported a signature of ten miRNAs, identifying three protective miRs (miR-20a, miR106a, and miR-17-5p), and seven risky miRs (miR-31, miR-222, miR148a, miR-221, miR-146b, miR-200b, miR-193a). The protective miRNAs were expressed at higher level in the low risk group and the risky miRNAs were expressed at higher level in the high risk group compared to in the low risk group. The protective and risky nature of these miRNAs was predictive of their oncosuppressive or pro-tumor roles (Srinivasan S et al. 2011). Also Hayes et al. performed an interesting study about glioblastoma, miRs, and survival (Hayes J et al. 2015). They found a biologically relevant 9-microRNAs signature that predicts patients survival in glioblastoma (miR-124a, miR-10b, miR-222, miR-34a, miR-182, miR-148a,

miR-145, miR-370, and miR-9). All these miRNAs had an already demonstrated role in glioblastoma, with the exception of miR-370.

Different studies reported the tumor-suppressive activity of miR-340 in human cancers. This miRNA was first reported to play an oncosuppressive role by Wu et al. They found that miR-340 was able to inhibit breast cancer cell migration and invasion by targeting c-Met, and that loss of its expression was associated with tumor metastasis and poor prognosis (Wu ZS et al. 2011). Another work reported that miR-340 cooperates with miR-137 and miR-124 to regulate colorectal cancer growth via inhibition of Warburg effect (Sun Y et al. 2012). In osteosarcoma, miR-340 was found down-regulated compared to normal tissue, and it was identified ROCK-1 as a target of miR-340. miR-340 overexpression was correlated with ROCK-1 down-regulation, leading to the inhibition of cell proliferation, migration and invasion (Zhou X et al. 2013). Further, it was reported that miR-340 and ROCK-1 expression levels were respectively decreased and increased in pediatric osteosarcoma tissues compared to normal bone tissues. Low miR-340 expression, high ROCK-1 level, and the combined miR-340 down-regulation and ROCK-1 up-regulation may be considered as bad prognostic factor in pediatric osteosarcoma (Cai H et al. 2014). More recently, Poenitzsch et al. demonstrated for the first time the pleiotropic regulation of the RAS-RAF-MAPKs pathway by miR-340 in melanoma, resulting in a strong tumor-suppressive activity (Poenitzsch AM et al. 2014). In addition, Fernandez et al. characterized the tumor-suppressive activity of miR-340 in lung cancer, where it mediated cell growth inhibition and apoptosis activation by an accumulation of p27 (Fernandez S et al. 2014). In fact, they found that miR-340 directly targeted three different post-transcriptional negative regulators of p27 (PUM1, PUM2 and SKP2). Finally, Yamashita et al. reported that miR-340 suppressed the stem-like cell function of glioma-initiating cells (Yamashita D et al. 2015). In particular, they identified miR-340 as a novel miRNA whose expression was significantly lower in glioma initiating cells and in glioma cell lines compared to normal stem cells. Further, they observed that miR-340 suppressed not only glioblastoma initiating cell proliferation and invasion *in vitro*, but also glioblastoma initiating cells tumor formation in nude mice brain. Their findings indicate that miR-340 could acts as a tumor-suppressor in glioma initiating cells, particularly affecting gliomagenesis and extensive tumor invasion. Moreover, they found that PLAT was directly targeted by miR-340 and mediated its effects. In addition to PLAT, miR-340 overexpression in glioma initiating cells decreased Sox2, c-MET, CD44, and DNMT1 expression. c-MET and CD44 regulated cell invasion, while Sox2 and CD44 were crucial for the maintenance of stem phenotype.

Definitely, identification of new biomarkers that play a central role in the progression of GBM will benefit diagnosis and targeted therapies of this disease. In this study, we demonstrated that miR-340 has a strong oncosuppressive role in GBM. We investigated miR-340 expression, functional role and mechanism of action *in vitro* and *in vivo*. Our data, together with that

obtained from “The Cancer Genome Atlas” (TCGA) database, demonstrated that miR-340 expression is significantly lower in GBM samples compared to normal brain. More importantly, data from two different cohorts of GBM patients (61 primary GBM specimens present in our lab and 352 from TCGA) demonstrated that this miRNA is over-expressed in LTS compared to STS. Furthermore, in both these cohorts, statistical analysis revealed that patients with higher expression of miR-340 displayed a significant longer survival and, finally, a better prognosis. Taken together, these data suggest that higher expression of miR-340 is a significant predictor of good prognosis in GBM.

Our *in vitro* functional studies showed that addition of miR-340 in glioblastoma cells determined a significant block of cell cycle that led to an inhibition of cell proliferation, a decrease of anchorage independent cell growth, and an increase in Temozolomide induced apoptosis. Further, we demonstrated that miR-340 is able to directly bind two different regions on N-RAS 3’UTR, thus strongly inhibiting N-RAS expression. The RAS protein family consists of 4 highly homologous enzymes (N-RAS, H-RAS, K-RAS4A and K-RAS4B). These are signal molecules that regulate cell fates by coupling receptor activation to downstream effector pathways that control different cellular responses, such as proliferation, resistance to therapy and survival. Activating mutations of RAS proteins are common in human cancers. In particular, N-RAS activating mutations were found in hematopoietic cancers, colorectal cancer and melanoma. In glioblastoma, N-RAS activation could be due to a direct mutation (5%) or to other alterations, such as amplification, overexpression of growth factor receptor or aberrations in other RAS pathway genes (Knobbe CB et al 2004). Recently, several miRNAs -miR-181d, let-7, miR-143- have been reported to suppress RAS expression and function as tumor-suppressor, suggesting that miRNAs targeting RAS may have an important role in carcinogenesis. In particular, the study of Wang et al. demonstrated the strong oncosuppressive activity of miR-181d in glioma (Wang XF et al. 2012). They found that this miRNA was down-regulated in human glioma tissues, with a concomitant up-regulation of its targets K-RAS and BCL-2. Moreover, Lee et al. demonstrated a strong tumor-suppressive role of let-7a in glioblastoma, by targeting N-RAS (Lee ST et al.2011); also Wang et al. revealed the anti-tumor activity of miR-143 in glioblastoma, via targeting N-RAS and so enhanced Temozolomide induced apoptosis (Wang L et al. 2014).

Our findings indicated that miR-340, targeting N-RAS, decreased the activation of its downstream pathways, mediated by AKT and ERKs kinases. Rescue experiments using dominant positive mutants of AKT and ERKs clearly showed that both these pathways are involved in miR-340 mediated effects in glioblastoma. In summary, we have identified a new link between miR-340 and N-RAS, which is a novel constituent of GBM tumorigenesis.

In animal models, it has been demonstrated that several tumor-suppressor miRNA replacement therapies, using either virus-mediated transduction or non-viral vehicle, had inhibitory effects on tumor growth and

metastasis formation. For example, Esquela-Kerscher et al. reported a reduced tumor growth by viral transfer of let-7 in mouse models of lung cancer (Esquela-Kerscher A et al. 2008). Furthermore, tumor-suppressor miRNA uptake is believed to confer no adverse effects to normal cells, because the pathways regulated by them are already activated by endogenous miRNAs. In the present study we found that the lentiviral mediated overexpression of miR-340 in glioblastoma cells was able to inhibit cell growth in nude mice, thus suggesting its possible use as therapeutic molecule.

In conclusion, we observed for the first time a direct relation between miR-340 expression and survival in GBM, and demonstrated that miR-340 has a powerful oncosuppressive effect in vitro and in vivo, mediated, at least in part, by N-RAS targeting via its downstream pathways of ERKs and AKT kinases. Our findings suggest miR-340 as a novel potential tool for glioblastoma prognosis and diagnosis, as well as a new and useful molecular targeted therapeutic to enhance GBM survival.

6. CONCLUSIONS

Our findings report miR-340 expression as a novel constituent of long-term survivor glioblastoma patients molecular signature. We demonstrated that this miRNA is down-regulated in glioblastoma, but its levels were higher in LTS patients compared to STS. Moreover, we found a direct correlation between miR-340 expression and overall survival of a wide cohort of glioblastoma patients. Based on these data, miR-340 levels may be considered as a favorable prognostic factor in glioblastoma. Further, we provided evidence of a strong tumor-suppressive activity of miR-340 *in vitro*, and found N-RAS as a new target of this miRNA directly involved in the determination of multiple miR-340 effects. miR-340 had an anti-tumoral activity not only in glioblastoma cell lines, but also in tumor xenografts in nude mice. Taken together, these results may represent the pre-clinical validation for considering the use of miR-340 as a novel potential therapeutic tool for glioblastoma treatment.

7. REFERENCES

- Agarwala SS and Kirkwood JM. Temozolomide, a novel alkylating agent with activity in the central nervous system, may improve the treatment of advanced metastatic melanoma. *The oncologist* 2000; 5: 144-151.
- Bartel DP. MicroRNAs: genomics, biogenesis, mechanism, and function. *Cell* 2004; 116: 281-297.
- Bobola MS, Emond MJ, Blank A et al. Apurinic endonuclease activity in adult gliomas and time to tumor progression after alkylating agent-based chemotherapy and after radiotherapy. *Clin Cancer Res* 2004; 10: 7875-7883.
- Bogler O, Huang HJ and Cavenee WK. Loss of wild-type p53 bestows a growth advantage on primary cortical astrocytes and facilitates their in vitro transformation. *Cancer research* 1995; 55: 2746-2751.
- Bottoni A, Zatelli MC, Ferracin M et al. Identification of differentially expressed microRNAs by microarray: a possible role for microRNA genes in pituitary adenomas. *Journal of cellular physiology* 2007; 210: 370-377.
- Brown PD, Krishnan S, Sarkaria JN et al. Phase I/II trial of erlotinib and temozolomide with radiation therapy in the treatment of newly diagnosed glioblastoma multiforme: North Central Cancer Treatment Group Study N0177. *J Clin Oncol* 2008; 26: 5603-5609.
- Cai H, Lin L, Cai H, Tang M and Wang Z. Combined microRNA-340 and ROCK1 mRNA profiling predicts tumor progression and prognosis in pediatric osteosarcoma. *International journal of molecular sciences* 2014; 15: 560-573.
- Calin GA, Dumitru CD, Shimizu M et al. Frequent deletions and down-regulation of micro- RNA genes miR15 and miR16 at 13q14 in chronic lymphocytic leukemia. *Proceedings of the National Academy of Sciences of the United States of America* 2002; 99: 15524-15529.
- Calin GA, Ferracin M, Cimmino A et al. A MicroRNA signature associated with prognosis and progression in chronic lymphocytic leukemia. *The New England journal of medicine* 2005; 353: 1793-1801.
- Cancer Genome Atlas Research Network. Comprehensive genomic characterization defines human glioblastoma genes and core pathways. *Nature* 2008; 455: 1061-1068.

- Chan JA, Krichevsky AM and Kosik KS. MicroRNA-21 is an antiapoptotic factor in human glioblastoma cells. *Cancer research* 2005; 65: 6029-6033.
- Chen CZ, Li L, Lodish HF and Bartel DP. MicroRNAs modulate hematopoietic lineage differentiation. *Science*, New York, NY 2004; 303: 83-86.
- Chen JF, Mandel EM, Thomson JM et al. The role of microRNA-1 and microRNA-133 in skeletal muscle proliferation and differentiation. *Nature genetics* 2006; 38: 228-233.
- Ciafre SA, Galardi S, Mangiola A et al. Extensive modulation of a set of microRNAs in primary glioblastoma. *Biochemical and biophysical research communications* 2005; 334: 1351-1358.
- Costinean S, Zaneni N, Pekarsky Y et al. Pre-B cell proliferation and lymphoblastic leukemia/high-grade lymphoma in E(mu)-miR155 transgenic mice. *Proceedings of the National Academy of Sciences of the United States of America* 2006; 103: 7024-7029.
- Dear TN and Kefford RF. Molecular oncogenetics of metastasis. *Molecular aspects of medicine* 1990; 11: 243-324.
- Dietrich J, Diamond EL and Kesari S. Glioma stem cell signaling: therapeutic opportunities and challenges. *Expert review of anticancer therapy* 2010; 10: 709-722.
- Dietrich J, Imitola J and Kesari S. Mechanisms of Disease: the role of stem cells in the biology and treatment of gliomas. *Nature clinical practice* 2008; 5: 393-404.
- Dolecek TA, Propp JM, Stroup NE and Kruchko C. CBTRUS statistical report: primary brain and central nervous system tumors diagnosed in the United States in 2005-2009. *Neuro-oncology* 2012; 14 Suppl 5: v1-49.
- Downward J. Targeting RAS signalling pathways in cancer therapy. *Nature reviews* 2003; 3: 11-22.
- Dresemann G, Weller M, Rosenthal MA et al. Imatinib in combination with hydroxyurea versus hydroxyurea alone as oral therapy in patients with progressive pretreated glioblastoma resistant to standard dose temozolomide. *Journal of neuro-oncology* 2010; 96: 393-402.
- Eis PS, Tam W, Sun L et al. Accumulation of miR-155 and BIC RNA in human B cell lymphomas. *Proceedings of the National Academy of Sciences of the United States of America* 2005; 102: 3627-3632.

Engelman JA, Luo J and Cantley LC. The evolution of phosphatidylinositol 3-kinases as regulators of growth and metabolism. *Nat Rev Genet* 2006; 7: 606-619.

Engelman JA. Targeting PI3K signalling in cancer: opportunities, challenges and limitations. *Nature reviews* 2009; 9: 550-562.

Esau C, Kang X, Peralta E et al. MicroRNA-143 regulates adipocyte differentiation. *The Journal of biological chemistry* 2004; 279: 52361-52365.

Esquela-Kerscher A, Trang P, Wiggins JF et al. The let-7 microRNA reduces tumor growth in mouse models of lung cancer. *Cell cycle (Georgetown, Tex)* 2008; 7: 759-764.

Esteller M, Risques RA, Toyota M et al. Promoter hypermethylation of the DNA repair gene O(6)-methylguanine-DNA methyltransferase is associated with the presence of G:C to A:T transition mutations in p53 in human colorectal tumorigenesis. *Cancer research* 2001; 61: 4689-4692.

Esteller M, Toyota M, Sanchez-Cespedes M et al. Inactivation of the DNA repair gene O6-methylguanine-DNA methyltransferase by promoter hypermethylation is associated with G to A mutations in K-ras in colorectal tumorigenesis. *Cancer research* 2000; 60: 2368-2371.

Fernandez S, Risolino M, Mandia N et al. miR-340 inhibits tumor cell proliferation and induces apoptosis by targeting multiple negative regulators of p27 in non-small cell lung cancer. *Oncogene* 2014; 0.

Friedman HS, Keir S, Pegg AE et al. O6-benzylguanine-mediated enhancement of chemotherapy. *Molecular cancer therapeutics* 2002; 1: 943-948.

Galanis E, Buckner JC, Maurer MJ et al. Phase II trial of temsirolimus (CCI-779) in recurrent glioblastoma multiforme: a North Central Cancer Treatment Group Study. *J ClinOncol* 2005; 23: 5294-5304.

Giese A, Bjerkvig R, Berens ME and Westphal M. Cost of migration: invasion of malignant gliomas and implications for treatment. *J ClinOncol* 2003; 21: 1624-1636.

Gomez-Manzano C, Fueyo J, Jiang H et al. Mechanisms underlying PTEN regulation of vascular endothelial growth factor and angiogenesis. *Annals of neurology* 2003; 53: 109-117.

Gregory RI and Shiekhattar R. MicroRNA biogenesis and cancer. *Cancer research* 2005; 65: 3509-3512.

Gressens P. Mechanisms and disturbances of neuronal migration. *Pediatric research* 2000; 48: 725-730.

- Gu J, Liu Y, Kyritsis AP and Bondy ML. Molecular epidemiology of primary brain tumors. *Neurotherapeutics* 2009; 6: 427-435.
- Guan Y, Mizoguchi M, Yoshimoto K et al. MiRNA-196 is upregulated in glioblastoma but not in anaplastic astrocytoma and has prognostic significance. *Clin Cancer Res* 2010; 16: 4289-4297.
- Hanahan D and Folkman J. Patterns and emerging mechanisms of the angiogenic switch during tumorigenesis. *Cell* 1996; 86: 353-364.
- Hayes J, Thygesen H, Tumilson C et al. Prediction of clinical outcome in glioblastoma using a biologically relevant nine-microRNA signature. *Molecular oncology* 2015; 9: 704-714.
- He L, Thomson JM, Hemann MT et al. A microRNA polycistron as a potential human oncogene. *Nature* 2005; 435: 828-833.
- Hegi ME, Diserens AC, Gorlia T et al. MGMT gene silencing and benefit from temozolomide in glioblastoma. *The New England journal of medicine* 2005; 352: 997-1003.
- Hermansen SK and Kristensen BW. MicroRNA biomarkers in glioblastoma. *Journal of neuro-oncology* 2013; 114: 13-23.
- Hottinger AF and Khakoo Y. Update on the management of familial central nervous system tumor syndromes. *Current neurology and neuroscience reports* 2007; 7: 200-207.
- Hovinga KE, Shimizu F, Wang R et al. Inhibition of notch signaling in glioblastoma targets cancer stem cells via an endothelial cell intermediate. *Stem cells (Dayton, Ohio)* 2010; 28: 1019-1029.
- Hu B, Guo P, Bar-Joseph I et al. Neuropilin-1 promotes human glioma progression through potentiating the activity of the HGF/SF autocrine pathway. *Oncogene* 2007; 26: 5577-5586.
- Huang HS, Nagane M, Klingbeil CK et al. The enhanced tumorigenic activity of a mutant epidermal growth factor receptor common in human cancers is mediated by threshold levels of constitutive tyrosine phosphorylation and unattenuated signaling. *The Journal of biological chemistry* 1997; 272: 2927-2935.
- Huang YT, Hsu T, Kelsey KT and Lin CL. Integrative analysis of micro-RNA, gene expression, and survival of glioblastoma multiforme. *Genetic epidemiology* 2014; 39: 134-143.

Huse JT and Holland EC. Targeting brain cancer: advances in the molecular pathology of malignant glioma and medulloblastoma. *Nature reviews* 2010; 10: 319-331.

Jain RK, di Tomaso E, Duda DG, Loeffler JS, Sorensen AG and Batchelor TT. Angiogenesis in brain tumours. *Nat Rev Neurosci* 2007; 8: 610-622.

Jain RK. Normalization of tumor vasculature: an emerging concept in antiangiogenic therapy. *Science*, New York, NY 2005; 307: 58-62.

Jiang L, Mao P, Song L et al. miR-182 as a prognostic marker for glioma progression and patient survival. *The American journal of pathology* 2012; 177: 29-38.

Johnson SM, Grosshans H, Shingara J et al. RAS is regulated by the let-7 microRNA family. *Cell* 2005; 120: 635-647.

Kerbel RS. Tumor angiogenesis. *The New England journal of medicine* 2008; 358: 2039-2049.

Kluiver J, Poppema S, de Jong D et al. BIC and miR-155 are highly expressed in Hodgkin, primary mediastinal and diffuse large B cell lymphomas. *The Journal of pathology* 2005; 207: 243-249.

Knobbe CB, Reifenberger J and Reifenberger G. Mutation analysis of the Ras pathway genes NRAS, HRAS, KRAS and BRAF in glioblastomas. *Actaneuropathologica* 2004; 108: 467-470.

Kreisl TN, Lassman AB, Mischel PS et al. A pilot study of everolimus and gefitinib in the treatment of recurrent glioblastoma (GBM). *Journal of neuro-oncology* 2009; 92: 99-105.

Krex D, Klink B, Hartmann C et al. Long-term survival with glioblastoma multiforme. *Brain* 2007; 130: 2596-2606.

Kwak PB, Iwasaki S and Tomari Y. The microRNA pathway and cancer. *Cancer science* 2010; 101: 2309-2315.

Lakomy R, Sana J, Hankeova S et al. MiR-195, miR-196b, miR-181c, miR-21 expression levels and O-6-methylguanine-DNA methyltransferase methylation status are associated with clinical outcome in glioblastoma patients. *Cancer science* 2011; 102: 2186-2190.

Lassman AB, Rossi MR, Raizer JJ et al. Molecular study of malignant gliomas treated with epidermal growth factor receptor inhibitors: tissue analysis from North American Brain Tumor Consortium Trials 01-03 and 00-01. *Clin Cancer Res* 2005; 11: 7841-7850.

- Lee ST, Chu K, Oh HJ et al. Let-7 microRNA inhibits the proliferation of human glioblastoma cells. *Journal of neuro-oncology* 2011; 102: 19-24.
- Lee Y, Jeon K, Lee JT, Kim S and Kim VN. MicroRNA maturation: stepwise processing and subcellular localization. *The EMBO journal* 2002; 21: 4663-4670.
- Lewis BP, Shih IH, Jones-Rhoades MW, Bartel DP and Burge CB. Prediction of mammalian microRNA targets. *Cell* 2003; 115: 787-798.
- Liu G, Yuan X, Zeng Z et al. Analysis of gene expression and chemoresistance of CD133+ cancer stem cells in glioblastoma. *Molecular cancer* 2006; 5: 67.
- Liu L and Gerson SL. Targeted modulation of MGMT: clinical implications. *Clin Cancer Res* 2006; 12: 328-331.
- Louis DN, Ohgaki H, Wiestler OD et al. The 2007 WHO classification of tumours of the central nervous system. *Actaneuropathologica* 2007; 114: 97-109.
- Mariani L, McDonough WS, Hoelzinger DB et al. Identification and validation of P311 as a glioblastoma invasion gene using laser capture microdissection. *Cancer research* 2001; 61: 4190-4196.
- Metzler M, Wilda M, Busch K, Viehmann S and Borkhardt A. High expression of precursor microRNA-155/BIC RNA in children with Burkitt lymphoma. *Genes, chromosomes & cancer* 2004; 39: 167-169.
- Michaud K, Solomon DA, Oermann E et al. Pharmacologic inhibition of cyclin-dependent kinases 4 and 6 arrests the growth of glioblastoma multiforme intracranial xenografts. *Cancer research* 2010; 70: 3228-3238.
- Network. CGAR. Cancer Genome Atlas Research Network. Comprehensive genomic characterization defines human glioblastoma genes and core pathways. *Nature* 2008; 455: 1061-1068.
- Neyns B, Sadones J, Joosens E et al. Stratified phase II trial of cetuximab in patients with recurrent high-grade glioma. *Ann Oncol* 2009; 20: 1596-1603.
- Niyazi M, Zehentmayr F, Niemoller OM et al. MiRNA expression patterns predict survival in glioblastoma. *Radiation oncology (London, England)* 2011; 6: 153.
- Norden AD, Drappatz J and Wen PY. Antiangiogenic therapies for high-grade glioma. *Nat Rev Neurol* 2009; 5: 610-620.
- Ohgaki H and Kleihues P. Genetic alterations and signaling pathways in the evolution of gliomas. *Cancer science* 2009; 100: 2235-2241.

- Ohgaki H and Kleihues P. Population-based studies on incidence, survival rates, and genetic alterations in astrocytic and oligodendroglial gliomas. *Journal of neuropathology and experimental neurology* 2005; 64: 479-489.
- Oliner J, Min H, Leal J et al. Suppression of angiogenesis and tumor growth by selective inhibition of angiopoietin-2. *Cancer cell* 2004; 6: 507-516.
- Pallante P, Visone R, Ferracin M et al. MicroRNA deregulation in human thyroid papillary carcinomas. *Endocrine-related cancer* 2006; 13: 497-508.
- Petrocca F, Vecchione A and Croce CM. Emerging role of miR-106b-25/miR-17-92 clusters in the control of transforming growth factor beta signaling. *Cancer research* 2008; 68: 8191-8194.
- Plowman J, Waud WR, Koutsoukos AD, Rubinstein LV, Moore TD and Grever MR. Preclinical antitumor activity of temozolomide in mice: efficacy against human brain tumor xenografts and synergism with 1,3-bis(2-chloroethyl)-1-nitrosourea. *Cancer research* 1994; 54: 3793-3799.
- Poenitzsch Strong AM, Setaluri V and Spiegelman VS. MicroRNA-340 as a modulator of RAS-RAF-MAPK signaling in melanoma. *Archives of biochemistry and biophysics* 2014; 563: 118-124.
- Pope WB, Lai A, Nghiemphu P, Mischel P and Cloughesy TF. MRI in patients with high-grade gliomas treated with bevacizumab and chemotherapy. *Neurology* 2006; 66: 1258-1260.
- Porter KR, McCarthy BJ, Freels S, Kim Y and Davis FG. Prevalence estimates for primary brain tumors in the United States by age, gender, behavior, and histology. *Neuro-oncology* 2010; 12: 520-527.
- Poulsen HS, Grunnet K, Sorensen M et al. Bevacizumab plus irinotecan in the treatment patients with progressive recurrent malignant brain tumours. *Acta oncologica (Stockholm, Sweden)* 2009; 48: 52-58.
- Quintavalle C, Donnarumma E, Iaboni M et al. Effect of miR-21 and miR-30b/c on TRAIL-induced apoptosis in glioma cells. *Oncogene* 2012; 32: 4001-4008.
- Quintavalle C, Garofalo M, Zanca C et al. miR-221/222 overexpression in human glioblastoma increases invasiveness by targeting the protein phosphate PTPmu. *Oncogene* 2010; 31: 858-868.
- Quintavalle C, Mangani D, Roscigno G et al. MiR-221/222 target the DNA methyltransferase MGMT in glioma cells. *PloS one* 2013; 8: e74466.
- Rajaraman P, Melin BS, Wang Z et al. Genome-wide association study of glioma and meta-analysis. *Human genetics* 2012; 131: 1877-1888.

Reardon DA, Dresemann G, Taillibert S et al. Multicentre phase II studies evaluating imatinib plus hydroxyurea in patients with progressive glioblastoma. *British journal of cancer* 2009; 101: 1995-2004.

Reifenberger G, Liu L, Ichimura K, Schmidt EE and Collins VP. Amplification and overexpression of the MDM2 gene in a subset of human malignant gliomas without p53 mutations. *Cancer research* 1993; 53: 2736-2739.

Reifenberger G, Weber RG, Riehm V et al. Molecular characterization of long-term survivors of glioblastoma using genome- and transcriptome-wide profiling. *International journal of cancer* 2014; 135: 1822-1831.

Schratt GM, Tuebing F, Nigh EA et al. A brain-specific microRNA regulates dendritic spine development. *Nature* 2006; 439: 283-289.

Schubert S, Shannon K and Bollag G. Hyperactive Ras in developmental disorders and cancer. *Nature reviews* 2007; 7: 295-308.

Sekulic A, Migden MR, Oro AE et al. Efficacy and safety of vismodegib in advanced basal-cell carcinoma. *The New England journal of medicine* 2012; 366: 2171-2179.

Shen Q, Goderie SK, Jin L et al. Endothelial cells stimulate self-renewal and expand neurogenesis of neural stem cells. *Science (New York, NY)* 2004; 304: 1338-1340.

Shete S, Hosking FJ, Robertson LB et al. Genome-wide association study identifies five susceptibility loci for glioma. *Nature genetics* 2009; 41: 899-904.

Sidransky D, Mikkelsen T, Schwechheimer K, Rosenblum ML, Cavanaugh W and Vogelstein B. Clonal expansion of p53 mutant cells is associated with brain tumour progression. *Nature* 1992; 355: 846-847.

Snuderl M, Fazlollahi L, Le LP et al. Mosaic amplification of multiple receptor tyrosine kinase genes in glioblastoma. *Cancer cell* 2011; 20: 810-817.

Srinivasan S, Patric IR and Somasundaram K. A ten-microRNA expression signature predicts survival in glioblastoma. *PloS one* 2011; 6: e17438.

Stommel JM, Kimmelman AC, Ying H et al. Coactivation of receptor tyrosine kinases affects the response of tumor cells to targeted therapies. *Science (New York, NY)* 2007; 318: 287-290.

Stott FJ, Bates S, James MC et al. The alternative product from the human CDKN2A locus, p14(ARF), participates in a regulatory feedback loop with p53 and MDM2. *The EMBO journal* 1998; 17: 5001-5014.

Stupp R, Hegi ME, Mason WP et al. Effects of radiotherapy with concomitant and adjuvant temozolomide versus radiotherapy alone on survival in glioblastoma in a randomised phase III study: 5-year analysis of the EORTC-NCIC trial. *The Lancet* 2009; 10: 459-466.

Stupp R, Mason WP, van den Bent MJ et al. Radiotherapy plus concomitant and adjuvant temozolomide for glioblastoma. *The New England journal of medicine* 2005; 352: 987-996.

Sun Y, Zhao X, Zhou Y and Hu Y. miR-124, miR-137 and miR-340 regulate colorectal cancer growth via inhibition of the Warburg effect. *Oncology reports* 2012; 28: 1346-1352.

Szerlip NJ, Pedraza A, Chakravarty D et al. Intratumoral heterogeneity of receptor tyrosine kinases EGFR and PDGFRA amplification in glioblastoma defines subpopulations with distinct growth factor response. *Proceedings of the National Academy of Sciences of the United States of America* 2012; 109: 3041-3046.

Tavazoie SF, Alarcon C, Oskarsson T et al. Endogenous human microRNAs that suppress breast cancer metastasis. *Nature* 2008; 451: 147-152.

Tran B and Rosenthal MA. Survival comparison between glioblastoma multiforme and other incurable cancers. *J ClinNeurosci* 2010; 17: 417-421.

Van den Bent MJ, Brandes AA, Rampling R et al. Randomized phase II trial of erlotinib versus temozolomide or carmustine in recurrent glioblastoma: EORTC brain tumor group study 26034. *J ClinOncol* 2009; 27: 1268-1274.

Vescovi AL, Galli R and Reynolds BA. Brain tumour stem cells. *Nature reviews* 2006; 6: 425-436.

Volinia S, Calin GA, Liu CG et al. A microRNA expression signature of human solid tumors defines cancer gene targets. *Proceedings of the National Academy of Sciences of the United States of America* 2006; 103: 2257-2261.

Vousden KH and Lane DP. p53 in health and disease. *Nat Rev Mol Cell Biol* 2007; 8: 275-283.

Wang L, Shi ZM, Jiang CF et al. MiR-143 acts as a tumor suppressor by targeting N-RAS and enhances temozolomide-induced apoptosis in glioma. *Oncotarget* 2014; 5: 5416-5427.

Wang XF, Shi ZM, Wang XR et al. MiR-181d acts as a tumor suppressor in glioma by targeting K-ras and Bcl-2. *Journal of cancer research and clinical oncology* 2012; 138: 573-584.

Weber F, Teresi RE, Broelsch CE, Frilling A and Eng C. A limited set of human MicroRNA is deregulated in follicular thyroid carcinoma. *The Journal of clinical endocrinology and metabolism* 2006; 91: 3584-3591.

Wen PY, Yung WK, Lamborn KR et al. Phase I/II study of imatinibmesylate for recurrent malignant gliomas: North American Brain Tumor Consortium Study 99-08. *Clin Cancer Res* 2006; 12: 4899-4907.

Wu Z, Sun L, Wang H et al. MiR-328 expression is decreased in high-grade gliomas and is associated with worse survival in primary glioblastoma. *PloS one* 2012; 7: e47270.

Wu ZS, Wu Q, Wang CQ et al. miR-340 inhibition of breast cancer cell migration and invasion through targeting of oncoprotein c-Met. *Cancer* 2011; 117: 2842-2852.

Yamashita D, Kondo T, Ohue S et al. miR340 Suppresses the Stem-like Cell Function of Glioma-Initiating Cells by Targeting Tissue Plasminogen Activator. *Cancer research* 2015; 75: 1123-1133.

Yoshino Y, Aoyagi M, Tamaki M, Duan L, Morimoto T and Ohno K. Activation of p38 MAPK and/or JNK contributes to increased levels of VEGF secretion in human malignant glioma cells. *International journal of oncology* 2006; 29: 981-987.

Zhi F, Chen X, Wang S et al. The use of hsa-miR-21, hsa-miR-181b and hsa-miR-106a as prognostic indicators of astrocytoma. *Eur J Cancer* 2010; 46: 1640-1649.

Zhou X, Wei M and Wang W. MicroRNA-340 suppresses osteosarcoma tumor growth and metastasis by directly targeting ROCK1. *Biochemical and biophysical research communications* 2013; 437: 653-658.

LIST OF PUBLICATIONS

Quintavalle C, Mangani D, Roscigno G, Romano G, Diaz-Lagares A, Iaboni M, Donnarumma E, **Fiore D**, De Marinis P, Soini Y, Esteller M, Condorelli G. MiR-221/222 target the DNA methyltransferase MGMT in glioma cells. PloSone 2013; 8: e74466.

Quintavalle C*, **Fiore D***, De Micco F, Visconti G, Focaccio A, Golia B, Riciardelli B, Donnarumma E, Bianco A, Zabatta MA, Troncone G, Colombo A, Briguori C, Condorelli G. Impact of a high loading dose of atorvastatin on contrast-induced acute kidney injury. Circulation 2012; 126: 3008-3016.

***Co-first authors**

Quintavalle C, Donnarumma E, Iaboni M, Roscigno G, Garofalo M, Romano G, **Fiore D**, De Marinis P, Croce CM, Condorelli G. Effect of miR-21 and miR-30b/c on TRAIL-induced apoptosis in glioma cells. Oncogene 2012; 32: 4001-4008.

Other publications:

Briguori C, Donnarumma E, Quintavalle C, **Fiore D**, Condorelli G. Contrast-induced acute kidney injury: potential new strategies. Curr Opin Nephrol Hypertens. 2015 Jan 19. [Epub ahead of print].

Quintavalle C, Donnarumma E, **Fiore D**, Briguori C, Condorelli G. Therapeutic strategies to prevent contrast-induced acute kidney injury. Curr Opin Cardiol. 2013 Nov;28(6):676-82.

Quintavalle C, Brenca M, De Micco F, **Fiore D**, Romano S, Romano MF, Apone F, Bianco A, Zabatta MA, Troncone G, Briguori C, Condorelli G. (2011). In vivo and in vitro assessment of pathways involved in contrast media-induced renal cells apoptosis.. CELL DEATH & DISEASE, vol. 2, ISSN: 2041-4889, doi: 10.1038/cddis.2011.38

miR-221/222 Target the DNA Methyltransferase MGMT in Glioma Cells

Cristina Quintavalle^{1,2}*, Davide Mangani¹*, Giuseppina Roscigno^{1,2}, Giulia Romano³, Angel Diaz-Lagares⁴, Margherita Iaboni¹, Elvira Donnarumma³, Danilo Fiore¹, Pasqualino De Marinis⁵, Ylermi Soini⁶, Manel Esteller⁴, Gerolama Condorelli^{1,2*}

1 Department of Molecular Medicine and Medical Biotechnology, "Federico II" University of Naples, Naples, Italy, **2** IEOS, CNR, Naples, Italy, **3** Fondazione IRCCS SDN, Naples, Italy, **4** Epigenetic and Cancer Biology Program (PEBC) IDIBELL, Hospital Duran i Reynals, Barcelona, Spain, **5** Ospedale Cardarelli, Naples, Italy, **6** Department of Pathology and Forensic Medicine, Institute of Clinical Medicine, Pathology and Forensic Medicine, School of Medicine, Cancer Center of Eastern Finland, University of Eastern Finland, Kuopio, Finland

Abstract

Glioblastoma multiforme (GBM) is one of the most deadly types of cancer. To date, the best clinical approach for treatment is based on administration of temozolomide (TMZ) in combination with radiotherapy. Much evidence suggests that the intracellular level of the alkylating enzyme O⁶-methylguanine–DNA methyltransferase (MGMT) impacts response to TMZ in GBM patients. MGMT expression is regulated by the methylation of its promoter. However, evidence indicates that this is not the only regulatory mechanism present. Here, we describe a hitherto unknown microRNA-mediated mechanism of MGMT expression regulation. We show that miR-221 and miR-222 are upregulated in GBM patients and that these paralogues target MGMT mRNA, inducing greater TMZ-mediated cell death. However, miR-221/miR-222 also increase DNA damage and, thus, chromosomal rearrangements. Indeed, miR-221 overexpression in glioma cells led to an increase in markers of DNA damage, an effect rescued by re-expression of MGMT. Thus, chronic miR-221/222-mediated MGMT downregulation may render cells unable to repair genetic damage. This, associated also to miR-221/222 oncogenic potential, may poor GBM prognosis.

Citation: Quintavalle C, Mangani D, Roscigno G, Romano G, Diaz-Lagares A, et al. (2013) miR-221/222 Target the DNA Methyltransferase MGMT in Glioma Cells. PLoS ONE 8(9): e74466. doi:10.1371/journal.pone.0074466

Editor: Russell O. Pieper, University of California-San Francisco, United States of America

Received: June 10, 2013; **Accepted:** July 31, 2013; **Published:** September 19, 2013

Copyright: © 2013 Quintavalle et al. This is an open-access article distributed under the terms of the Creative Commons Attribution License, which permits unrestricted use, distribution, and reproduction in any medium, provided the original author and source are credited.

Funding: This work was partially supported by funds from Associazione Italiana Ricerca sul Cancro, to GC (grant n.ro 10620), MERIT (RBNE08E8CZ_002) to GC, POR Campania FSE 2007-2013, Project CRÈME to GC. CQ and MI was supported by the "Federazione Italiana Ricerca sul Cancro" Post-Doctoral Research Fellowship. GR was supported by a MERIT project Fellowship. ADL was supported by the Angeles Alvaríño-2009 postdoctoral fellowship from the Xunta de Galicia and European Social Fund and at present is the recipient of a Sara Borrell postdoctoral contract (CD12/00738) from the Instituto de Salud Carlos III at the Spanish Ministry of Economy and Competitiveness. The funders had no role in study design, data collection and analysis, decision to publish, or preparation of the manuscript.

Competing interests: The authors have declared that no competing interests exist.

* E-mail: gecondor@unina.it

© These authors contributed equally to this work.

Introduction

Glioblastoma multiforme (GBM) is the most common and deadly primary tumor of the central nervous system. Despite several therapeutic advances, the prognosis for GBM remains poor, with a median survival lower than 15 months [1,2]. Currently, first-line therapy for GBM comprises surgery with the maximum feasible resection, followed by a combination of radiotherapy and treatment with the alkylating agent temozolomide (TMZ), also referred to by its brand name Temodal [3,4,5]. TMZ is a methylating agent that modifies DNA in several positions, one of them being O⁶-methylguanine MeG (O⁶MeG) [6]. If the methyl group is not removed before cell division, this modified guanine preferentially pairs with thymine

during DNA replication, triggering the DNA mismatch repair (MMR) pathway, DNA double-strand breaks, and, therefore, the apoptotic pathway [7,8]. O⁶-methylguanine–methyltransferase (MGMT) is a suicide cellular DNA repair enzyme ubiquitously expressed in normal human tissues. MGMT does not act as a part of a repair complex but works alone [9]. To neutralize the cytotoxic effects of alkylating agents, such as TMZ, it rapidly reverses alkylation at the O⁶ position of guanine, transferring the alkyl group to an internal cysteine residue in its active site. In this form, the enzyme is inactive and, thus, requires *de novo* protein synthesis. In tumors, high levels of MGMT activity are associated with resistance to alkylating agents [10]. In contrast, epigenetic silencing of MGMT gene expression by promoter methylation

results in sensitization to therapy [11,12]. However, some studies have reported that MGMT promoter methylation does not always correlate with MGMT expression and with response to therapy [13,14]. Therefore, the existence of other mechanisms of MGMT regulation should be postulated.

MicroRNAs (miRs) are small regulatory molecules that have a role in cancer progression and in tumor therapy response [15,16]. By negatively regulating the expression of their targets, miRs can act as tumor suppressors or oncogenes [17]. miRs may also regulate DNA damage response and DNA repair, interfering with the response to chemotherapy or radiotherapy [18]. Several studies have indicated that the modulation of miR expression levels is a possible therapeutic strategy for cancer.

The paralogues miR-221 and miR-222 have frequently been found to be dysregulated in glioblastoma and astrocytomas [19,20,21,22]. Their upregulation increases glioma cell proliferation, motility, and *in vivo* growth in mouse models. miR-221/222 have also been shown to be implicated in cellular sensitivity to tumor necrosis factor-related apoptosis-inducing ligand (TRAIL)-treatment [23,24,25]. In this manuscript, we provide evidence that miR-221 and miR-222 regulate MGMT expression levels in glioblastoma, increasing the response to TMZ, but due to their oncogenic potential, affect overall patient survival negatively.

Materials and Methods

Cell culture and transfection

U87MG, T98G, LN428, LN308, A172, and HEK-293 cells were grown in DMEM. LN229 were grown in Advanced DMEM (Gibco, Life technologies, Milan, Italy). T98G, U87MG, and LN229 were from ATCC (LG Standards, Milan Italy); LN428, LN308, and A172 were kindly donated by Frank Furnari (La Jolla University). Media were supplemented with 10% heat-inactivated fetal bovine serum (FBS) -5% FBS for LN229 -2 mM L-glutamine, and 100 U/ml penicillin/streptomycin. All media and supplements were from Sigma Aldrich (Milan, Italy). For overexpression of miRs, cells at 50% confluency were transfected using Oligofectamine (Invitrogen, Milan, Italy) and 100nM pre-miR-221 or pre-miR-222, a scrambled miR or anti-miR-221/222 (Applied Biosystems, Milan, Italy). For overexpression of MGMT, cells were transfected using Lipofectamine and Plus Reagent with 4 µg of MGMT cDNA (Origene, Rockville MD USA). Temozolomide was purchased from Sigma Aldrich (Milan, Italy).

Human Glioma samples

A total of 34 formalin-fixed, paraffin-embedded (FFPE) tissue samples were collected from the archives of the Department of Pathology, University Hospital of Kuopio, Finland. Permission to use the material was obtained from the National Supervisory Authority for Welfare and Health of Finland, and the study was accepted by the ethical committee of the Northern Savo Hospital District, Kuopio, Finland.

Primary cell cultures

Glioblastoma specimens were obtained as previously described [19]. Samples were mechanically disaggregated, and the lysates grown in DMEM-F12 medium supplemented with 10% FBS, 1% penicillin streptomycin, and 20 ng/ml epidermal growth factor (EGF; Sigma-Aldrich, Milan, Italy). To determine the glial origin of the isolated cells, we stained the cultures for glial fibrillary acidic protein (GFAP), a protein found in glial cells.

Protein isolation and Western blotting

Cells were washed twice in ice-cold PBS and lysed in JS buffer (50 mM HEPES pH 7.5 containing 150 mM NaCl, 1% Glycerol, 1% Triton X100, 1.5mM MgCl₂, 5mM EGTA, 1 mM Na₃VO₄, and 1X protease inhibitor cocktail). Protein concentration was determined by the Bradford assay (BioRad, Milan, Italy) using bovine serum albumin (BSA) as the standard, and equal amounts of proteins were analyzed by SDS-PAGE (12.5% acrylamide). Gels were electroblotted onto nitrocellulose membranes (GE Healthcare, Milan, Italy). For immunoblot experiments, membranes were blocked for 1 hr with 5% non-fat dry milk in Tris-buffered saline (TBS) containing 0.1% Tween-20, and incubated at 4°C overnight with primary antibody. Detection was performed by peroxidase-conjugated secondary antibodies using the enhanced chemiluminescence system (GE Healthcare, Milan, Italy). Primary antibodies used were: anti-β-actin from Sigma-Aldrich (Milan Italy); anti-caspase-3 and anti-PARP from Santa Cruz Biotechnologies (Santa Cruz, CA, USA), anti-γH2AX from Millipore (Milan, Italy), anti-p53, p^{ser15} p53, and phosphorylated-ATM from Cell Signaling Technology (Milan, Italy).

RNA extraction and Real-Time PCR

Cell culture: Total RNA (microRNA and mRNA) were extracted using Trizol (Invitrogen, Milan, Italy) according to the manufacturer's protocol.

Tissue specimens

Total RNA (miRNA and mRNA) from FFPE tissue specimens was extracted using RecoverAll Total Nucleic Acid isolation Kit (Ambion, Life Technologies, Milan, Italy) according to the manufacturer's protocol. Reverse transcription of total miRNA was performed starting from equal amounts of total RNA/sample (1µg) using miScript reverse Transcription Kit (Qiagen, Milan, Italy), and with SuperScript® III Reverse Transcriptase (Invitrogen, Milan, Italy) for mRNA. Quantitative analysis of MGMT, β-actin (as an internal reference), miR-221, miR-222, and RNU5A (as an internal reference) were performed by RealTime PCR using specific primers (Qiagen, Milan, Italy), miScript SYBR Green PCR Kit (Qiagen, Milan, Italy), and iQ™ SYBR Green Supermix (Bio-Rad, Milan, Italy), respectively. The reaction for detection of mRNAs was performed as follows: 95°C for 15', 40 cycles of 94°C for 15", 60°C for 30", and 72°C for 30". The reaction for detection of miRNAs was performed as follows: 95°C for 15', 40 cycles of 94°C for 15", 55°C for 30", and 70°C for 30". All reactions were run in triplicate. The threshold cycle (CT) is defined as the fractional cycle number

at which the fluorescence passes the fixed threshold. For relative quantization, the $2^{-\Delta\Delta CT}$ method was used as previously described [26]. Experiments were carried out in triplicate for each data point, and data analysis was performed by using a Bio-Rad software (Bio-Rad, Milan, Italy).

Luciferase assay

The 3' UTR of the human MGMT gene was PCR amplified using the following primers: MGMT-Fw: 5'TCTAGAGTATGTGCAGTAGGATGGATG3'; MGMT-Rv: 5'TCCAGAGCTACAGTTTCCCTTCC3', and cloned downstream of the Renilla luciferase stop codon in pGL3 control vector (Promega, Milan, Italy). A deletion was introduced into the miRNA-binding sites with the QuikChange Mutagenesis Kit (Stratagene, La Jolla CA USA) using the following primers: MGMT-mut Fw: 5'CTATATCCAAAAGGGAAACCTGTAGCTCTTGC 3'. MGMT-mut Rv: 5'-GCAGAGCTACACGTTTCCCTTTGGATATAG 3'. HEK-293 cells were co-transfected with 1.2 µg of plasmid and 400 µg of a Renilla luciferase expression construct, pRL-TK (Promega, Milan, Italy), with Lipofectamine 2000 (Invitrogen, Milan, Italy). Cells were harvested 24 hrs post-transfection and assayed with Dual Luciferase Assay (Promega, Milan, Italy) according to the manufacturer's instructions. Three independent experiments were performed in triplicate.

Cell death quantification

Cell viability was evaluated with the CellTiter 96 Aqueous One Solution Cell Proliferation Assay (Promega, Milan, Italy) according to the manufacturer's protocol. Metabolically active cells were detected by adding 20 µL of MTS to each well. After 2 hrs of incubation, the plates were analyzed in a Multilabel Counter (BioTek, Milan, Italy). For caspase-3 inhibition experiments, ZVAD-Fmk was purchased from Calbiochem.

Comet assay

Alkaline comet assay was performed according to manufacturer's instructions (Trevigen, Gaithersburg, Maryland, USA). Briefly, 12×10^4 glioblastoma cell lines were transfected with miRs or MGMT cDNA and then treated with TMZ in 6-well plates. Cells were collected and then combined with LMAgarose. The mixture was applied to Comet slides and kept at 4°C in the dark for 10'. The slides were immersed in pre-chilled lysis buffer for 30 min. The slides were washed and then electrophoresis was carried out. The slides were fixed in 70% ethanol for 5 min and let dry overnight. SYBR green was added and comets were photographed at 100 x microscopes (Carl Zeiss Inc., NY, USA).

γH2AX flow cytometric analysis

Treated cells were fixed with 2% paraformaldehyde for 1 hr. Fixed cells were permeabilized with 0.1% Triton-X100/PBS for 5 min on ice. Blocking was done in PBS+2% BSA. Anti-phosphorylated H2Ax antibody (Ser139, γH2Ax, Millipore, Milan, Italy) was diluted in PBS and then FITC-conjugated goat anti-mouse antibody (Santa Cruz Biotechnology, CA, USA) was

used. Cells were analyzed with a Becton Dickinson FACScan flow cytometer.

Caspase Assay

The assay was performed using the Colorimetric CaspACE™ Assay System, (Promega, Milan, Italy) as reported in the instruction manual. Briefly, T98G cells were transfected with miR-221 and/or MGMT cDNA, plated in 96-well plates, and then treated with 300 µMol of temozolomide or with 10 µMol of ZVAD-Fmk. After treatments, 100 µl caspase-3/-7 reagent was added to each well for 1 hr in the dark. The plates were analyzed in a Multilabel Counter (BioTek, Milan, Italy).

MGMT Methylation Analysis

DNA methylation status in the CpG island of MGMT was established by PCR analysis of bisulfite modified genomic DNA, which induces chemical conversion of unmethylated, but not methylated, cytosine to uracil. DNA was extracted from cell lines using the DNeasy blood and tissue kit (Qiagen, Milan, Italy). DNA (1 µg) was modified with sodium bisulfite using the EZ DNA methylation-gold kit (Zymo Research, CA, USA) according to the manufacturer's instructions. Methylation-specific polymerase chain reaction (MSP) was performed with primers specific for either methylated or the modified unmethylated DNA. Primer sequences for the unmethylated reaction were 5'TTTGTGTTTTGATGTTTGTAGTTTTTGT3' (forward primer) and 5'AACTCCACACTCTTCCAAAAACAAAACA3' (reverse primer), and for the methylated reaction they were 5'TTTCGACGTTTCGTAGTTTTTCGC3' (forward primer) and 5'GCACTCTCCGAAAACGAAACG3' (reverse primer.) The annealing temperature was 59°C. The cell line SW48 and *in vitro* methylated DNA (CpGenome Universal Methylated DNA, Millipore) were used as a positive control for the methylation of MGMT and DNA from normal lymphocytes used as a negative control. Controls without DNA were used for each set of methylation-specific PCR assays. The methylation-specific PCR product was loaded directly onto 2% agarose gels, stained with syber safe, and examined under ultraviolet illumination.

Colony Assay

Cells were transfected with scrambled miR or miR-221 for 24 hrs, harvested, and 2.4×10^4 cells plated in 6-well plates. After 24 hrs, cells were treated with 300 µMol TMZ for 24 hrs, as indicated. Cells were transferred to 100-mm dishes and grown for 6 days. Finally, the cells were colored with 0.1% crystal violet dissolved in 25% methanol for 20 min at 4°C. Dishes were washed with water, left to dry on the bench, and then photographs taken.

Statistical analysis

Student's *t* test and nonparametric Mann-Whitney tests were used to determine differences between values for normally and, respectively, not normally distributed variables. A probability level <0.05 was considered significant throughout

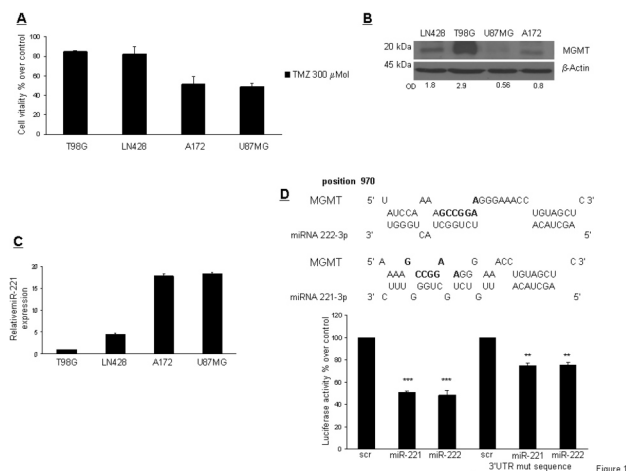


Figure 1. TMZ sensitivity and MGMT and miR-221/222 expression in glioma cells. (A) Glioma cells were treated with TMZ (300 μMol) for 24 hr. Cell viability was evaluated with an MTT assay. (B) Western blot analysis of MGMT expression in glioblastoma cells. (C) Real time PCR of miR-221 expression in glioblastoma cells. (D) RNA Hybrid prediction analyzes of miR-222, miR-221, and MGMT 3' UTR. In bold are shown the mutated oligonucleotides. Luciferase activity of HEK-293 cells transiently co-transfected with the luciferase reporter containing wild-type MGMT-3'UTR or mutant MGMT-3'UTR in the presence of pre-miR-222, miR-221, or scrambled oligonucleotide. Representative of at least three independent experiments. *** $p < 0.001$ versus control, ** $p < 0.0037$ versus control.

doi: 10.1371/journal.pone.0074466.g001

the analysis. Data were analyzed with GraphPad Prism (San Diego, CA, USA) for Windows.

Results

Sensitivity of human glioma cell lines to temozolomide

We analyzed the sensitivity to TMZ of human glioma cell lines by exposing the cells to 300 μMol TMZ for 48 hours and then assessing cell viability with the MTT assay (Figure 1A). We observed different TMZ sensitivities, which correlated with MGMT levels analyzed by Western blot (Figure 1B). We also observed an inverse correlation between the level of MGMT (Figure 1B) and miR-221 expression in glioma cell lines (Figure 1C). An RNA hybrid alignment bioinformatics search identified a possible binding site for miR-221/222 at position 970 of the 3' UTR of *MGMT*.

To examine whether miR-221/222 interfered with *MGMT* expression by directly targeting the predicted 3' UTR region, we cloned this region downstream of a luciferase reporter gene in the pGL3 vector. HEK-293 cells were co-transfected with the reporter plasmid plus the negative control miR (scrambled miR), miR-221, or miR-222. Only transfection of either miR-221 or miR-222 with the wild-type *MGMT*-3'UTR reporter plasmid led to a significant decrease of luciferase activity. On the

contrary, co-expression of the scrambled miR had no effect (Figure 1D). In addition, miR-221/222's effect on the promoter of *MGMT* was reduced with the mutant *MGMT*-3'UTR reporter, in which the seed sequence was mutated. Together, these results demonstrate that miR-221/222 directly target *MGMT*-3'UTR, thereby reducing *MGMT* expression.

miR-221/222 target MGMT protein and mRNA

In order to establish a causal link between miR-221/222 and *MGMT* expression, we transfected T98G cells with either pre-miR-221 or pre-miR-222 for 72 hrs and then analyzed MGMT levels by Western blot and real time-PCR. Upon miR transfection, MGMT protein and mRNA were downregulated (Figure 2A). In contrast, MGMT expression was increased upon transfection with anti-miR-221 or -222 in U87MG cells (Figure 2B). Similarly, miR-221/222, induced downregulation of MGMT in LN428 cells, another TMZ-resistant glioma cell line (Figure 2C), and in A375 cells, a TMZ-resistant melanoma cell line (Figure 2D). Since *MGMT* expression is mainly dependent on the methylation status of its promoter [27], we determined if miR-221/222 acted by modulating *MGMT* promoter methylation. To this end, we performed a bisulfite modification assay by PCR using specific primers for both methylated and unmethylated *MGMT* promoter. As shown in Figure 2E, miR-221/222 expression in T98G cells, or anti-miR expression in U87MG cells, did not modify the methylation profile of the *MGMT* promoter.

miRs-221/222 modulate TMZ sensitivity in glioma cells

To verify if miR-221/222 play a role in the modulation of TMZ sensitivity because of their effects on MGMT expression, we characterized the viability of T98G, LN428, and A375 cells transfected with miR-221/222 and then treated with TMZ for 24 hrs. As shown in Figure 3A, miR-221/222 transfection increased the response to TMZ. These results were also confirmed by proliferation and colony assays (Figure 3B and 3C). To establish a causal link between miR-221 expression and MGMT downregulation, we performed a rescue experiment with simultaneous overexpression of miR-221 and MGMT cDNA in two different cell lines (T98G and LN428). As shown in Figure 3D, the effect of miR-221 on TMZ response was abolished by MGMT overexpression. We then verified in nine different glioblastoma primary cell lines and in six glioma cell lines any correlation between miR-221 expression and TMZ sensitivity. As shown, TMZ sensitivity positively correlated with the expression level of miR-221 (Figure 3E).

miR-221 promotes apoptotic cell death

In order to evaluate the mechanism of TMZ-induced cell death, we assessed the presence of apoptotic cells by PI staining and flow cytometry upon miR-221 transfection and TMZ treatment. We found that TMZ increased apoptotic cell death in miR-221-overexpressing cells compared with control cells. Interestingly, this effect was rescued by the co-expression of MGMT cDNA with miR-221 (Figure 4A). Caspase-3/7 activation assay further confirmed the involvement of the apoptotic machinery. As shown in Figure 4B, miR-221 expression increased caspase-3 activity upon

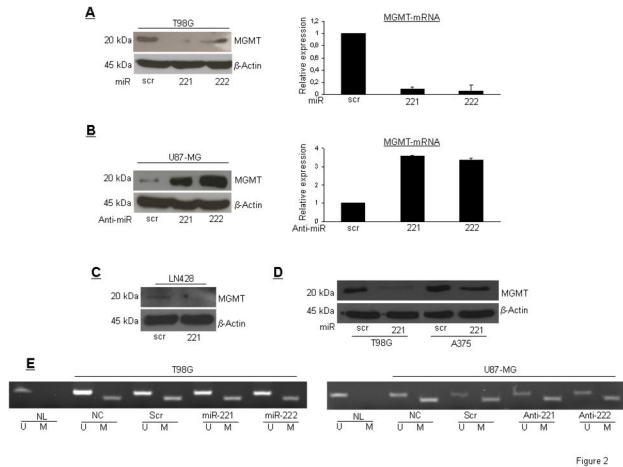


Figure 2

Figure 2. miR-221/222 target MGMT. (A) Western blot analysis and real time PCR of MGMT protein and RNA after miR-221/222 transfection of T98G cells. (B) Western blot analysis and real time PCR of MGMT protein and RNA after anti-miR-221 and -222 transfection of U87MG cells. (C) Western blot of MGMT expression upon miR-221 transfection of LN428 cells. (D) Western blot analysis of MGMT expression in T98G cells, as a control, and the melanoma cell line A375 upon miR-221 transfection. (E) Analysis of methylation status of MGMT promoter in T98G and U87MG upon miR- or anti-miR-221/222 transfection. U is for the un-methylated form, M for methylated form, NL is for normal lymphocytes, used as control.

doi: 10.1371/journal.pone.0074466.g002

TMZ treatment, while the co-expression of MGMT cDNA with miR-221 abolished this effect. Simultaneous treatment with the caspase inhibitor ZVAD-fmk and TMZ was able to decrease caspase activity, confirming that TMZ induced cell death by a caspase-mediated mechanism. Caspase-3 activation, observed by Western blot in miR-221-transfected cells after 24 hrs of TMZ treatment, was rescued by MGMT cDNA (Figure 4C). Coherently, we observed an increase in cell viability after miR-221 transfection and simultaneous treatment with TMZ and ZVAD-fmk (Figure 4D).

miR-221 promotes DNA damage after TMZ treatment

MGMT activity repairs DNA by removing DNA adducts caused by TMZ treatment. The absence of MGMT increases cell death upon exposure to TMZ, but, as a long-term effect, may increase DNA damage, and thus the accumulation of mutations. We investigated whether miR-221 may increase DNA damage upon TMZ treatment by down-modulating MGMT expression. This was assessed by a comet assay, which quantifies double-stranded DNA (dsDNA) breaks, in T98G cells transfected with miR-221 or a scrambled sequence and then treated with TMZ at different times. We found that miR-221 produced a significant enhancement of dsDNA breaks (Figure 5A). To strengthen our hypothesis, we looked for the phosphorylation status of histone H2AX (γ H2AX) at Ser139, which reflects dsDNA break formation. As shown in Figure 5B,

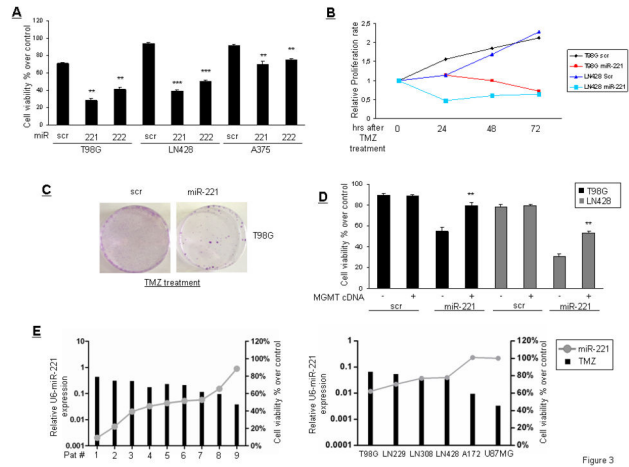


Figure 3

Figure 3. miR-221 modulates TMZ sensitivity. (A) Cell viability of T98G, LN428, and A375 cells transfected with miR-221 and miR-222 upon TMZ treatment (300 μ Mol) for 24 hrs. **p value<0.0082 versus scr column, ***p value<0.005 versus scr column. (B) Growth curve of T98G and LN428 cells transfected or not with miR-221 after 24 hrs of treatment with TMZ. (C) Colony assay of T98G and LN428 cells transfected with miR-221 and then treated for 24 hrs with TMZ (300 μ Mol). Cells were left to grow for 6 days after treatment removal. (D) MGMT expression rescues cell viability after TMZ treatment in T98G and LN428 cells overexpressing miR-221 **p value<0.0082 versus untransfected MGMT column. (E) Correlation between miR-221 expression and TMZ sensitivity in nine primary glioblastoma cell lines and in six glioblastoma cell lines.

doi: 10.1371/journal.pone.0074466.g003

miR-221 significantly increased γ H2AX, as assessed by immunocytofluorescence (upper panel) or by Western blot (lower panel), suggesting that miR overexpression may induce DNA damage. This effect was even stronger in the presence of TMZ, but was rescued by MGMT cDNA (Figure 5B, middle panel). Furthermore, we also observed an increase of other DNA damage markers, such as P-ATM, P-p53^{ser15} and PARP cleavage, upon miR-221 transfection; this was even stronger upon treatment with both miR-221 and TMZ (Figure 5C). These effects were rescued by the simultaneous expression of MGMT with miR-221. Taken together, these data suggest that the targeting of MGMT by miR-221 increases DNA damage. This effect was amplified by TMZ treatment.

MGMT and miR-221 expression in glioblastoma patients

We then evaluated the expression of MGMT and miR-221 in human glioblastoma samples. Patients were clustered into two separate groups: a long survival (survival >15 months) group and a short survival (survival <15 months) group, according to common classification [2].

We first analyzed the methylation profile of the MGMT promoter, and then MGMT mRNA and miR-221 levels. We performed methylation-specific PCR (MSP) on 33 human

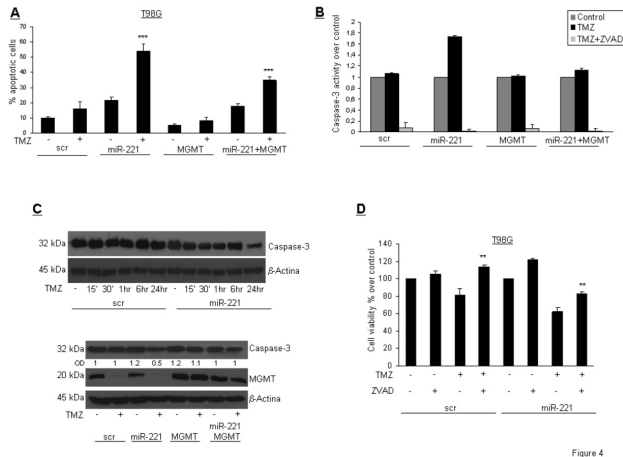


Figure 4

Figure 4. miR-221 promotes DNA damages upon TMZ treatment. (A) Apoptotic cell death assessed by FACS in T98G cells transfected with miR-221 or scrambled sequence and MGMT and treated with TMZ for 24 hrs. *** p value < 0.005 versus untransfected MGMT column. (B) Active caspase-3 quantification in T98G cells as indicated and treated with TMZ for 24 hrs in the presence or absence of 3 hrs pre-treatment with ZVAD-fmk. (C) Upper panel Time course analysis of caspase-3 activation upon TMZ treatment in T98G cells transfected with miR-221 or with scrambled sequence. Lower panel Western blot analysis of caspase-3 activation after miR-221 and MGMT transfection. (D) Cell viability of T98G cells transfected with miR-221 or with scrambled sequence treated with TMZ for 24 hrs in the presence or absence of 3 hrs pre-treatment with ZVAD-fmk. ** p value < 0.0034 versus only treated TMZ column, Student's t test.

doi: 10.1371/journal.pone.0074466.g004

glioblastoma paraffin-embedded tissues, and found 27 to be unmethylated and 4 to be methylated (samples 2, 21, 22, and 28) (Figure S1). For two samples (#31 and #32), it was not possible to define the *MGMT* promoter methylation profile. We then analyzed the effect of miR-221 on *MGMT* regulation among 15 unmethylated samples from which we obtained sufficient RNA for real time PCR analysis. We identified 4 long- (#1, #4, #10, and #14) and 11 short- (#6, #7, #8, #12, #13, #17, #18, #23, #25, #32, and #33) survival patients. We found that the short-survival group exhibited a higher miR-221 level and a lower *MGMT* level compared with the long-survival group (Figure 6 A,B). These data supports our in vitro evidence of an inverse correlation between miR-221 and *MGMT* expression. Furthermore, this observation identifies miR-221 as a negative prognostic factor for survival.

Discussion

Much evidence suggests that the intracellular level of the alkylating enzyme *MGMT* affects TMZ response in GBM patients [10,11]. Low levels of *MGMT* are associated with a better TMZ response, because in the absence of *MGMT* the cells are not able to repair the TMZ-induced base mismatch.

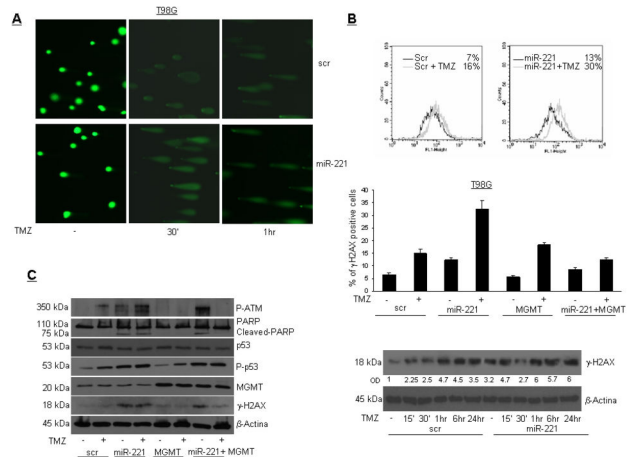


Figure 5

Figure 5. miR-221 promotes DNA damage. (A) Alkaline comet assay of T98G cells transfected with miR-221 and treated with TMZ for the indicated times. (B) Analysis of γH2AX in T98G cells transfected with scrambled control miR or miR-221, treated with TMZ in the presence or in the absence of *MGMT* cDNA, by immunocytofluorescence (upper and medium panel) or by Western blot (lower panel). (C) Western blot analysis of the indicated proteins upon transfection of T98G cells with miR-221 and *MGMT* cDNA and TMZ treatment for 24 hrs.

doi: 10.1371/journal.pone.0074466.g005

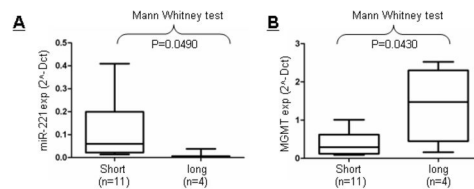


Figure 6. Association of miR-221 and MGMT expression. Mann-Whitney U test analysis was performed to evaluate the association between miR-221 and *MGMT* expression in long- and short-survival groups of patients. The expression of miR-221 ($2^{-\Delta Ct}$) (A-B) and *MGMT* ($2^{-\Delta Ct}$) are inversely correlated with patient survival ($p < 0.0490$ and $p = 0.043$, respectively).

doi: 10.1371/journal.pone.0074466.g006

Hence, double-strand DNA breaks, DNA mismatch repair, and the apoptotic pathway are activated. *MGMT* expression is regulated by the methylation of its promoter. *MGMT* promoter methylation lowers *MGMT* levels and accounts for a greater TMZ response when associated with radiotherapy. However, a fraction of patients with unmethylated *MGMT* show some TMZ response, suggesting that promoter methylation is not the only regulatory mechanism of *MGMT* expression [13,14].

In the present study, we addressed this specific issue by investigating the involvement of miRs in *MGMT* regulation. First, we characterized TMZ sensitivity in a subset of

glioblastoma cell lines and primary cells obtained from GBM patients. We found that the analyzed glioblastoma cell lines (T98G, LN428, U87MG, and A172) expressed different levels of miR-221/222 and displayed a consistent difference in MGMT expression. This inverse correlation was also observed in glioblastoma biopsies.

Bioinformatics identified a possible miR-221/222 binding site on *MGMT*. This was confirmed by a luciferase assay and overexpression experiments. The effect of miR-221/222 on MGMT levels was direct and not related to *MGMT* promoter methylation, since miR transfection did not alter the *MGMT* methylation profile. Instead, we found evidence that miR-221/222 regulated MGMT levels, leading to increased TMZ-induced apoptosis, reduced anchorage-independent growth, and reduced cell viability. Overexpression of MGMT cDNA with miR-221/222 rescued the effects on TMZ sensitivity. This result was not restricted to glioma cells, but was obtained also in other cancer cells sensitive to TMZ, such as human malignant melanoma.

It has been demonstrated that *MGMT* may be a target also of other miRs, such as miR-181, in GBM [28]. Zhang et al. demonstrated that miR-181d targets *MGMT* 3' UTR, and reported an inverse correlation between miR-181d and MGMT levels in human GBM samples, in particular in those samples in which the *MGMT* promoter was unmethylated [28]. However, the modest correlation between miR-181d and MGMT suggested that other miRs may regulate MGMT expression. Therefore, miR-221/222 may be part of this cohort.

MGMT expression may be regulated also thought the p53 pathway. Blough et al. provided evidence that p53 regulates MGMT expression in murine astrocytes, and presented data suggesting that p53 contributes to the regulation of MGMT gene expression in the human astrocytic glioma cell line SF767 [29].

In this manuscript, we demonstrate that miR-221 overexpression increases DNA damage in glioma cells. In fact, miR-221-overexpressing glioma cells exhibited an increase in DNA damage markers, such as P-ATM, P-p53, cleaved PARP, and γ H2AX. These markers were activated even in the absence of TMZ, and became increased upon TMZ treatment. MGMT participates in the repair of DNA. Thus, miR-221/222 induces chronic MGMT downregulation, rendering the cells unable to repair DNA damage. It is well established that miR221/222 are oncogenic microRNAs that are upregulated in a number of human tumors [30,31,32]. In GMB tissue and cell lines, upregulated miR-222 and miR-221 expression correlated with the stage of the disease, cell motility, and TRAIL response [19,23,31,33]. We found that miR-221 is a negative prognostic factor, since it is up regulated in short-survival patients and is downregulated in long-survival ones. However, we did not observe the expected correlation between miR-221 expression and response to temozolomide/survival. Arguably, overall survival and therapy response have to be linked to other factors. It therefore seems that the pro-oncogenic effect of miR-221 is more powerful than its potentiation of the response to temozolomide.

The role of MGMT in DNA damage repair has been investigated also in animal models. Reduced expression of this

repair enzyme has been thought to result in a spontaneous 'mutator' phenotype and to promote neoplastic lesions in the presence of either endogenous or exogenous sources of alkylation stress. Sakumi, et al. showed that *Mgmt*^{-/-} mice develop thymic lymphomas and lung adenomas to a greater extent when exposed to methylnitrosourea (MNU), suggesting that the DNA repair methyltransferase protected these mice from MNU-induced tumorigenesis [34]. Sandercock et al. reported that MGMT-deficient cells exhibited an increased mutational burden, but only following exposure to specific environmental mutagens [35]. Takagi et al. demonstrated that mice with mutations in *Mgmt* as well as in the DNA mismatch repair gene *Mlh1* developed numerous tumors after being administered MNU. When exposed to a sub-lethal dose of MNU (1mM), the mutation frequency in *Mgmt*^{-/-}/*Mlh1*^{-/-} cells was up to 12 times that of untreated cells; this effect was not present in control mice [36]. Walter et al. generated transgenic mice overexpressing MGMT in brain and liver, or in lung [37]. They found that expression of the transgene correlated with a reduced prevalence of MNU-induced tumors in liver and in lung and also with reduced spontaneous hepatocellular carcinoma. Reese et al. found that overexpression of MGMT decreased the incidence and increased the latency of thymic lymphoma induction in mice with both heterozygous and wild type p53 alleles [38]. This protective effect was described also by Allay et al., who reported that the incidence of lymphomas was much lower in MGMT transgenic mice compared with controls [39]. Those studies thus suggest that MGMT, other than being involved in the response to therapy, is also involved in DNA repair. Therefore, its inactivation may produce devastating effects on DNA integrity.

In summary, we have provided evidence of the existence of an adjunct mechanism of MGMT regulation, besides promoter methylation, involving miR targeting its 3' UTR. We have also shown that overexpression of miR-221/222 produces an increase in sensitivity to TMZ via a reduction in the level of MGMT. On the other hand, these miRs increase DNA damage, conferring oncogenic features to glioma cells. This may link miR-221/222 to poor GBM prognosis.

Supporting Information

Figure S1. Methylation-specific PCR analyses for MGMT methylation in glioblastoma human tumors. 33 glioblastoma samples were used for analysis. The SW48 cell line and *in vitro* methylated DNA (IVD) are shown as a positive control for methylation, normal lymphocytes (NL) as a negative control for methylation, and water (H₂O) as a negative PCR control. U and M indicate the presence of unmethylated or methylated MGMT, respectively. Red colour is for methylated samples, green for unmethylated and orange for undetermined samples. (TIF)

Acknowledgements

We wish to thank Dr. Michael Latronico for the extensive revision of the manuscript.

Author Contributions

Conceived and designed the experiments: CQ GC. Performed the experiments: G. Roscigno CQ DM ADL G. Romano.

Analyzed the data: DF ED MI GC. Contributed reagents/materials/analysis tools: ME YS PD. Wrote the manuscript: CQ GC.

References

- Wen PY, Kesari S (2008) Malignant Gliomas in Adults. *N Engl J Med* 359: 492-507. doi:10.1056/NEJMra0708126. PubMed: 18669428.
- Louis DN, Ohgaki H, Wiestler OD, Cavenee WK, Burger PC et al. (2007) The 2007 WHO Classification of Tumours of the Central Nervous System. *Acta Neuropathol* 114: 97-109. doi:10.1007/s00401-007-0243-4. PubMed: 17618441.
- Stupp R, Hegi ME (2013) Brain cancer in 2012: Molecular characterization leads the way. *Nat Rev Clin Oncol* 10: 69-70. doi:10.1038/nrclinonc.2012.240. PubMed: 23296110.
- Stupp R, Mason WP, van den Bent MJ, Weller M, Fisher B et al. (2005) Radiotherapy plus concomitant and adjuvant temozolomide for glioblastoma. *N Engl J Med* 352: 987-996. doi:10.1056/NEJMoa043330. PubMed: 15758009.
- Stupp R, Hegi ME, Mason WP, van den Bent MJ, Taphoorn MJB et al. (2009) Effects of radiotherapy with concomitant and adjuvant temozolomide versus radiotherapy alone on survival in glioblastoma in a randomised phase III study: 5-year analysis of the EORTC-NCIC trial. *Lancet Oncol* 10: 459-466. doi:10.1016/S1470-2045(09)70025-7. PubMed: 19269895.
- Mrugala MM, Chamberlain MC (2008) Mechanisms of Disease: temozolomide and glioblastoma-look to the future. *Nat Clin Pract Oncol* 5: 476-486. doi:10.1038/ncpgasthep1210. PubMed: 18542116.
- Roos WP, Batista LFZ, Naumann SC, Wick W, Weller M et al. (2006) Apoptosis in malignant glioma cells triggered by the temozolomide-induced DNA lesion O6-methylguanine. *Oncogene* 26: 186-197. PubMed: 16819506.
- Bignami M, O'Driscoll M, Aquilina G, Karran P (2000) Unmasking a killer. DNA O6-methylguanine and the cytotoxicity of methylating agents. *Mutat Res* 462: 71-82.
- Gerson SL (2002) Clinical Relevance of MGMT in the Treatment of Cancer. *J Clin Oncol* 20: 2388-2399. doi:10.1200/JCO.2002.06.110. PubMed: 11981013.
- Gerson SL (2004) MGMT: its role in cancer aetiology and cancer therapeutics. *Nat Rev Cancer* 4: 296-307. doi:10.1038/nrc1319. PubMed: 15057289.
- Hegi ME, Liu L, Herman JG, Stupp R, Wick W et al. (2008) Correlation of O6-Methylguanine Methyltransferase (MGMT) Promoter Methylation With Clinical Outcomes in Glioblastoma and Clinical Strategies to Modulate MGMT Activity. *J Clin Oncol* 26: 4189-4199. doi:10.1200/JCO.2007.11.5964. PubMed: 18757334.
- Dunn J, Baborie A, Alam F, Joyce K, Moxham M et al. (2009) Extent of MGMT promoter methylation correlates with outcome in glioblastomas given temozolomide and radiotherapy. *Br J Cancer* 101: 124-131. doi:10.1038/sj.bjc.6605127. PubMed: 19536096.
- Krex D, Klink B, Hartmann C, von Deimling A, Pietsch T et al. (2007) Long-term survival with glioblastoma multiforme. *Brain* 130: 2596-2606. doi:10.1093/brain/awm204. PubMed: 17785346.
- Weller M, Stupp R, Reifenberger G, Brandes AA, van den Bent MJ et al. (2010) MGMT promoter methylation in malignant gliomas: ready for personalized medicine? *Nat. Rev Neurol* 6: 39-51. doi:10.1038/nrneuro.2009.197.
- Calin GA, Croce CM (2006) MicroRNA signatures in human cancers. *Nat Rev Cancer* 6: 857-866. doi:10.1038/nrc1997. PubMed: 17060945.
- Gregory RI, Shiekhattar R (2005) MicroRNA biogenesis and cancer. *Cancer Res* 65: 3509-3512. doi:10.1158/0008-5472.CAN-05-0298. PubMed: 15867338.
- Garofalo M, Condorelli G, Croce CM (2008) MicroRNAs in diseases and drug response. *Curr Opin Pharmacol* 8: 661-667. doi:10.1016/j.coph.2008.06.005. PubMed: 18619557.
- Negrini M, Ferracin M, Sabbioni S, Croce CM (2007) MicroRNAs in human cancer: from research to therapy. *J Cell Sci* 120: 1833-1840. doi:10.1242/jcs.03450. PubMed: 17515481.
- Quintavalle C, Garofalo M, Zanca C, Romano G, Iaboni M et al. (2012) miR-221/222 overexpression in human glioblastoma increases invasiveness by targeting the protein phosphatase PTPmu. *Oncogene* 31: 858-868. doi:10.1038/onc.2011.280. PubMed: 21743492.
- Conti A, Aguenouz MH, Torre D, Tomasello C, Cardali S et al. (2009) miR-21 and 221 upregulation and miR-181b downregulation in human grade II-IV astrocytic tumors. *J Neuro Oncol* 93: 325-332. doi:10.1007/s11060-009-9797-4. PubMed: 19159078.
- Ciafrè SA, Galardi S, Mangiola A, Ferracin M, Liu CG et al. (2005) Extensive modulation of a set of microRNAs in primary glioblastoma. *Biochem Biophys Res Commun* 334: 1351-1358. doi:10.1016/j.bbrc.2005.07.030. PubMed: 16039986.
- Garofalo M, Quintavalle C, Romano G, Croce CM, Condorelli G (2012) miR221/222 in Cancer: Their Role in Tumor Progression and Response to Therapy. *Curr Mol Med* 12: 27-33. doi:10.2174/156652412798376170. PubMed: 22082479.
- Garofalo M, Di Leva G, Romano G, Nuovo G, Suh SS et al. (2009) miR-221&222 regulate TRAIL resistance and enhance tumorigenicity through PTEN and TIMP3 downregulation. *Cancer Cell* 16: 498-509. doi:10.1016/j.ccr.2009.10.014. PubMed: 19962668.
- Garofalo M, Condorelli GL, Croce CM, Condorelli G (2010) MicroRNAs as regulators of death receptors signaling. *Cell Death Differ* 2: 200-8. PubMed: 19644509.
- Garofalo M, Romano G, Di Leva G, Nuovo G, Jeon Y-J et al. (2011) EGFR and MET receptor tyrosine kinase-altered microRNA expression induces tumorigenesis and gefitinib resistance in lung cancers. *Nat Med* 18: 74-82. doi:10.1038/nm.2577. PubMed: 22157681.
- Livak KJ, Schmittgen TD (2001) Analysis of relative gene expression data using real-time quantitative PCR and the 2(-Delta Delta C(T)) Method. *Methods* 25: 402-408. doi:10.1006/meth.2001.1262. PubMed: 11846609.
- Esteller M, Hamilton SR, Burger PC, Baylin SB, Herman JG (1999) Inactivation of the DNA Repair: Gene O6-Methylguanine-DNA Methyltransferase by Promoter Hypermethylation is a Common Event in Primary Human Neoplasia. *Cancer Res* 59: 793-797.
- Zhang W, Zhang J, Hoadley K, Kushwaha D, Ramakrishnan V et al. (2012) miR-181d: a predictive glioblastoma biomarker that downregulates MGMT expression. *Neuro Oncol* 14: 712-719. doi:10.1093/neuonc/nos089. PubMed: 22570426.
- Blough MD, Zlatescu MC, Cairncross JG (2007) O6-Methylguanine-DNA Methyltransferase Regulation by p53 in Astrocytic Cells. *Cancer Res* 67: 580-584. doi:10.1158/0008-5472.CAN-06-2782. PubMed: 17234766.
- Pallante P, Visone R, Ferracin M, Ferraro A, Berlingieri MT et al. (2006) MicroRNA deregulation in human thyroid papillary carcinomas. *Endocr Relat Cancer* 13: 497-508. doi:10.1677/erc.1.01209. PubMed: 16728577.
- Conti A, Aguenouz M, La Torre D, Tomasello C, Cardali S et al. (2009) miR-21 and 221 upregulation and miR-181b downregulation in human grade II-IV astrocytic tumors. *J Neuro Oncol* 93: 325-332. doi:10.1007/s11060-009-9797-4. PubMed: 19159078.
- Pineau P, Volinia S, McJunkin K, Marchio A, Battiston C et al. (2010) miR-221 overexpression contributes to liver tumorigenesis. *Proc Natl Acad Sci U S A* 107: 264-269. doi:10.1073/pnas.0907904107. PubMed: 20018759.
- Ciafrè SA, Galardi S, Mangiola A, Ferracin M, Liu CG et al. (2005) Extensive modulation of a set of microRNAs in primary glioblastoma. *Biochem Biophys Res Commun* 334: 1351-1358. doi:10.1016/j.bbrc.2005.07.030. PubMed: 16039986.
- Sakumi K, Shiraishi A, Shimizu S, Tsuzuki T, Ishikawa T et al. (1997) Methylnitrosourea-induced Tumorigenesis in MGMT Gene Knockout Mice. *Cancer Res* 57: 2415-2418. PubMed: 9192819.
- Sandercock LE, Hahn JN, Li L, Luchman HA, Giesbrecht JL et al. (2008) Mgmt deficiency alters the in vivo mutational spectrum of tissues exposed to the tobacco carcinogen 4-(methylnitrosamino)-1-(3-pyridyl)-1-butanone (NNK). *Carcinogenesis* 29: 866-874. doi:10.1093/carcin/bgn030. PubMed: 18281247.
- Takagi Y, Takahashi M, Sanada M, Ito R, Yamaizumi M et al. (2003) Roles of MGMT and MLH1 proteins in alkylation-induced apoptosis and mutagenesis. *DNA Repair (Amst)* 2: 1135-1146. doi:10.1016/S1568-7864(03)00134-4. PubMed: 13679151.
- Walter CA, Lu J, Bhakta M, Mitra S, Dunn W et al. (1993) Brain and liver targeted overexpression of O6-methylguanine DNA methyltransferase in transgenic mice. *Carcinogenesis* 14: 1537-1543. doi:10.1093/carcin/14.8.1537. PubMed: 8353838.
- Reese JS, Allay E, Gerson SL (2001) Overexpression of human O6-alkylguanine DNA alkyltransferase (AGT) prevents MNU induced

lymphomas in heterozygous p53 deficient mice. *Oncogene* 20: 5258-5263.

39. Allay E, Veigl M, Gerson SL (1999) Mice over-expressing human O6 alkylguanine-DNA alkyltransferase selectively reduce O6

methylguanine mediated carcinogenic mutations to threshold levels after N-methyl-N-nitrosourea. *Oncogene* 18: 3783-3787.

Impact of a High Loading Dose of Atorvastatin on Contrast-Induced Acute Kidney Injury

Cristina Quintavalle, PhD*; Danilo Fiore, PhD*; Francesca De Micco, PhD; Gabriella Visconti, MD; Amelia Focaccio, MD; Bruno Golia, MD; Bruno Ricciardelli, MD; Elvira Donnarumma, PhD; Antonio Bianco, PhD; Maria Assunta Zabatta, PhD; Giancarlo Troncone, MD, PhD; Antonio Colombo, MD; Carlo Briguori, MD, PhD; Gerolama Condorelli, MD, PhD

Background—The role of statins in the prevention of contrast-induced acute kidney injury (CIAKI) is controversial.

Methods and Results—First, we investigated the in vivo effects of atorvastatin on CIAKI. Patients with chronic kidney disease enrolled in the Novel Approaches for Preventing or Limiting Events (NAPLES) II trial were randomly assigned to (1) the atorvastatin group (80 mg within 24 hours before contrast media [CM] exposure; n=202) or (2) the control group (n=208). All patients received a high dose of *N*-acetylcysteine and sodium bicarbonate solution. Second, we investigated the in vitro effects of atorvastatin pretreatment on CM-mediated modifications of intracellular pathways leading to apoptosis or survival in renal tubular cells. CIAKI (ie, an increase >10% of serum cystatin C concentration within 24 hours after CM exposure) occurred in 9 of 202 patients in the atorvastatin group (4.5%) and in 37 of 208 patients in the control group (17.8%) ($P=0.005$; odds ratio=0.22; 95% confidence interval, 0.07–0.69). CIAKI rate was lower in the atorvastatin group in both diabetics and nondiabetics and in patients with moderate chronic kidney disease (estimated glomerular filtration rate, 31–60 mL/min per 1.73 m²). In the in vitro model, pretreatment with atorvastatin (1) prevented CM-induced renal cell apoptosis by reducing stress kinases activation and (2) restored the survival signals (mediated by Akt and ERK pathways).

Conclusions—A single high loading dose of atorvastatin administered within 24 hours before CM exposure is effective in reducing the rate of CIAKI. This beneficial effect is observed only in patients at low to medium risk. (*Circulation*. 2012;126:3008-3016.)

Key Words: apoptosis ■ contrast media ■ kidney ■ prevention ■ statins

Iodinated contrast media (CM) are used in both diagnostic and interventional cardiovascular procedures. In addition to the risk of allergic reactions, the major concern in regard to CM use is a deterioration of kidney function termed *contrast-induced acute kidney injury* (CIAKI). The reported incidence of CIAKI varies widely (<1% to >50%), depending on the patient population, the baseline risk factors, and the definition.¹ Hemodynamic changes of renal blood flow, which lead to hypoxia of the renal medulla, and direct toxic effects of CM on renal cells are thought to contribute to the pathogenesis of CIAKI.² We have observed previously both in vitro and in vivo that CM induce apoptotic cell death via 3 important signaling pathways: (1) the reactive oxygen species (ROS) pathway, (2) the Jun N-terminal kinase (JNK)/p38

pathway, and (3) the intrinsic apoptosis pathway, which are triggered by CM in this sequence.^{3,4} The causal relationship between these 3 sequential pathways supports the investigation of novel therapeutic approaches to prevent CIAKI.

Clinical Perspective on p 3016

Statins exert several effects through their non-lipid-related mechanisms. These so-called pleiotropic effects encompass several mechanisms that modify inflammation responses, endothelial function, plaque stability and thrombus formation, and the apoptotic pathway.^{5–7} The effectiveness of statin pretreatment in reducing the incidence of CIAKI has been examined in some observational^{8–10} and randomized studies.^{11–13} Because of the controversial results, there is a general

Received March 6, 2012; accepted October 22, 2012.

From the Department of Cellular and Molecular Biology and Pathology, Federico II University of Naples, and IEOS, CNR Naples (C.Q., D.F., G.C.); Laboratory of Interventional Cardiology and Department of Cardiology, Clinica Mediterranea, Naples (F.D.M., G.V., A.F., B.G., B.R., C.B.); Fondazione IRCCS-SDN, Naples (E.D.); Dipartimento di Scienze Biomorfologiche e Funzionali, Università di Napoli Federico II, Naples (A.B., M.A.Z., G.T.); and Laboratory of Interventional Cardiology, San Raffaele Hospital, Milan (A.C.), Italy.

*The first 2 authors contributed equally to this work.

The online-only Data Supplement is available with this article at <http://circ.ahajournals.org/lookup/suppl/doi:10.1161/CIRCULATIONAHA.112.103317/-/DC1>.

Correspondence to Gerolama Condorelli, MD, PhD, Department of Cellular and Molecular Biology and Pathology, and IEOS, CNR, Federico II University of Naples, Via Pansini, 5, I-80121, Naples, Italy. E-mail gecondor@unina.it; or Carlo Briguori, MD, PhD, Laboratory of Interventional Cardiology, Clinica Mediterranea, Via Orazio, 2, I-80121, Naples, Italy. E-mail carlobriguori@clinicamediterranea.it

© 2012 American Heart Association, Inc.

Circulation is available at <http://circ.ahajournals.org>

DOI: 10.1161/CIRCULATIONAHA.112.103317

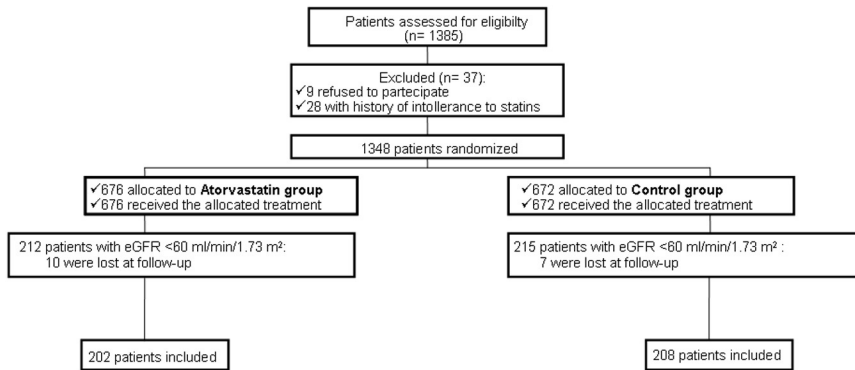


Figure 1. Flow of participants through each stage of the trial according to the CONSORT guidelines. eGFR indicates estimated glomerular filtration rate.

consensus that statins merit further study for the prevention of CIAKI. In the present study, we investigated (1) the *in vivo* effects of atorvastatin pretreatment on CIAKI and (2) the *in vitro* effects of atorvastatin pretreatment on CM-mediated modifications of intracellular pathways leading to apoptosis or survival in renal tubular cells.

Methods

Patient Population

The patients included in the present study represent the subgroup with chronic kidney disease (CKD) enrolled in the Novel Approaches for Preventing or Limiting Events (NAPLES) II trial⁷ (Figure 1). The design of the NAPLES II trial has been reported previously. From January 2005 to December 2008, 1348 naive patients (ie, those not taking statins) scheduled for elective coronary angiography or percutaneous coronary intervention in *de novo* lesions in native coronary arteries were considered eligible for the study. The day before the procedure, all eligible patients were randomly assigned to atorvastatin treatment (atorvastatin group) or to no atorvastatin treatment (control group). Randomization was performed by a 1:1 ratio with computer-generated random numbers. Patients randomized in the atorvastatin group started atorvastatin treatment (80 mg) within 24 hours before CM exposure. The prophylaxis for CIAKI in all patients with CKD included (1) *N*-acetylcysteine (NAC) (Fluimucil, Zambon Group SpA, Milan, Italy; 1200 mg PO twice daily, the day before and the day of administration of CM) and (2) hydration with sodium bicarbonate solution¹⁴ (154 mEq/L in dextrose and H₂O). It was administered with the initial intravenous bolus of 3 mL/kg per hour for 1 hour immediately before CM injection, followed by 1 mL/kg per hour during contrast exposure and for 6 hours after the procedure.^{14,15} Iodixanol (Visipaque, GE) a nonionic, iso-osmolar (290 mOsm/kg of water) contrast agent, was used in all patients. CKD was defined as an estimated glomerular filtration rate (eGFR) <60 mL/min per 1.73 m².¹⁶ The risk score for predicting CIAKI was calculated according to the following algorithm: hypotension (integer score 5), intra-aortic balloon pump support (integer score 5), congestive heart failure (integer score 4), age >75 years (integer score 4), diabetes mellitus (integer score 3), eGFR <60 mL/min per 1.73 m² (integer score 2–6), preexisting anemia (integer score 3), and CM volume (integer score 1 for each 100 mL). The global scores ≤5, 6 to 10, 11 to 16, and >16 anticipate a CIAKI risk of 7.5%, 14%, 26.1%, and 57.3%, respectively.¹⁷ Serum creatinine (sCr), cystatin C (sCyC), blood urea nitrogen, sodium, and potassium were measured the day before the procedure and at 24 and 48 hours and 1 week after CM administration. Additional measurements were performed in all instances in which there was a deterioration of baseline renal function. The primary outcome measure was the development of CIAKI, defined as an increase in sCyC concentration 10% above the baseline value at 24 hours after administration of CM.¹⁸ Secondary outcome measures were (1) an increase of sCr concentration ≥0.5 mg/dL at 48 hours from baseline value and (2) an increase of sCr concentration

≥25% at 48 hours from baseline value. To address whether a single high (80 mg) dose of atorvastatin may affect the sCr or sCyC levels, we analyzed an additional 20 patients with CKD not scheduled for CM exposure and not enrolled in the original NAPLES II trial. The clinical characteristics of the 20 enrolled patients are summarized in Table I in the online-only Data Supplement. The trial was conducted in 2 interventional cardiology centers in Italy and was approved by our ethics committees.

Culture Conditions and Reagents

Two cell lines were utilized: Madin Darby distal nonhuman tubular epithelial (MDCK) cells and human embryonic proximal tubules (HK2) cells. MDCK cells were grown in a 5% CO₂ atmosphere in Dulbecco's modified Eagle's medium containing 10% heat-inactivated fetal bovine serum, 2 mmol/L L-glutamine, and 100 U/mL penicillin-streptomycin. HK2 cell lines were grown in Dulbecco's modified Eagle's medium–F12 mixture with 10% heat-inactivated fetal bovine serum, 2 mmol/L L-glutamine, and 100 U/mL penicillin-streptomycin. Cells were routinely passaged when 80% to 85% confluent. Media, sera, and antibiotics for cell culture were from Sigma-Aldrich (Milan, Italy). Protein electrophoresis reagents were from Bio-Rad (Richmond, VA), and Western blotting and enhanced chemiluminescence reagents were from GE Healthcare (Milan, Italy). The following antibodies were used for immunoblotting: anti-β-actin (Sigma-Aldrich), anti-phospho-JNK, anti-caspase-3, anti-phosphoserine¹⁵ p53, anti-p53, anti-phospho-Akt, anti-Akt, anti-phospho-ERK, anti-ERK, anti-HSP70 (Cell Signaling, Danvers, MA), and anti-JNK (DB Bioscience, Milan, Italy).

Atorvastatin was kindly donated by Pfizer (Pfizer Inc, New York, NY), and NAC was donated by Zambon (Zambon Group SpA, Milan, Italy). MDCK and HK2 cells were pretreated with atorvastatin at a dose of 0.2 μmol/L¹⁹ or 100 μmol of NAC.⁴ The dose of atorvastatin was selected according to the standard doses used in cell lines. Iodixanol was used in all experiments.

Caspase Assay

The assay was performed with the use of the Colorimetric CaspACE Assay System (Promega, Madison, WI) according to the manufacturer's protocol. Briefly, MDCK cells were pretreated with 0.2 μmol/L atorvastatin for 12 hours and then treated for 3 hours with iodixanol. Cells were harvested in caspase assay buffer, and proteins were quantified by Bradford assay. Fifty micrograms of protein was used.

Protein Isolation and Western Blotting

Cellular pellets were washed twice with cold phosphate-buffered saline and resuspended in JS buffer (HEPES 50 mmol/L, NaCl 150 mmol/L, 1% glycerol, 1% Triton X-100, 1.5 mmol/L MgCl₂, 5 mmol/L EGTA) containing Proteinase Inhibitor Cocktail (Roche, Basel, Switzerland). Solubilized proteins were incubated for 1 hour on ice. After centrifugation at 13 200 rpm for 10 minutes at 4°C, lysates were collected as supernatants. Eighty micrograms of sample extract was resolved on a 12% sodium dodecyl sulfate–polyacrylamide gel with the use of a mini-gel apparatus (Bio-Rad Laborato-

ries) and transferred to Hybond-C extra nitrocellulose (GE Healthcare). Membrane was blocked for 1 hour with 5% nonfat dry milk in Tris-buffered saline containing 0.05% Tween-20 and incubated overnight at 4°C with specific antibodies. The indicated antibody was used for immunoblotting. Washed filters were then incubated for 45 minutes with horseradish peroxidase-conjugated anti-rabbit or anti-mouse secondary antibodies (GE Healthcare) and visualized with chemiluminescence detection (GE Healthcare).

Cell Death Quantification

Cell vitality was evaluated with the CellTiter 96 AQueous One Solution Cell Proliferation Assay (Promega), according to the manufacturer's protocol. The assay is based on reduction of 3-(4,5-dimethylthiazol-2-yl)-5-(3-carboxymethoxyphenyl)-2-(4-sulfophenyl)-2H-tetrazolium inner salt (MTS) to a colored product that is measured spectrophotometrically. Cells were plated in 96-well plates in triplicate, stimulated, and incubated at 37°C in a 5% CO₂ incubator. Iodixanol and atorvastatin were used in vitro at doses and times indicated. Metabolically active cells were detected by adding 20 μL of MTS to each well. After 30 minutes of incubation, the plates were analyzed on a Multilabel Counter (Bio-Rad). Apoptosis was also analyzed via propidium iodide incorporation in permeabilized cells by flow cytometry. The cells (2×10⁵) were washed in phosphate-buffered saline and resuspended in 200 μL of a solution containing 0.1% sodium citrate, 0.1% Triton X-100, and 50 μg/mL propidium iodide (Sigma-Aldrich). After incubation at 4°C for 30 minutes in the dark, nuclei were analyzed with a Becton Dickinson FACScan flow cytometer. Cellular debris was excluded from analyses by raising the forward scatter threshold, and the DNA content of the nuclei was registered on a logarithmic scale. The percentage of elements in the hypodiploid region was calculated.

Biological Material

Exfoliated cell pellets from the urine of 10 enrolled and randomly selected patients (5 in each group) were collected by centrifugation at 1200 rpm for 25 minutes. A fraction of urine samples was sent to the pathologist for cytological analysis and a fraction to the laboratory for in vitro assay. All samples were stored at -80°C for a maximum of 2 months. Urine samples were resuspended in ice-cold TRAP (Tris-HCl 10 mmol/L, pH 7.5, MgCl₂ 1 mmol/L, EGTA 1 mmol/L, phenylmethylsulfonyl 0.1 mmol/L, β-mercaptoethanol 5 mmol/L, CHAPS 0.5%, and glycerol 10%) and incubated on ice for 1 hour. The lysate was centrifuged for 20 minutes at 13 200 rpm at 4°C. The supernatant was collected. The presence of tubular cells was assessed with the use of morphological criteria on cytospin preparations stained by standard Papanicolaou staining methods. To this end, cell block preparations were employed. To ensure their adequacy, cell blocks were stained with hematoxylin and eosin. Caspase-3 expression was detected with the use of rabbit polyclonal antibody (Cell Signaling 9661, Danvers, MA). Signal was developed by the polyvalent LSAB-peroxidase Dako kit (Dako, Denmark).

Statistical Analysis

The sample size was selected to demonstrate a reduction in the primary end point of CIAKI from 20% in the control group to 10% in the atorvastatin group.^{18,20} With the use of a 2-sided χ² test with a significance level of 0.05, a total of at least 400 randomized patients (200 in each arm) provided the study with 80% power. This is a prespecified secondary end point of the NAPLES II trial.

Continuous variables are given as mean±1 SD or median and first and third quartiles, when appropriate. The Student *t* and nonparametric Mann-Whitney tests were used to determine differences between values for normally and nonnormally distributed variables, respectively. Categorical variables were reported as percentage and were analyzed by either χ² or Fisher exact test, as appropriate. Multiplicity issues were addressed with the use of the Bonferroni adjustment. To test the impact of the prophylactic regimen (as defined by the 2 treatment groups) on changes in sCyC concentration, we used a linear mixed model, taking into account the clustered features of the data, after transforming sCyC levels into a natural

Table 1. Clinical Characteristics of Patients Enrolled in the 2 Groups

	Control Group (n=208)	Atorvastatin Group (n=202)
Age, y	70±8	70±6
Male	120 (58)	103 (51)
Weight, kg	75±15	76±13
Height, m	1.67±0.5	1.65±0.5
Body mass index, kg/m ²	28±5	28±4
Blood pressure, mm Hg		
Systolic	150±22	151±23
Diastolic	76±10	77±13
Mean	101±13	102±15
LV ejection fraction, %	50±8	50±9
Systemic hypertension	182 (87.5)	172 (85.5)
Diabetes mellitus	80 (38.5)	89 (44)
Drugs		
ACE inhibitor	83 (40)	76 (38)
Calcium channel blocker	64 (31)	64 (32)
Angiotensin II receptor inhibitor	64 (31)	66 (33)
Diuretics	100 (48)	111 (55)
β-blockers	137 (66)	131 (65)
Procedure performed		
Coronary angiography	68 (23)	78 (27)
PCI	140 (77)	124 (73)
Volume of contrast media, mL	184±78	177±74
Contrast ratio >1	55 (26)	51 (25)

Continuous values are expressed as mean±SD; categorical values are expressed as total number and percentage of the global population (in parentheses). LV indicates left ventricular; ACE, angiotensin-converting enzyme; and PCI, percutaneous coronary intervention.

logarithm (to overcome the problem of nonnormal distribution). Specifically, we considered the treatment strategy (as defined in the control and atorvastatin groups), time period, and time×treatment strategy interaction as fixed effects and patients as a random effect. *P*<0.05 was considered significant throughout the analysis. Data were analyzed with SPSS 13.0 (Chicago, IL) for Windows. The authors had full access to and take responsibility for the integrity of the data. All authors have read and agree to the manuscript as written.

Results

Clinical Results

The clinical and biochemical characteristics were well matched between the 2 groups (Tables 1 and 2). sCyC increased significantly more in the control group than in the atorvastatin group (*P*=0.005; *F*=5.52 by repeated-measures ANOVA; Figure 2A). CIAKI occurred in 9 of 202 patients in the atorvastatin group (4.5%) and in 37 of 208 patients in the control group (17.8%) (*P*=0.005; odds ratio=0.22; 95% confidence interval, 0.07–0.69; Figure 2B). sCr increased significantly more in the control group than in the atorvastatin group (*P*=0.018; *F*=4.97 by repeated-measures ANOVA). An increase of sCr concentration ≥0.5 mg/dL at 48 hours from baseline value occurred in 7 of 202 patients (3.5%) in the atorvastatin group and in 16 of 208 patients (7.7%) in the control

Table 2. Biochemical Characteristics of Patients Enrolled in the 2 Groups

	Control Group (n=208)	Atorvastatin Group (n=202)
Serum creatinine, median (range), mg/dL	1.29 (0.88–1.61)	1.32 (0.96–1.62)
Serum cystatin C, median (range), mg/dL	1.25 (1.0–1.59)	1.23 (1.06–1.62)
eGFR, mL/min per 1.73 m ²	43±14	42±13
≤30 mL/min per 1.73 m ²	38 (18.5)	37 (18.5)
Contrast nephropathy risk score*	7.5±2.7	8.1±2.8
Serum urea nitrogen, mg/dL		
Baseline	78±31	80±35
After 48 h	70±30	76±35
Serum sodium, mEq/L		
Baseline	140±5	140±3
After 48 h	140±5	141±4
Serum potassium, mEq/L		
Baseline	4.7±0.7	4.6±0.7
After 24 h	4.5±0.7	4.6±0.7

Continuous values are expressed as median and first and third quartiles (serum creatinine and cystatin C) or mean±SD; categorical values are expressed as total number and percentage of the global population (in parentheses). eGFR indicates estimated glomerular filtration rate.

*According to Mehran et al.¹⁷

group ($P=0.085$). An increase of sCr concentration $\geq 25\%$ at 48 hours from baseline value occurred in 6 of 202 patients (3%) in the atorvastatin group and in 14 of 208 patients (7%) in the control group ($P=0.10$) (Figure I in the online-only Data Supplement). We also performed a stratified analysis to determine the benefit of atorvastatin according to the severity of CKD (eGFR ≤ 30 versus 31–60 mL/min per 1.73 m²) and the presence of diabetes mellitus (Figure 2C). The rate of CIAKI was lower in the atorvastatin group in both diabetics and nondiabetics and in patients with eGFR 31 to 60 mL/min per

1.73 m². On the contrary, no difference was observed in the subgroup with severe CKD (eGFR ≤ 30 mL/min per 1.73 m²). We observed that neither sCr nor sCyC was altered by administration of a single high (80 mg) atorvastatin loading dose (Figure II in the online-only Data Supplement).

One-year outcome was available in 402 of 410 patients (98%). Clinical and biochemical characteristics of the patients are reported in Tables II and III in the online-only Data Supplement. Major adverse events (including death and dialysis) occurred in 37 of 402 patients (9%). In particular, death occurred in 29 patients (7%) and chronic dialysis in 8 patients (2%). Major adverse events occurred in 9 of 45 patients (20%) with CIAKI (ie, a CyC $\geq 10\%$ at 24 hours after contrast exposure) and in 28 of 357 patients (7.8%) without CIAKI ($P=0.013$).

Atorvastatin Effects on CM-Induced Renal Cell Damage

In both MDCK and HK2 cells exposed to CM, pretreatment with atorvastatin induced an increase in cell vitality and a reduction of cell death (Figure 3). This protective effect was evident after 6 hours and reached a peak at 12 hours of atorvastatin pretreatment. Interestingly, we observed that pretreatment with atorvastatin reduced the CM-induced activation of caspase-3, JNK, and p53 (Figures 4 and 5).

We then evaluated the effects of atorvastatin pretreatment on survival signals mediated by Akt and ERK pathways. CM induced a strong reduction of the phosphorylated (activated) forms of Akt and ERK (Figure 5C and 5D). Interestingly, atorvastatin almost completely restored the survival signal in kidney cells. We performed a further experiment to investigate the effect of 2 hours of NAC pretreatment (100 mmol/L) in the presence of atorvastatin (0.2 μ mol/L) on cell death after 3-hour incubation with iodixanol (200 mg/mL). The beneficial effect of the combination of NAC and atorvastatin was higher than that obtained with the NAC or atorvastatin alone ($P=0.010$; $F=10.5$ by ANCOVA test; Figures 3C, 3D, and 4B). Finally, we did not observe any involvement of the

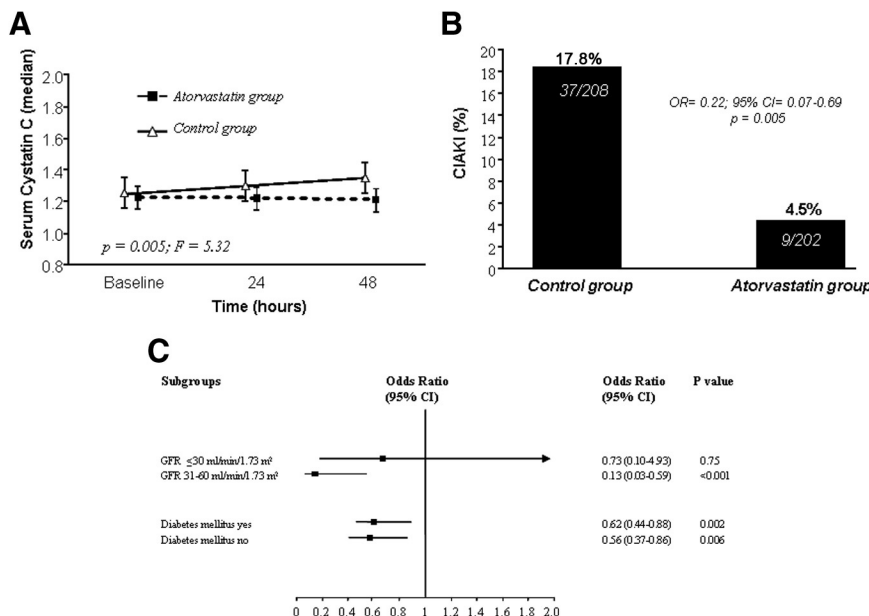


Figure 2. A, Serum cystatin C concentration at baseline and 24 and 48 hours after contrast media administration in the control group (open symbol, continuous line) and in the atorvastatin group (closed symbol, dashed line); $P=0.005$; $F=5.32$ by linear mixed model. **B**, Incidence of contrast-induced acute kidney injury (CIAKI) in control and atorvastatin groups. **C**, Benefit of atorvastatin according to severity of chronic kidney disease (estimated glomerular filtration rate [GFR] ≤ 30 vs 31–60 mL/min per 1.73 m²) and presence of diabetes mellitus. CI indicates confidence interval.

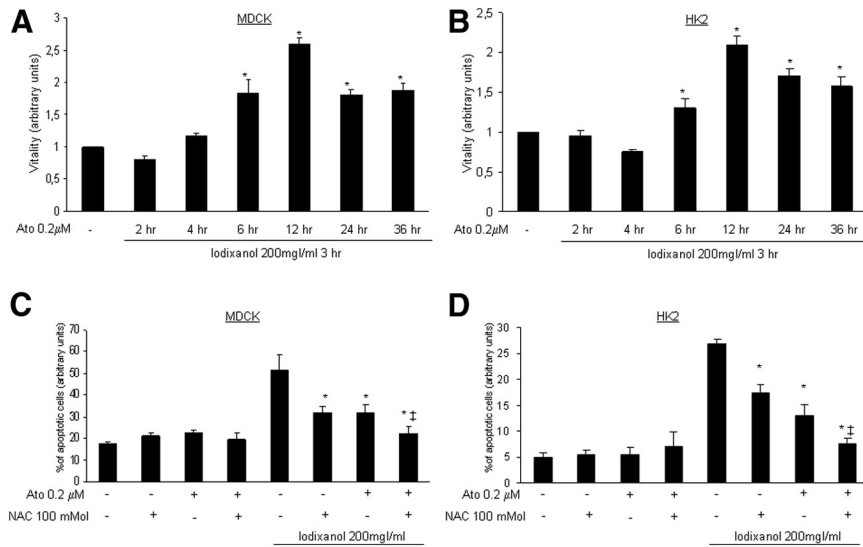


Figure 3. Effects of atorvastatin (Ato) (0.2 μmol/L) pretreatment for different times (2, 4, 6, 12, 24, 36 hours) on contrast media-induced Madin Darby distal nonhuman tubular epithelial (MDCK) and human embryonic proximal tubules (HK2) cell damage, assessed as viability (cell titer proliferation assay) (A and B) and percentage of apoptotic cells evaluated by fluorescence-activated cell sorting analysis (C and D). Pretreatment with both *N*-acetylcysteine (NAC) (100 mmol) and atorvastatin (0.2 μmol/L) was more effective than each single compound alone in the prevention of contrast media-induced apoptosis; * $P < 0.001$ vs column (NAC- and atorvastatin-); ‡ $P = 0.03$ vs columns (NAC- and atorvastatin+) and (NAC+ and atorvastatin-). All cells were incubated for 3 hours with iodixanol (200 mg iodine/mL). Each experiment was repeated 3 times. In A and B, a mixed linear model for repeated measures was used, with Bonferroni adjustment. In C and D, the Student *t* test was used.

JAK/STAT pathway in atorvastatin renal cell protection. Indeed, no differences in HSP70 protein (one of the signaling molecules of this pathway) expression have been detected in cells treated with atorvastatin (Figure 5B).

To clarify the clinical impact of these features, we evaluated the activation of JNK, p53, and caspase-3 in epithelial tubular cells collected at 24 and 48 hours after CM exposure from 10 patients (5 in the atorvastatin group and 5 in the control group). The presence of epithelial tubular cells was confirmed by immunohistochemistry by hematoxylin and eosin staining (Figure 7). In controls, an increase of both JNK and p53 phosphorylation (activation) was observed at 24 and 48 hours after CM exposure (Figure 6A through 6C). In contrast, in all 5 atorvastatin-treated patients, we observed a significant reduction of JNK and p53 phosphorylation (Figure 6B through 6D). Cells collected from patients were also analyzed immunohistochemically with anti-caspase-3 antibodies. Consistent with Western blot data, the activation of pro-caspase-3 at 24 and 48 hours was observed in the control group but not in the atorvastatin group (Figure 7).

Discussion

Clinical Findings

The present study demonstrates that a single high (80 mg) loading dose of atorvastatin administered within 24 hours

before CM exposure is effective in reducing the rate of CIAKI. This beneficial effect was observed in patients with and without diabetes mellitus as well as in those with moderate CKD (eGFR 31–60 mL/min per 1.73 m²). On the contrary, no advantage was evident in patients with severe CKD (eGFR ≤30 mL/min per 1.73 m²).

At present, the evidence for the use of statins to prevent CIAKI is conflicting and inconclusive.^{8–12,21} A number of considerations may be involved in the conflicting results.

First, the sample size is often modest to detect significant differences in the CIAKI rate. This may often be due to the enrollment of patients at low risk for CIAKI.¹⁷ The lack of observed benefit may therefore represent a type II error (ie, concluding that a benefit does not exist when one really does).²² Toso et al,¹² for example, did not observe any significant effect of atorvastatin loading dose on the CIAKI rate. However, the 304 patients enrolled in that study were insufficient to detect the expected 50% relative decrease in CIAKI rate in the atorvastatin group (from 15% in the placebo group) with 90% power at the conventional, 2-sided significance level of 5%. Indeed, >350 subjects in each group would have been required to test the hypothesis. Moreover, our study is also underpowered to demonstrate the impact of the atorvastatin loading dose in preventing CIAKI with the use of the current sCr cutoffs.²³ Indeed, with an

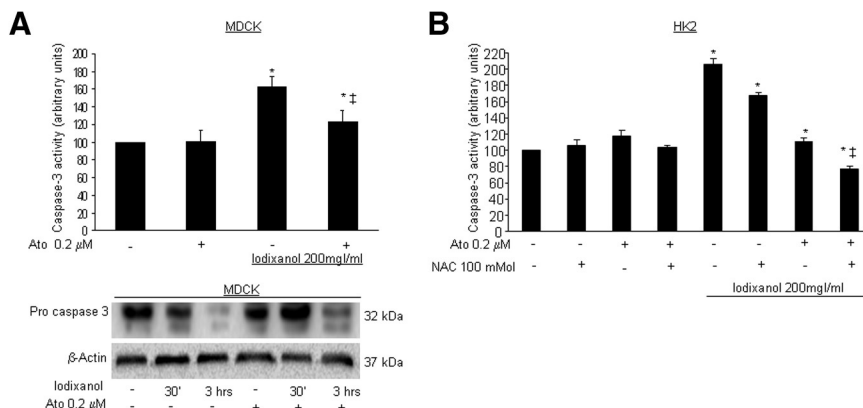


Figure 4. Effect of atorvastatin (Ato) (0.2 μmol/L) pretreatment on contrast media-induced Madin Darby distal nonhuman tubular epithelial (MDCK) (A) and human embryonic proximal tubules (HK2) (B) cell damage, assessed by caspase-3 assay or by Western blot of pro-caspase-3. * $P < 0.001$ vs control; ‡ $P < 0.001$ vs column (iodixanol+ and atorvastatin-). Pretreatment with both *N*-acetylcysteine (NAC) (100 mmol) and atorvastatin (0.2 μmol/L) was more effective than each single compound alone in the prevention of contrast media-induced caspase-3 activation. * $P < 0.001$ vs column [NAC- and atorvastatin-]; ‡ $P = 0.03$ vs columns (NAC- and atorvastatin+) and (NAC+ and atorvastatin-). Each experiment was repeated 3 times. The Student *t* test was used.

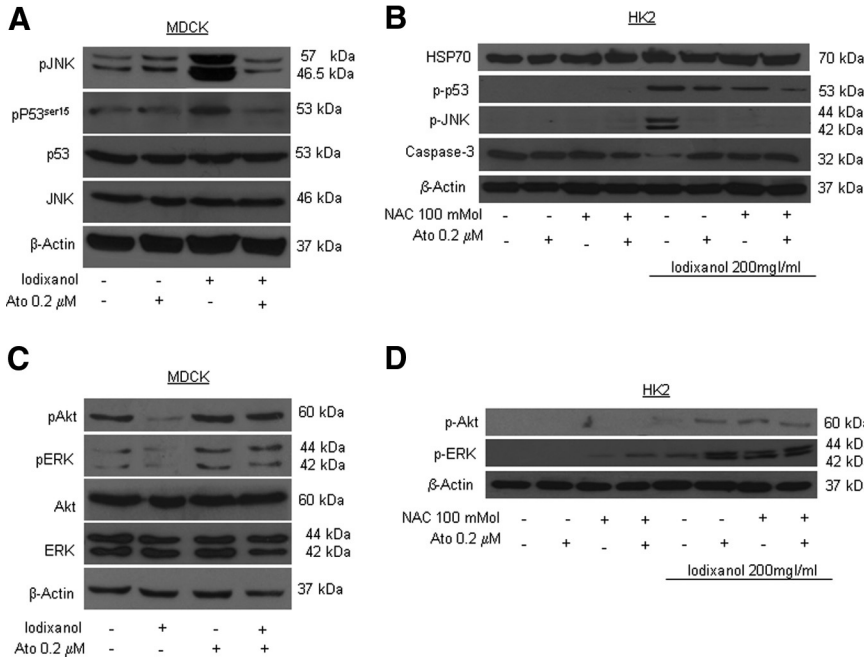


Figure 5. Western blot analysis showing the effect of atorvastatin (Ato) (0.2 $\mu\text{mol/L}$) pretreatment on contrast media-induced activation of Jun N-terminal kinase (JNK) and p53 in Madin Darby distal nonhuman tubular epithelial (MDCK) (A) and human embryonic proximal tubules (HK2) (B) renal cells. The activation of JNK and p53 was evaluated by detection of the phosphorylated (activated) form of the proteins (pJNK and pP53^{ser15}). Pretreatment with both *N*-acetylcysteine (NAC) (100 mmol) and atorvastatin (0.2 $\mu\text{mol/L}$) was more effective than each single compound alone. No differences of HSP70 protein (one of the signaling molecules of the JAK/STAT pathway) expression have been detected in cells treated with atorvastatin (B) in Western blot analysis, showing that atorvastatin (0.2 $\mu\text{mol/L}$) pretreatment induced an increase of the phosphorylated (activated) levels of both Akt and ERK (pAkt and pERK) in the presence of iodixanol in MDCK (C) and HK2 (D) cells.

absolute sCr increase ≥ 0.5 mg/dL as primary end point, to demonstrate a reduction from 10% to 5%, ≈ 1000 patients (450 in each arm) would be required.¹⁴ In addition, when the $\geq 25\%$ sCr increase is selected as the primary end point, to demonstrate a reduction of CIAKI from 5% to 2%, ≈ 1200 patients (600 in each arm) would be required.^{15,18,24} In the present study, we used sCyC as a marker of kidney function to detect CIAKI for several reasons: (1) sCyC is more sensitive than sCr to rapidly detect acute changes in renal function^{25,26}; (2) sCyC allows an early (24 hours) diagnosis of CIAKI^{18,27}; and (3) sCyC predicts the occurrence of major adverse events at follow-up in patients with CKD undergoing CM exposure.^{18,20}

The second consideration is primary end point definition. In the negative Prevention of Radiocontrast Medium Induced

Nephropathy Using Short-Term High-Dose Simvastatin in Patients With Renal Insufficiency Undergoing Coronary Angiography (PROMISS) trial,¹¹ the authors hypothesized an absolute sCr difference between baseline and 48 hours of 0.36 mg/dL in the simvastatin group and 1.1 mg/dL in the control group. This means that, with a baseline sCr level of 1.2 mg/dL, the authors expected a peak increase in the sCr concentration of 28% for the simvastatin group and 92% percent for the control group. Although such a large effect size has been observed in a single-center CIAKI trial,²⁸ multicenter trials generally produce a much smaller effect, with an absolute sCr difference between baseline and 48 hours ≤ 0.20 mg/dL and a peak increase in the sCr concentration of 20% to 30%.^{24,25,29–31} In addition, the absolute sCr difference is generally not a good primary outcome because it

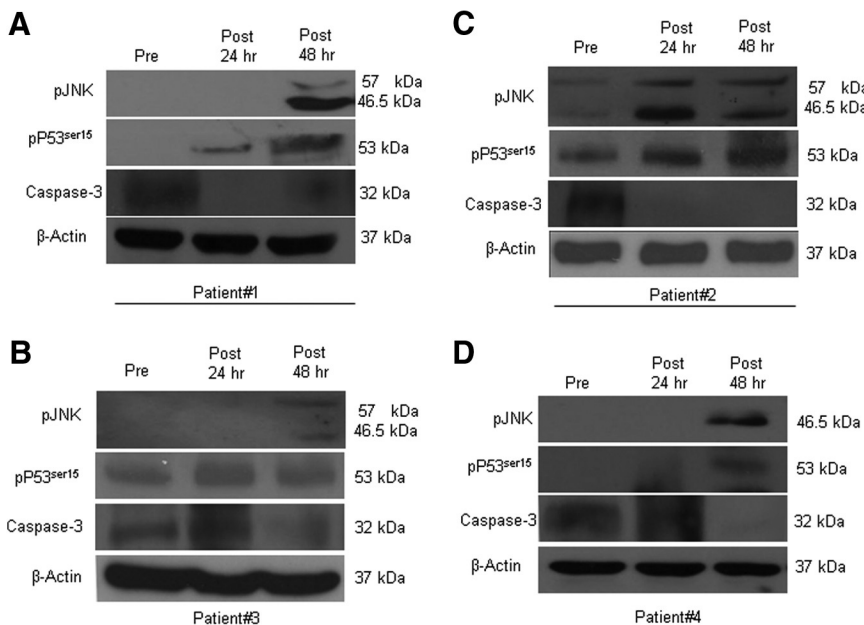


Figure 6. In vivo effects of contrast media on epithelial tubular renal cells. Western blot analysis assessing Jun N-terminal kinase (JNK) and p53 phosphorylation (activation) levels in epithelial tubular cells from 2 patients in the control group (A through C) and 2 patients in the atorvastatin group (B through D) is shown. The analysis revealed that activation of JNK and p53 was higher in the control group than in the atorvastatin group.

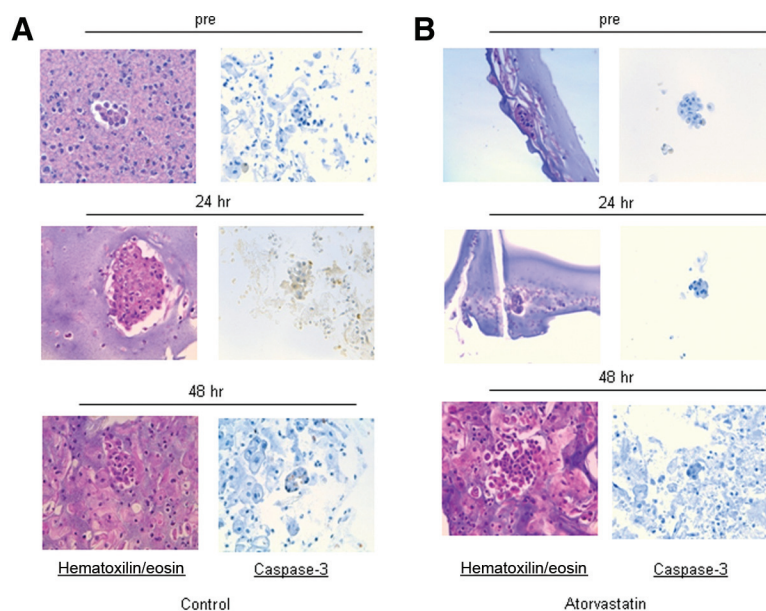


Figure 7. Immunohistochemistry of kidney tubular cells. Urine cytological cell block was prepared as described in Methods. This specimen type was used to perform a specific tubular cell marker immunostaining preparation (hematoxylin and eosin staining $\times 400$) and to assess the activation of active caspase-3 in patients in the control group (A) and atorvastatin group (B) at different times.

has not been validated to predict adverse outcomes (such as CIAKI).

The third consideration is type and dose of statin administered. Although results of retrospective studies (which included patients receiving a multitude of statins) may suggest the presence of a class effect,⁸ the majority of prospective randomized trials demonstrating prevention of CIAKI in patients undergoing CM exposure used short-term pretreatment with high doses of atorvastatin. Some evidence also exists on the better prophylactic effect of a high versus a low statin dose.^{32,33} Thus, when a strategy of short-term pretreatment with statins before CM exposure is adopted, it would be appropriate to use potent statins at high doses.

Mechanisms of Prevention of CM-Induced Renal Cell Damage by Atorvastatin

The cornerstone of the prophylaxis of CIAKI is hydration; however, strategies to prevent CM-induced renal cell apoptosis seem to play a clinical role. Previous studies have demonstrated that CM induce an increase in ROS production.^{3,34} This leads to eventual activation of the stress kinases JNK1/2 and p38. For this reason, clinical trials have been performed with the use of various antioxidant compounds with the aim of lowering the occurrence of CIAKI by scavenging ROS. The present study shows the additive protective effect of atorvastatin over the combined administration of sodium bicarbonate solution and NAC; this supports the hypothesis that the combination of different antioxidant compounds seems to be more effective than a single agent in preventing CIAKI.¹⁴ The Acetylcysteine for Prevention of Renal Outcomes in Patients Undergoing Coronary and Peripheral Vascular Angiography (ACT) trial showed no advantages in routine NAC use.³⁵ However, several aspects need to be addressed before one reaches the strong conclusion that NAC should be abandoned, including baseline CKD severity, consistency of hydration protocol, and impact of CM selection. Indeed, a recent meta-analysis of 30 trials showed a renoprotective benefit with NAC.³⁶ NAC pretreat-

ment inhibits CM-induced ROS production and therefore inhibits JNK and p38 activation as well as apoptosis, suggesting the existence of a specific target for NAC upstream of the apoptosis-executing stress kinases in the CM-activated signaling pathway.^{3,4,37} Atorvastatin may work at a different level in preventing activation of the intrinsic apoptotic pathway. Statins reduces the intracellular ROS levels in many cellular systems^{38,39} by acting on the inhibition of ROS-producing enzymes. In our *in vitro* model, pretreatment with a high dose of atorvastatin reduced contrast-induced JNK activation, which therefore led to intrinsic apoptosis pathway activation.⁴⁰ On the contrary, activation of the JAK2/STAT5 pathway does not seem to have a role in the protective effect of atorvastatin on contrast-induced renal cell damage; indeed, unlike asialo-erythropoietin, atorvastatin does not induce an increase in HSP70 cellular levels.⁴¹ Atorvastatin induces an increase in the survival signals and a reduction of the death signals mediated by CM treatment of kidney cells. This effect was time dependent, reaching a maximum effect at 12 hours of statin incubation. We also, for the first time, confirmed *in vivo* these mechanisms. *In vitro* studies addressing the pathophysiology of CM-induced apoptosis have been criticized because of several limitations, including the following: (1) assessment of only 1 potential mechanism of CM-induced renal cell damage in the absence of confounding variables that can be found *in vivo* (eg, hypoxia due to hemodynamic changes or other systemic mechanisms); (2) exposure to a constant concentration of CM to all cell lines, whereas *in vivo* the more distal epithelial tubular cells are exposed to much higher concentrations; (3) the potentially high dose of CM; and (4) differences in the tested drug/compound metabolism and transport across cell membranes. Cultured cells are attached with their basolateral membrane to the culture dish. This may preclude the access of atorvastatin to the cells through the active mechanism because the organic amino-transporting polypeptide is mainly present on the basolateral side of the epithelial renal cells.⁴² Of note, however, the cytochrome 3A4, which metabolizes atorvastatin into active

metabolites, is consistently expressed in proximal tubular epithelial cells.⁴³ Moreover, several studies indicate that the parent drug is equipotent to the active metabolites in vitro.⁴⁴

Study Limitations

The present study is a prespecified secondary end point of the NAPLES II trial, which was designed to assess whether a single, high (80 mg), loading (within 24 hours) dose of atorvastatin is effective in preventing elevation of biomarkers of myocardial infarction after elective coronary stent implantation.⁷ The lack of randomization of the patients with CKD may represent a limitation. However, the most important characteristics of the 2 groups were well balanced, without significant differences. The present study was powered with sCyC as a marker of kidney damage. The current gold standard for kidney function is still sCr. Having the sCr cutoffs as primary end points would have required a much larger (>1000 patients) sample size to detect the beneficial prophylactic effect of atorvastatin. Moreover, serum CyC is a reliable marker for both an early (24 hours) diagnosis of CIAKI and for predicting the occurrence of major adverse events at follow-up in patients with CKD undergoing CM exposure.¹⁸ Finally, the 4% loss to follow-up rate should be taken into account when our results are interpreted. Indeed, although the 17 patients lost at follow-up were largely similar to those analyzed (online-only Data Supplement), every patient lost to follow-up can be considered a potential threat to robust and precise inference.

Conclusions

A single high loading dose of atorvastatin administered within 24 hours before CM exposure is effective in reducing the rate of CIAKI by preventing CM-induced epithelial tubular renal cell apoptosis and increasing the survival signaling pathways. The advantage of adding an atorvastatin loading dose to the sodium bicarbonate solution and NAC seems to be effective in patients at low to medium risk but not in those at high risk.

Sources of Funding

This work was supported in part by funds from Associazione Italiana Ricerca sul Cancro (grant 10620) to Dr Condorelli, MERIT (RBNE08E8CZ 002) to Dr Condorelli, and PON01-02342 to Dr Briguori. Dr Quintavalle is a recipient of a Federazione Italiana Ricerca sul Cancro (FIRC) fellowship. Dr De Micco is recipient of PON01-02342 fellowship.

Disclosures

None.

References

1. McCullough PA. Contrast-induced acute kidney injury. *J Am Coll Cardiol.* 2008;51:1419–1428.
2. Tumlin J, Stacul F, Adam A, Becker CR, Davidson C, Lameire N, McCullough PA, CIN Consensus Working Panel. Pathophysiology of contrast-induced nephropathy. *Am J Cardiol.* 2006;98:14K–20K.
3. Quintavalle C, Brenca M, De Micco F, Fiore D, Romano S, Romano MF, Apone F, Bianco A, Zabatta MA, Troncone G, Briguori C, Condorelli G. In vivo and in vitro assessment of pathways involved in contrast media-induced renal cells apoptosis. *Cell Death Dis.* 2011;2:e155.
4. Romano G, Briguori C, Quintavalle C, Zanca C, Rivera NV, Colombo A, Condorelli G. Contrast agents and renal cell apoptosis. *Eur Hearth J.* 2008;29:2569–2576.

5. Gauthaman K, Manasi N, Bongso A. Statins inhibit the growth of variant human embryonic stem cells and cancer cells in vitro but not normal human embryonic stem cells. *Br J Pharmacol.* 2009;157:962–973.
6. Rosenson RS, Tangney CC. Antiatherothrombotic properties of statins. *JAMA.* 1998;279:1643–1650.
7. Briguori C, Visconti G, Focaccio A, Golia B, Chieffo A, Castelli A, Mussardo M, Montorfano M, Ricciardelli B, Colombo A. Novel Approaches for Preventing or Limiting Events (NAPLES) II trial: impact of a single high loading dose of atorvastatin on periprocedural myocardial infarction. *J Am Coll Cardiol.* 2009;54:2157–2163.
8. Khanal S, Attallah N, Smith DE, Kline-Rogers E, Share D, O'Donnell MJ, Moscucci M. Statin therapy reduces contrast-induced nephropathy: an analysis of contemporary percutaneous interventions. *Am J Med.* 2005;118:843–849.
9. Lev EI, Kornowski R, Vaknin-Assa H, Ben-Dor I, Brosh D, Teplitsky I, Fuchs S, Battler A, Assali A. Effect of previous treatment with statins on outcome of patients with ST-segment elevation myocardial infarction treated with primary percutaneous coronary intervention. *Am J Cardiol.* 2009;103:165–169.
10. Patti G, Nusca A, Chello M, Pasceri V, D'Ambrosio A, Vetrovec GW, Di Sciascio G. Usefulness of statin pretreatment to prevent contrast-induced nephropathy and to improve long-term outcome in patients undergoing percutaneous coronary intervention. *Am J Cardiol.* 2008;101:279–285.
11. Jo S-H, Koo B-K, Park J-S, Kang H-J, Cho Y-S, Kim Y-J, Youn T-J, Chung W-Y, Chae I-H, Choi D-J, Sohn D-W, Oh B-H, Park Y-B, Choi Y-S, Kim H-S. Prevention of Radiocontrast Medium Induced Nephropathy Using Short-Term High-Dose Simvastatin in Patients With Renal Insufficiency Undergoing Coronary Angiography (PROMISS) trial: a randomized controlled study. *Am Heart J.* 2008;155:499.e491–499.e498.
12. Toso A, Maioli M, Leoncini M, Gallopin M, Tedeschi D, Micheletti C, Manzone C, Amato M, Bellandi F. Usefulness of atorvastatin (80 mg) in prevention of contrast-induced nephropathy in patients with chronic renal disease. *Am J Cardiol.* 2010;105:288–292.
13. Patti G, Ricottini E, Nusca A, Colonna G, Pasceri V, D'Ambrosio A, Montinaro A, Di Sciascio G. Short-term, high-dose atorvastatin pretreatment to prevent contrast-induced nephropathy in patients with acute coronary syndromes undergoing percutaneous coronary intervention (from the ARMYDA-CIN [Atorvastatin for Reduction of MYocardial Damage During Angioplasty–Contrast-Induced Nephropathy] Trial. *Am J Cardiol.* 2011;108:1–7.
14. Briguori C, Airoldi F, D'Andrea D, Bonizzoni E, Morici N, Focaccio A, Michev I, Montorfano M, Carlino M, Cosgrave J, Ricciardelli B, Colombo A. Renal Insufficiency Following Contrast Media Administration Trial (REMEDIAL): a randomized comparison of 3 preventive strategies. *Circulation.* 2007;115:1211–1217.
15. Merten GJ, Burgess WP, Gray LV, Holleman JH, Roush TS, Kowalchuk GJ, Bersin RM, Van Moore A, Simonton CA III, Rittase RA, Norton HJ, Kennedy TP. Prevention of contrast-induced nephropathy with sodium bicarbonate: a randomized controlled trial. *JAMA.* 2004;291:2328–2334.
16. National Kidney Foundation. K/DOQI clinical practice guidelines for chronic kidney disease: evaluation, classification, and stratification. *Am J Kidney Dis.* 2002;39:S1–266.
17. Mehran R, Aymong ED, Nikolsky E, Lasic Z, Iakovou I, Fahy M, Mintz GS, Lansky AJ, Moses JW, Stone GW, Leon MB, Dangas G. A simple risk score for prediction of contrast-induced nephropathy after percutaneous coronary intervention: development and initial validation. *J Am Coll Cardiol.* 2004;44:1393–1399.
18. Briguori C, Visconti G, Rivera NV, Focaccio A, Golia B, Giannone R, Castaldo D, De Micco F, Ricciardelli B, Colombo A. Cystatin C and contrast-induced acute kidney injury. *Circulation.* 2010;121:2117–2122.
19. Posvar EL, Radulovic LL, Cilla DD, Whitfield LR, Sedman AJ. Tolerance and pharmacokinetics of single-dose atorvastatin, a potent inhibitor of HMG-CoA reductase, in healthy subjects. *J Clin Pharmacol.* 1996;36:728–731.
20. Solomon RJ, Mehran R, Natarajan MK, Doucet S, Katholi RE, Staniloae CS, Sharma SK, Labinaz M, Gelormini JL, Barrett BJ. Contrast-induced nephropathy and long-term adverse events: cause and effect? *Clin J Am Soc Nephrol.* 2009;4:1162–1169.
21. Zhang T, Shen LH, Hu LH, He B. Statins for the prevention of contrast-induced nephropathy: a systematic review and meta-analysis. *Am J Nephrol.* 2011;33:344–351.
22. Mehran R, Brar S, Dangas G. Contrast-induced acute kidney injury: underappreciated or a new marker of cardiovascular mortality? *J Am Coll Cardiol.* 2010;55:2210–2211.

23. Mehta RL, Kellum JA, Shah SV, Molitoris BA, Ronco C, Warnock DG, Levin A, Network AKI. Acute Kidney Injury Network: report of an initiative to improve outcomes in acute kidney injury. *Crit Care*. 2007; 11:R31.
24. Spargias K, Adreanides E, Demerouti E, Gkouziouta A, Manginas A, Pavlides G, Voudris V, Cokkinos DV. Iloprost prevents contrast-induced nephropathy in patients with renal dysfunction undergoing coronary angiography or intervention. *Circulation*. 2009;120:1793–1799.
25. Newman DJ, Thakkar H, Edwards RG, Wilkie M, White T, Grubb AO, Price CP. Serum cystatin C measured by automated immunoassay: a more sensitive marker of changes in GFR than serum creatinine. *Kidney Int*. 1995;47:312–318.
26. Dharmidharka VR, Kwon C, Stevens G. Serum cystatin C is superior to serum creatinine as a marker of kidney function: a meta-analysis. *Am J Kidney Dis*. 2002;40:221–226.
27. Rickli H, Benou K, Ammann P, Fehr T, Brunner-La Rocca HP, Petridis H, Riesen W, Wüthrich RP. Time course of serial cystatin C levels in comparison with serum creatinine after application of radiocontrast media. *Clin Nephrol*. 2004;61:98–102.
28. Attallah N, Yassine L, Musial J, Yee J, Fisher K. The potential role of statins in contrast nephropathy. *Clin Nephrol*. 2004;62:273–278.
29. Aspelin P, Aubry P, Fransson SG, Strasser R, Willenbrock R, Berg KJ; Nephrotoxicity in High-Risk Patients Study of Iso-Osmolar and Low-Osmolar Non-Ionic Contrast Media Study Investigators. Nephrotoxic effects in high-risk patients undergoing angiography. *N Engl J Med*. 2003;348:491–499.
30. Briguori C, Visconti G, Focaccio A, Airolidi F, Valgimigli M, Sangiorgi GM, Golia B, Ricciardelli B, Condorelli G; REMEDIAL II Investigators. Renal Insufficiency After Contrast Media Administration Trial II (REMEDIAL II): RenalGuard system in high-risk patients for contrast-induced acute kidney injury. *Circulation*. 2011;124:1260–1269.
31. Marenzi G, Assanelli E, Marana I, Lauri G, Campodonico J, Grazi M, De Metrio M, Galli S, Fabbicchi F, Montorsi P, Veglia F, Bartorelli AL. N-Acetylcysteine and contrast-induced nephropathy in primary angioplasty. *N Engl J Med*. 2006;354:2773–2782.
32. Xinwei J, Xianghua F, Jing Z, Xinshun G, Ling X, Weize F, Guozhen H, Yunfa J, Weili W, Shiqiang L. Comparison of usefulness of simvastatin 20 mg versus 80 mg in preventing contrast-induced nephropathy in patients with acute coronary syndrome undergoing percutaneous coronary intervention. *Am J Cardiol*. 2009;104:519–524.
33. Zhou X, Jin YZ, Wang Q, Min R, Zhang XY. Efficacy of high dose atorvastatin on preventing contrast induced nephropathy in patients underwent coronary angiography. *Zhonghua Xin Xue Guan Bing Za Zhi*. 2009;37:394–396.
34. Lee HC, Sheu SH, Yen HW, Lai WT, Chang JG. JNK/ATF2 pathway is involved in iodinated contrast media-induced apoptosis. *Am J Nephrol*. 2009;31:125–133.
35. ACT Investigators. Acetylcysteine for prevention of renal outcomes in patients undergoing coronary and peripheral vascular angiography. *Circulation*. 2011;124:1250–1259.
36. Kelly AM, Dwamena B, Cronin P, Bernstein SJ, Carlos RC. Meta-analysis: effectiveness of drugs for preventing contrast-induced nephropathy. *Ann Intern Med*. 2008;148:284–294.
37. Briguori C, Quintavalle C, De Micco F, Condorelli G. Nephrotoxicity of contrast media and protective effects of acetylcysteine. *Arch Toxicol*. 2011;85:165–173.
38. Takemoto M, Node K, Nakagami H, Liao Y, Grimm M, Takemoto Y, Kitakaze M, Liao JK. Statins as antioxidant therapy for preventing cardiac myocyte hypertrophy. *J Clin Invest*. 2001;108:1429–1437.
39. Wassmann S, Laufs U, Muller K, Konkol C, Ahlbory K, Baumer AT, Linz W, Bohm M, Nickenig G. Cellular antioxidant effects of atorvastatin in vitro and in vivo. *Arterioscler Thromb Vasc Biol*. 2002;22:300–305.
40. Dhanasekaran DN, Reddy EP. JNK signaling in apoptosis. *Oncogene*. 2008;27:6245–6251.
41. Yokomaku Y, Sugimoto T, Kume S, Araki S-i, Isshiki K, Chin-Kanasaki M, Sakaguchi M, Nitta N, Haneda M, Koya D, Uzu T, Kashiwagi A. Asialoerythropoietin prevents contrast-induced nephropathy. *J Am Soc Nephrol*. 2008;19:321–328.
42. Inui K-I, Masuda S, Saito H. Cellular and molecular aspects of drug transport in the kidney. *Kidney Int*. 2000;58:944–958.
43. Murray GI, McFadyen MCE, Mitchell RT, Cheung YL, Kerr AC, Melvin WT. Cytochrome P450 CYP3A in human renal cell cancer. *Br J Cancer*. 1999;79:1836–1842.
44. Lins RL, Matthys KE, Verpooten GA, Peeters PC, Dratwa M, Stolear JC, Lameire NH. Pharmacokinetics of atorvastatin and its metabolites after single and multiple dosing in hypercholesterolaemic haemodialysis patients. *Nephrol Dial Transplant*. 2003;18:967–976.

CLINICAL PERSPECTIVE

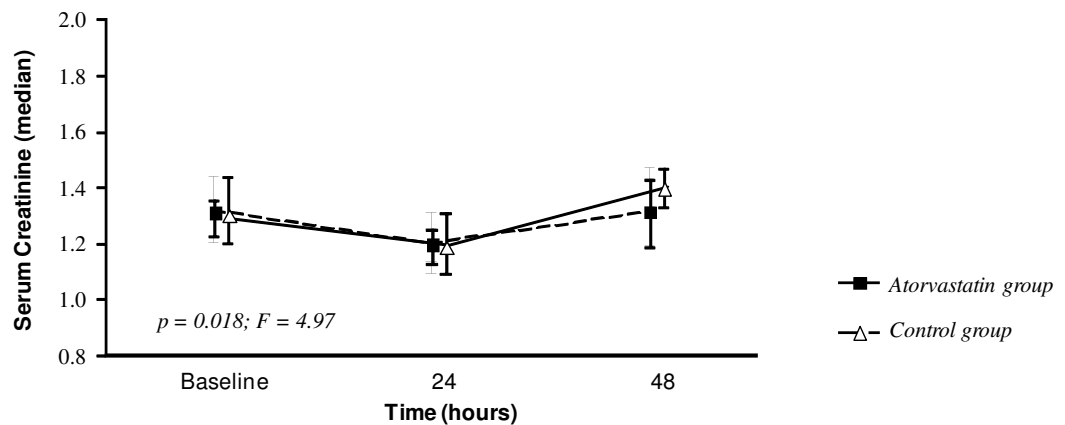
Patients with chronic kidney disease were randomly assigned to (1) the atorvastatin group (atorvastatin loading dose [80 mg] within 24 hours before contrast media exposure; n=202) or (2) the control group (n=208). All patients received a high dose of N-acetylcysteine and sodium bicarbonate solution. Contrast-induced acute kidney injury (defined as an increase >10% of serum cystatin C) occurred in 9 of 202 patients in the atorvastatin group (4.5%) and in 37 of 208 patients in the control group (17.8%) ($P=0.005$; odds ratio=0.22; 95% confidence interval, 0.07–0.69). In the in vitro model, pretreatment with atorvastatin (1) prevented contrast media-induced renal cell apoptosis by reducing activation of stress kinases and (2) restored survival signals (mediated by Akt and ERK pathways). The present study demonstrates that a single high loading dose of atorvastatin administered within 24 hours before contrast media exposure (on top of conventional strategies) is effective in reducing the rate of contrast-induced acute kidney injury by preventing contrast media-induced epithelial tubular renal cell apoptosis and increasing survival signaling pathways.

SUPPLEMENTAL MATERIAL

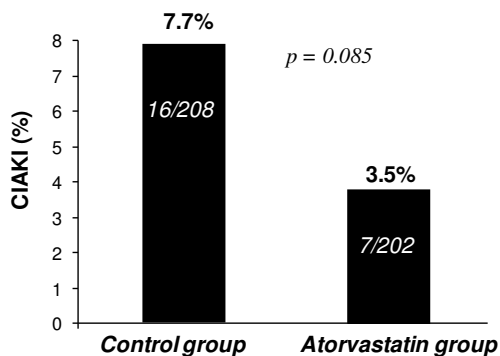
Effect of high loading dose of atorvastatin on serum creatinine concentrations after contrast media exposure. sCr increased significantly more in the *Control group* than in the *Atorvastatin group* ($p=0.018$; $F = 4.97$ by repeated measure of variance). An increase of sCr concentration ≥ 0.5 mg/dL at 48 hours from baseline value occurred in 7/202 (3.5%) patients in the *Atorvastatin group* and in 16/208 patients (7.7%) in the *Control group* ($p = 0.085$). An increase of sCr concentration $\geq 25\%$ at 48 hours from baseline value occurred in 6/202 (3%) patients in the *Atorvastatin group* and in 14/208 patients (7%) in the *Control group* ($p = 0.10$) (Figure 1S).

Figure1S

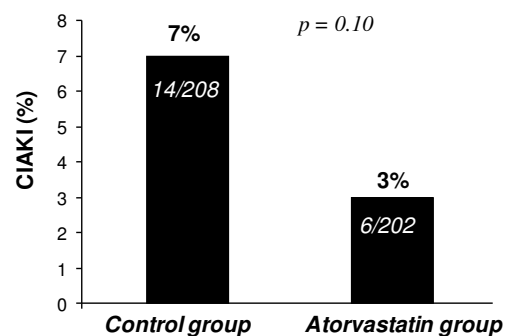
A



B



C



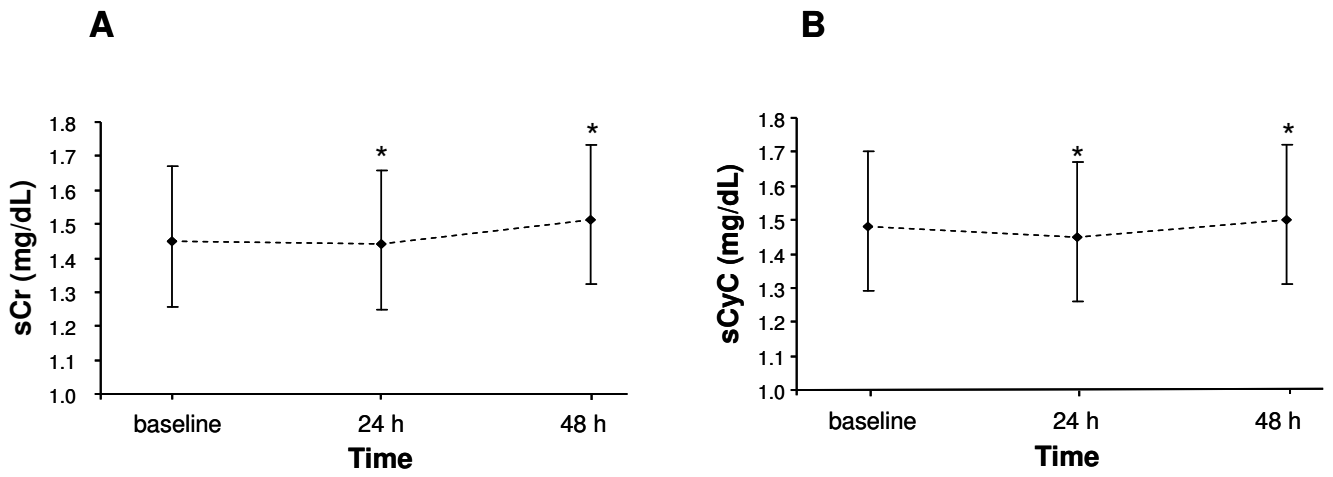
Effect of high loading dose of atorvastatin on serum creatinine and cystatin C concentrations. We analyzed 20 patients with chronic kidney disease and assessed the effects of a single high (80 mg) atorvastatin loading dose on renal function in the absence of contrast media exposure, using two surrogate markers of GFR, serum creatinine and cystatin C. These markers were measured simultaneously before and 24 h and 48 h after atorvastatin administration. These patients were not part of the original NAPLES II trial. This amendment of the NAPLES II trial was approved by our Ethic Committee, and all the 20 patients signed the informed consent. The clinical characteristics of the 20 enrolled patients are summarized in the Table 1S. We observed that neither serum creatinine nor cystatin C was altered by administration of a single high (80 mg) atorvastatin loading dose (Figure 2S).

Table1S. Clinical characteristics of the 20 patients.

Age, years	75±11
Male	10 (50%)
BMI (kg/m²)	28±6
sCr, mg/dL	1.45 (1.06-1.67)
eGFR, ml/min/1.73 m²	43±9
sCyC, mg/dL	1.48 (1.30-1.80)
Diabetes mellitus	9 (45%)
Hypertension	15 (75%)
LV ejection fraction, %	55±7
Drugs:	
ACE inhibitor	8 (40%)
Calcium channel blocker	6 (30%)
Angiotensin II receptor inhibitor	6 (30%)
Diuretics	10 (50%)
Beta blockers	14 (70%)

BMI = body mass index. sCr = serum creatinine; eGFR = estimated glomerular filtration rate; sCyC = serum cystatin C; LV = left ventricular. sCr and sCyC are expressed as median and Q1-Q3.

Figure 2S



*p >0.05 by paired *t* test versus baseline.

Patients lost at follow-up.

Table 2S. Clinical characteristics of the patients lost at follow-up

	Patients included (n= 410)	Patients lost at follow-up (n= 17)	P
Age (years)	70 ± 9	68 ± 6	0.53
Male	223 (54%)	10 (59%)	0.80
Body-mass index (kg/m²)	28±5	27±2	0.37
LV ejection fraction (%)	50±9	51±7	0.58
Systemic Hypertension	354 (86%)	15 (88%)	0.95
Diabetes Mellitus	169 (41%)	7 (41%)	0.80
Volume of contrast media (ml)	180±76	171±49	0.51
Contrast ratio >1	106 (26%)	4 (23%)	0.96

LV = left ventricular; Continuous values are expressed as mean ± standard deviation; categorical values are expressed as a total number and as a percentage of the global population (in parenthesis).

Table 3S. Clinical characteristics of the patients lost at follow-up.

	Patients included (n= 410)	Patients lost at follow-up (n= 17)	P
Serum creatinine, median (range), mg/dl	1.30 (0.88-1.62)	1.30 (1,20-1.45)	0.56
Serum cystatin C, median (range), mg/dl	1.25 1.0-1.62)	1.22 (1.02-1.55)	0.56
eGFR (ml/min/1.73 m²)	43 ± 14	45 ± 8	0.54
Contrast nephropathy risk score*	7.8 ± 2.7	8.1 ± 2.8	0.65

eGFR = estimated glomerular filtration rate. *According to Mehran et al. ⁷. Continuous values are expressed as median and first and third quartiles (serum creatinine and cystatin C) or mean ± standard deviation; categorical values are expressed as a total number and as a percentage of the global population (in parenthesis).

FIGURE LEGENDS Supplement

Figure 1S. Panel A: serum creatinine concentration at baseline, 24 and 48 hours after contrast media administration in the *Control group* (**open symbol, continuous line**) and in the *Atorvastatin group* (**closed symbol, dashed line**); **Panel B:** incidence of contrast-induced-acute kidney injury (CIAKI; defined as a serum creatinine increase ≥ 0.5 mg/dl at 48 hours) in the *Control group* and in the *Atorvastatin group*. **Panel C:** incidence of contrast-induced-acute kidney injury (CIAKI; defined as a serum creatinine increase $\geq 25\%$ at 48 hours) in the *Control group* and in the *Atorvastatin group*.

Figure 2S. Serum creatinine (panel A) and cystatin C (panel B) concentrations at baseline and at 24 and 48 hours after a single high (80 mg) loading dose of atorvastatin in patients with chronic kidney disease. * $p > 0.05$ by paired *t* test versus baseline.

Impact of a High Loading Dose of Atorvastatin on Contrast-Induced Acute Kidney Injury

Cristina Quintavalle, Danilo Fiore, Francesca De Micco, Gabriella Visconti, Amelia Focaccio, Bruno Golia, Bruno Ricciardelli, Elvira Donnarumma, Antonio Bianco, Maria Assunta Zabatta, Giancarlo Troncone, Antonio Colombo, Carlo Briguori and Gerolama Condorelli

Circulation. 2012;126:3008-3016; originally published online November 12, 2012;
doi: 10.1161/CIRCULATIONAHA.112.103317

Circulation is published by the American Heart Association, 7272 Greenville Avenue, Dallas, TX 75231
Copyright © 2012 American Heart Association, Inc. All rights reserved.
Print ISSN: 0009-7322. Online ISSN: 1524-4539

The online version of this article, along with updated information and services, is located on the
World Wide Web at:

<http://circ.ahajournals.org/content/126/25/3008>

Data Supplement (unedited) at:

<http://circ.ahajournals.org/content/suppl/2012/11/12/CIRCULATIONAHA.112.103317.DC1.html>

Permissions: Requests for permissions to reproduce figures, tables, or portions of articles originally published in *Circulation* can be obtained via RightsLink, a service of the Copyright Clearance Center, not the Editorial Office. Once the online version of the published article for which permission is being requested is located, click Request Permissions in the middle column of the Web page under Services. Further information about this process is available in the [Permissions and Rights Question and Answer](#) document.

Reprints: Information about reprints can be found online at:
<http://www.lww.com/reprints>

Subscriptions: Information about subscribing to *Circulation* is online at:
<http://circ.ahajournals.org/subscriptions/>

ORIGINAL ARTICLE

Effect of miR-21 and miR-30b/c on TRAIL-induced apoptosis in glioma cells

C Quintavalle^{1,2,7}, E Donnarumma^{3,7}, M Iaboni^{1,2}, G Roscigno^{1,2}, M Garofalo⁴, G Romano³, D Fiore¹, P De Marinis⁵, CM Croce⁴ and G Condorelli^{1,2,6}

Glioblastoma is the most frequent brain tumor in adults and is the most lethal form of human cancer. Despite the improvements in treatments, survival of patients remains poor. To define novel pathways that regulate susceptibility to tumor necrosis factor-related apoptosis-inducing ligand (TRAIL) in glioma, we have performed genome-wide expression profiling of microRNAs (miRs). We show that in TRAIL-resistant glioma cells, levels of different miRs are increased, and in particular, miR-30b/c and -21. We demonstrate that these miRs impair TRAIL-dependent apoptosis by inhibiting the expression of key functional proteins. T98G-sensitive cells treated with miR-21 or -30b/c become resistant to TRAIL. Furthermore, we demonstrate that miR-30b/c and miR-21 target respectively the 3' untranslated region of caspase-3 and TAp63 mRNAs, and that those proteins mediate some of the effects of miR-30 and -21 on TRAIL resistance, even in human glioblastoma primary cells and in lung cancer cells. In conclusion, we show that high expression levels of miR-21 and -30b/c are needed to maintain the TRAIL-resistant phenotype, thus making these miRs as promising therapeutic targets for TRAIL resistance in glioma.

Oncogene advance online publication, 10 September 2012; doi:10.1038/onc.2012.410

Keywords: glioblastoma; TRAIL; therapy; microRNA; treatment; apoptosis

INTRODUCTION

Glioblastomas are the most common primary tumors of the brain and are divided into four clinical grades on the basis of their histology and prognosis.¹ These tumors are highly invasive, very aggressive and are one of the most incurable forms of cancer in humans.² The treatment strategies for this disease have not changed appreciably for many years, and failure of treatment occurs in the majority of patients owing to the strong resistant phenotype. Therefore, the development of new therapeutic strategies is necessary for this type of cancer.

A novel interesting therapeutic approach is the reactivation of apoptosis using member of TNF (tumor necrosis factor)-family, of which the tumor necrosis factor-related apoptosis-inducing ligand (TRAIL) holds the greatest interest. Apoptosis is a particularly desirable treatment outcome, as it eradicates cancer cells without causing a major inflammatory response, which could provide unwanted survival signals. However, many cancers develop functional defects in the drug-induced apoptosis pathway, which may lead to constitutive or acquired resistance. To this end, alternative pathways, such as the one activated by death receptors including Fas/Apo-1, or DR4 (TRAIL-R1) and DR5 (TRAIL-R2), are being explored for cancer treatment. TRAIL is a relatively new member of the TNF family, known to induce apoptosis in a variety of cancers.³ Treatment with TRAIL induces programmed cell death in a wide range of transformed cells, both *in vivo* and *in vitro*, without producing significant effects in normal cells.^{3,4} Therefore, recombinant TRAIL or monoclonal antibodies against its receptors (TRAIL-R1 and TRAIL-R2) are in phase II/III

clinical trials for different kinds of tumors, either as a single agent or in combination with chemotherapy.^{5,6}

However, a significant proportion of human cancer cells are resistant to TRAIL-induced apoptosis, and the mechanisms of sensitization seem to differ among cell types. Different studies relate resistance to TRAIL-induced cell death to downstream factors. It has been shown that downregulation of two anti-apoptotic proteins such as PED (Phosphoprotein enriched in diabetes) or cellular-FLICE such as inhibitory protein (c-FLIP) can sensitize cells to TRAIL-induced apoptosis.^{7–9} However the mechanism of TRAIL resistance is still largely unknown.

miRs are a class of endogenous non-coding RNA of 19–24 nucleotides in length that has an important role in the negative regulation of gene expression blocking translation or directly cleaving the targeted mRNA.¹⁰ miRs are involved in the pathogenesis of most cancers.¹⁰ In the last few years, our understanding of the role of miRNA has expanded from the initially identified functions in the development of round worms to a highly expressed and ubiquitous regulators implicated in a wide array of critical processes, including proliferation, cell death and differentiation, metabolism and, importantly, tumorigenesis.¹¹ We have recently showed an important role of microRNAs in TRAIL sensitivity in non-small cell lung cancer (NSCLC).^{12–14}

In this study, to identify novel mechanisms implicated in TRAIL resistance in human glioma, we performed a genome-wide expression profiling of miRs in different cell lines. We found that miR-30b/c and -21 are markedly upregulated in TRAIL-resistant, and downregulated in TRAIL-sensitive glioma cells.

¹Department of Cellular and Molecular Biology and Pathology, 'Federico II' University of Naples, Naples, Italy; ²IEOS, CNR, Naples, Italy; ³Fondazione IRCCS SDN, Naples, Italy; ⁴Department of Molecular Virology, Immunology and Medical Genetics, Human Cancer Genetics Program, Comprehensive Cancer Center, The Ohio State University, Columbus, OH, USA; ⁵Neurosurgery Unit, Ospedale A. Cardarelli, Napoli, Italy and ⁶Facoltà di Scienze Biotechnologiche, 'Federico II' University of Naples, Naples, Italy. Correspondence: Professor G Condorelli, Department of Cellular and Molecular Biology and Pathology, 'Federico II' University of Naples, Via Pansini, 5, Ed 19 A, II floor, Naples 80131, Italy. E-mail: gecondor@unina.it

⁷These authors contributed equally to this work.

Received 28 February 2012; revised 13 June 2012; accepted 23 July 2012

Our experiments indicate that miR-30b/c and -21 modulate TRAIL sensitivity in glioma cells mainly by modulating caspase-3 and Tap63 expression and TRAIL-induced caspase machinery.

RESULTS

Selection of TRAIL-sensitive vs TRAIL-resistant glioma cell lines

We analyzed TRAIL sensitivity of different human glioma cell lines. Cells were exposed to TRAIL at two different concentrations for 24 h and cell death was assessed using the MTT assay (Figure 1a) or propidium iodide staining (Figure 1b). As shown in Figure 1, we can distinguish two sets of cells: TB10, LN229, U251 and U87MG cells exhibited total or partial TRAIL resistance, whereas T98G and LN18 cells underwent TRAIL-induced cell death.

miRs expression screening in TRAIL-resistant vs TRAIL-sensitive glioma cell lines

To investigate the involvement of miRs in TRAIL resistance in glioblastoma cell lines, we analyzed the miRs expression profile in the most TRAIL-resistant glioma cells (TB10 and LN229) vs the TRAIL-sensitive cells (T98G and LN18). The analysis was performed with a microarray chip containing 1150 miR probes, including 326 human and 249 mouse miRs, spotted in duplicates. Data obtained indicated that seven miRs (miR-21, -30b, -30c, -181a, -181d, -146 and -125b) were significantly overexpressed in resistant glioma cells with at least > 1.9-fold change (Table 1). Quantitative real-time-polymerase chain reaction (qRT-PCR) validated the microarray analysis (data not shown).

Role of miRs in TRAIL resistance in glioma

To test the role of these overexpressed miRs in TRAIL sensitivity in glioma, we transfected T98G TRAIL-sensitive cells with miR-21, -30b, -30c, -181a, -146 and -125b. TRAIL sensitivity was evaluated by MTT assay, propidium iodide staining and colony assay. We obtained significant results only for miR-30b/c and miR-21 that

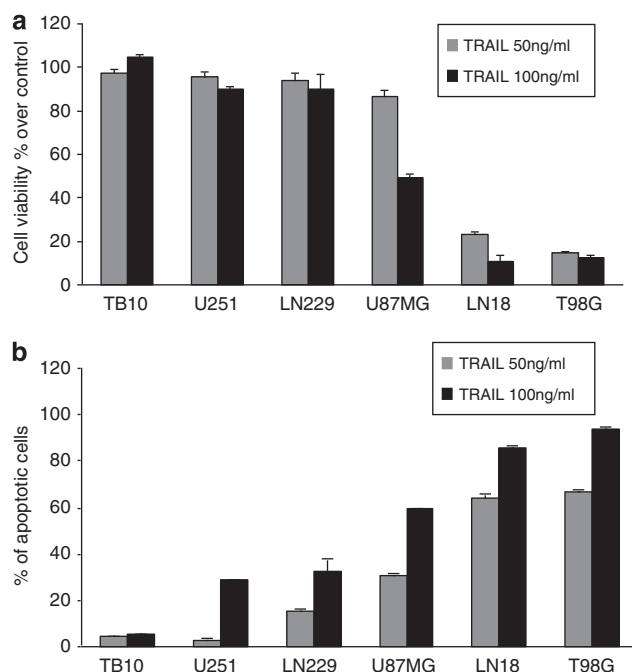


Figure 1. TRAIL sensitivity of glioblastoma cells. Glioblastoma cell lines (10^4 cell) were treated with superKiller TRAIL. After 24 h of treatment, the effect on cell death was assessed with MTT assay (a) or by propidium iodide staining and FACS analysis (b).

were then extensively investigated. In fact, data obtained with MTT assay and FACS analysis showed that the overexpression of miR-30b/c and -21 was able to revert TRAIL sensitivity in T98G (Figures 2a and b). Similar results were obtained in LN18 cells (Figures 2c and d). This effect was not restricted to glioma, as miR-30 and miR-21 were able to exert an anti-apoptotic action also in non small cell lung cancer (NSCLC) (Supplementary Figure 3B). We further evaluated TRAIL sensitivity by colony assay. T98G and LN18 cells were transfected with miR-scrambled, miR-30b/c and miR-21 for 48 h and then were treated with 50 or 100 ng/ml of superKiller TRAIL for 24 h. Cells were grown for 6 days and then coloured with crystal violet-methanol solution (Supplementary Figures 1A and B). The results indicated that both miRs induced an increase of TRAIL resistance.

To further explore the role of miR-21 and -30b/c on TRAIL sensitivity, we transfected U251 (Figure 3a) or LN229 (Figure 3b) TRAIL-resistant cells with anti-miR-21, -30b, 30c, or with a scrambled sequence. As shown in Figures 3a and b, transfection of the anti-miR sequences was able to sensitize U251 and LN229 cells to TRAIL. Anti-miR-21 and -30c were also able to sensitize to TRAIL the CALU-1-resistant non-small cell lung cancer (NSCLC) TRAIL-resistant cell lines (Supplementary Figure 3C), indicating that this effect was not restricted to glioma.

Identification of cellular targets of miR-30b/c and miR-21 in glioma cells

To identify cellular targets of miR-30b/c and -21, we used as first attempt a bioinformatic search, using programs available on the web including Pictar, TargetScan, miRanda and Microcosm target.

miR-21 targets different tumor suppressor genes and proteins potentially involved in TRAIL resistance in glioblastoma cells, such as PTEN (phosphatase and tensin homologue), PDCD4 (programmed cell death 4), TPM1 (Tropomyosin 1) and p53.¹⁵⁻¹⁷ Computer-assisted analysis identified the presence of evolutionary-conserved binding sites for miR-21 in *Tap63* gene. We focused our attention on this p53 family member, as it regulates the expression of TRAIL receptors and molecules involved in TRAIL signaling.¹⁸ We also searched for miR-30 targets and among them we focused on caspase-3.

TRAIL-resistant and TRAIL-sensitive glioma or NSCLC cells exhibited different levels of miR-21 and -30c assessed by either qRT-PCR (Figure 4a and Supplementary Figure 3A) or by northern blot analysis (Supplementary Figure 4). Interestingly, we observed a reduction of protein (Figure 4b and Supplementary Figure 3D) and mRNA (Figure 4c) levels of *Tap63* and caspase-3 upon, respectively, miR-21 or miR-30c and miR-30b (data not shown) transfection in TRAIL-sensitive cell lines. We didn't observe a

Table 1. microRNA identified in TRAIL-resistant glioma (LN229 and TB10) compared with TRAIL-sensitive (T98G, LN18) cells

miR	P-value	Fold difference
hsa-miR-125b1-A	6.09e - 05	3.033
hsa-miR-30b-A	9.14e - 05	2.041
hsa-miR-30c-A	0.0001199	2.337
hsa-miR-146b-A	0.0001556	5.972
hsa-miR-181a-5p-A	0.0004698	2.66
hsa-miR-181d-A	0.0004817	3.035
hsa-miR-21-A	0.0032482	1.949

miRNA expression profiles in TRAIL-sensitive vs TRAIL-resistant cells. miRNA screening was performed in triplicate for TRAIL-sensitive and TRAIL-resistant cell lines by a microarray as described in Materials and methods. A two-tailed, two-sample *t*-test was used ($P < 0.05$). Seven miRNAs were found to be significantly deregulated in TRAIL-resistant cells compared with the TRAIL sensitive.

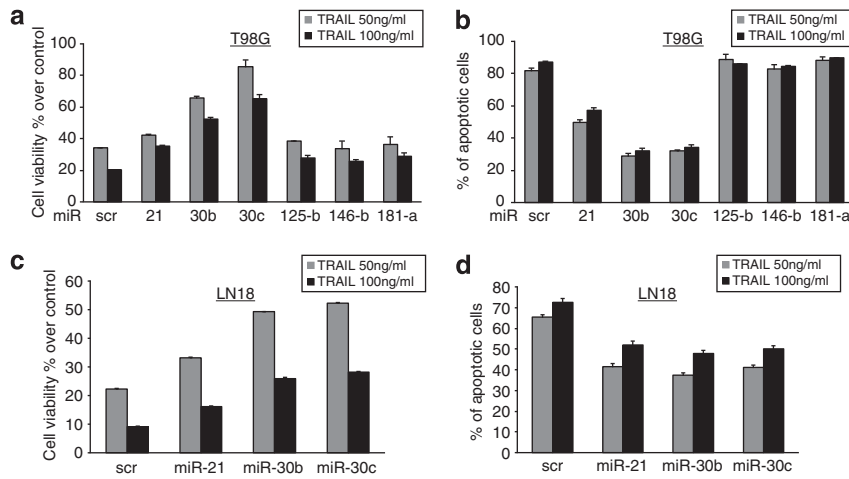


Figure 2. Effect of miR-21 and miR-30c overexpression on TRAIL-sensitive glioblastoma cells. T98G (a, b) cells were transfected with miR-21, miR-30b, miR-30c, miR-125b, miR-146b and miR-181a. LN18 (c, d) were transfected with miR-21, miR-30b and miR-30c. 10⁴ cells were then treated with two different concentrations of superkiller TRAIL. After 24 h of treatment, cell viability was assessed with MTT assay (a, c) or with propidium iodide staining and FACS analysis (b, d). Both miR-21 and miR-30 induce TRAIL resistance in glioma cells.

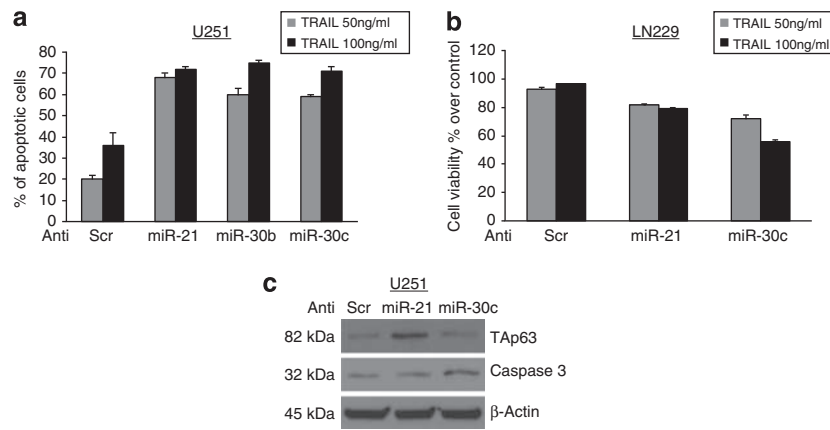


Figure 3. Effects of anti-miR-21 and anti-miR-30b/c on TRAIL sensitivity. Knock down of miR-21 and anti-miR-30b/c increases the percentage of apoptotic cells as assessed by propidium iodide staining in U251 cells (a) and decreases the cell viability of LN229 (b). (c) Tap63 and caspase-3 western blot analysis of U251 cells transfected with a scrambled sequence as negative control and with anti-miR-21 or anti-miR-30c, as indicated.

decrease in the levels of other caspases upon miR-30c transfection (Figure 4b). On the contrary, Tap63 and caspase-3 protein levels increased upon anti-miR-21 and anti-miR-30c transfection (Figure 3c and Supplementary Figure 3D) in TRAIL-resistant cell lines. To verify a direct link between the miR-21/Tap63 and miR-30b/c and caspase-3, we performed luciferase assay by co-transfecting pGL3-3' untranslated region (UTR) vectors along with miR-21 or miR-30c. The results obtained indicated a direct interaction of miR-21 with Tap63 and miR-30c with caspase-3 (Figure 4d). As indicated in Figure 4d, miR-30b and -30c have the same seed sequence that recognizes caspase-3, differing only at the latest four nucleotides of the 5'. Therefore, miR-30b down-regulates caspase-3 at the same extent than miR-30c (data not shown). Deletions in seed complementary sites rescued the repression of miR-21 and miR-30c on their identified targets (Figure 4d).

Validation of miR-21 and miR-30b/c mechanisms of action

To demonstrate that miR-21 and miR-30b/c, by downregulating Tap63 and caspase-3, are responsible for the TRAIL resistance observed in T98G and LN18 cells, we transfected T98G with

caspase-3 or Tap63 complementary DNAs lacking the miRNA-binding site in their 3'UTR or with a control vector and miR-30c (Figure 5a) or miR-21 (Figure 5b). Interestingly, transfection of Tap63 and caspase-3 was able to overcome the effects of miR-21 and miR-30c, decreasing cell viability and increasing apoptosis (Figures 5a and b). The data were confirmed by colony assay in T98G cells (Supplementary Figures 2A and B). Similar results were obtained when we analyzed miR-30b (data not shown). These rescue experiments proved the causative link between miR-21/Tap63 and caspase-3/miR-30b/c and TRAIL sensitivity.

Effect of miR-21 and miR-30c expression on TRAIL sensitivity in primary human glioma cell lines

MiR-21 and miR-30c expression levels were measured by qRT-PCR in nine different human primary cell lines (Figure 6a), eight derived from glioblastoma tumors (patient no. 1 to no. 8) and one from tissue surrounding the tumor (patient no. 9), and compared with TRAIL sensitivity. As shown in Figure 6b, TRAIL sensitivity correlated with miR-21 and miR-30c expression levels in all cases analyzed, with the exception of control sample that did not respond to TRAIL. Moreover, anti-miRs expression in TRAIL-

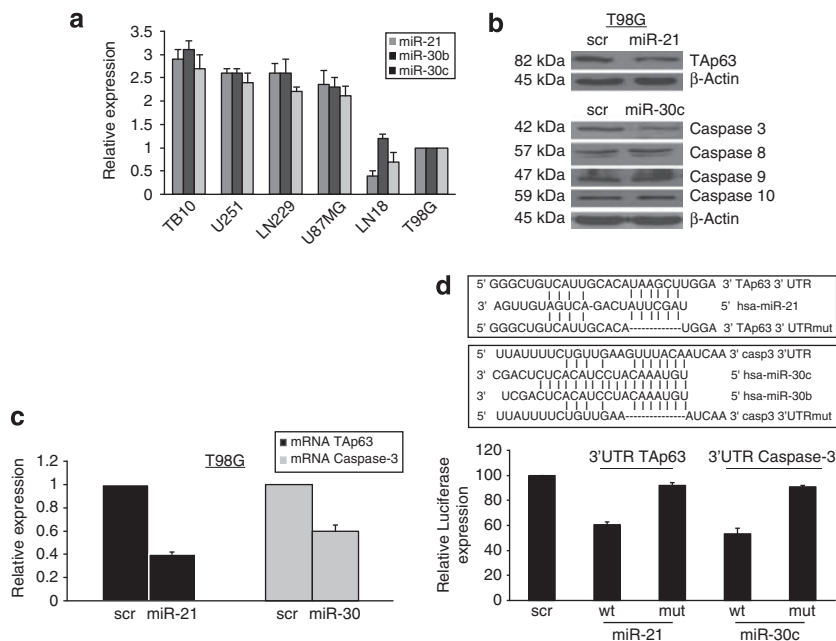


Figure 4. Tap63 and caspase-3 are targets of miR-21 and miR-30c. **(a)** qRT-PCR expression of miR-21, miR-30c and miR-30b in TB10, LN229, U251, U87MG, LN18 and T98G glioma cells. **(b)** Tap63 and caspase-3, caspase-8, caspase-9 and caspase-10 western blot analysis of T98G cells transfected with a scrambled sequence as negative control and with miR-21 and miR-30c, as indicated. **(c)** qRT-PCR of Tap63 and caspase-3 mRNA in T98G transfected with a negative control and with miR-21 and miR-30c, as indicated. **(d)** Alignment between miR-21 and 3'UTR Tap63 wild type or mutant and between miR-30c and 3'UTR caspase-3 wild type or mutant. Luciferase activity of PGL3-3'UTR Tap63 and of PGL3-3'UTR caspase-3 vector after HEK-293 transfection with scrambled miR, miR-21 and miR-30c wild type or mutated, as indicated.

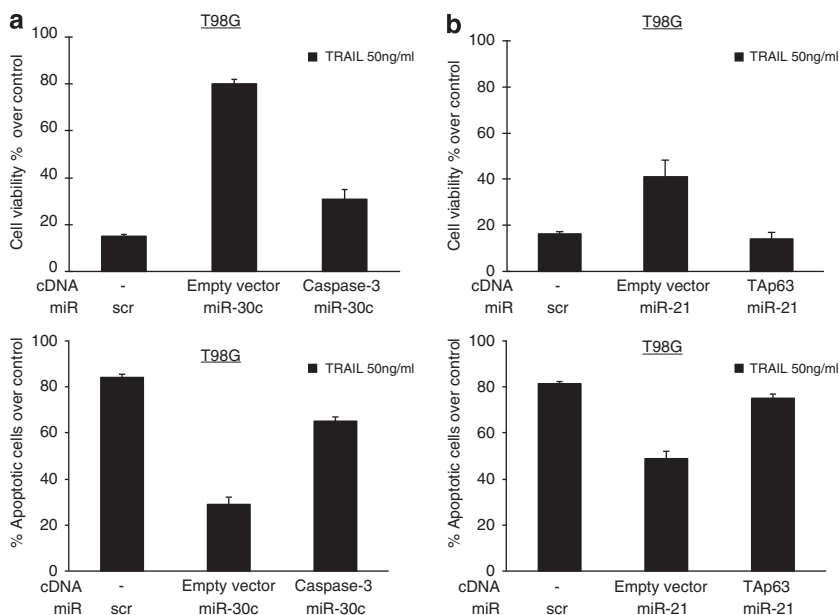


Figure 5. Validation of the involvement of caspase-3 and Tap63 in TRAIL sensitivity. Cell viability assay (upper panels) and propidium iodide staining (lower panels) of T98G cells transfected with miR-30c **(a)** and miR-21 **(b)** in the presence of cDNA for caspase-3 or Tap63.

resistant primary cultured cells (patient no. 1 and no. 2) was able to determine an increase of TRAIL sensitivity (Figure 6c) and concomitantly an increase of the levels of Tap63 and caspase-3 (Figure 6d).

DISCUSSION

Sensitization of cancer cells to apoptosis could be a valuable strategy to define new treatment options for cancer, in particular

when using agents that aim to directly activate apoptotic pathways. A promising agent is the death receptor ligand TRAIL,¹⁹ as it induces apoptosis in most cancer cells, but not in normal cells.^{20,21} Moreover, TRAIL exhibits potent tumoricidal activity *in vivo* in several xenograft models, including malignant glioma.^{22,23} Indeed, agonistic anti-TRAIL receptor monoclonal antibodies (mAbs), including mapatumumab (HGS-ETR1, anti-human DR4 mAb),²⁴ lexatumumab (HGS-ETR2, anti-human DR5 mAb)²⁵ and MD5-1 (anti-mouse DR5 mAb) are currently under

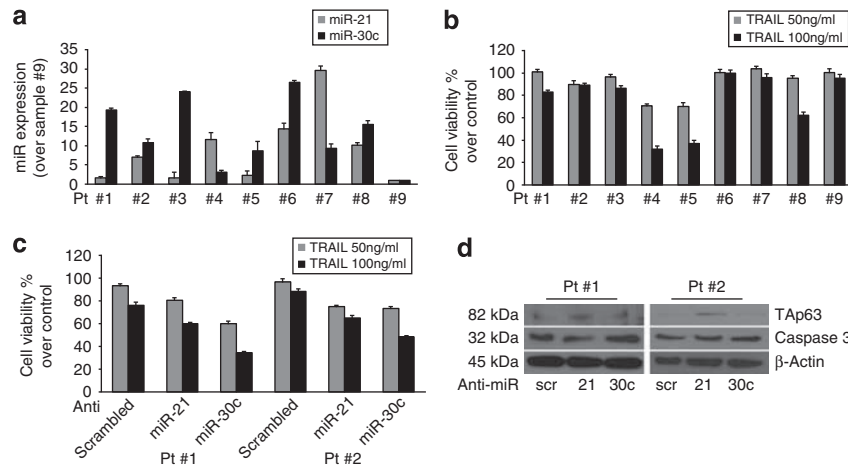


Figure 6. Effect of miR-21 and 30c on primary glioblastoma cell lines. **(a)** qRT-PCR analysis of miR-21 and miR-30c levels in eight primary glioblastoma cancer cell lines and one primary cell line derived from the surrounding tumor tissue used as control. **(b)** TRAIL sensitivity of primary cell lines (10^4 cells) treated with two different doses of SuperKiller TRAIL for 24 h, as indicated. **(c)** Cell viability assay of glioblastoma cells from two patients (#1 and #2) transfected with anti-miR-21 and anti-miR-30c and then treated with 50 ng/ml and 100 ng/ml of TRAIL for 24 h. Anti-miRs treatment sensitized glioblastoma cells to TRAIL. **(d)** Western blot analysis of TAP63 and caspase-3 after anti-miR-21 and anti-miR-30c transfection in patient #1 and #2.

intensive investigation. The former two mAbs have been tested in phase 1 clinical trials in patients with systemic malignancy, exhibiting excellent safety profiles. Anti-mouse DR5 mAb MD5-1 could also be administered safely without inducing hepatotoxicity either alone or in combination with histone deacetylase inhibitors in mice.²⁶ The induction of apoptosis by TRAIL is essentially dependent on the expression of specific TRAIL receptors and on the activation of caspases,²⁰ thus the regulation of the expression levels of those molecules is of fundamental importance.

MicroRNAs are emerging as key regulators of multiple pathways involved in cancer development and progression,^{27–29} and may become the next targeted therapy in glioma. The present study shows that microRNA expression may modulate TRAIL-induced apoptosis in glioma cells, by the regulation of caspase-3 and TAp63 levels. We analyzed the miRs profile of TRAIL-resistant compared with TRAIL-sensitive glioma cells. We then focused our attention on miR-30b/c and miR-21, as only these miRs among those identified by the array, demonstrated the ability to revert the TRAIL-sensitive phenotype. We also provided evidences that this regulation is not restricted to glioma, but it is present also in a different type of cancer such as NSCLC.

MiR-21 has been found overexpressed in high-grade glioma patients³⁰ and studies have identified different miR-21 key targets for glioma biology, such as *RECK*, *TIMP3*, *Spry2* and *Pdcd4* genes, which are suppressors of malignancy and inhibitors of matrix metalloproteinase.^{16,31–33} Moreover, levels of expression of miR-21 have been associated to patients survival.³⁴

Other studies indicate that knockdown of miR-21 in cultured glioblastoma cells triggers activation of caspases and leads to increased apoptotic cell death.³⁵ Corsten *et al.*³⁶ hypothesized that suppression of miR-21 might sensitize gliomas for cytotoxic tumor therapy. With the use of locked nucleic acid (LNA)-anti-miR-21 oligonucleotides and neural precursor cells (NPC) expressing a secretable variant of TRAIL (S-TRAIL), they showed that the combined suppression of miR-21 and NPC-S-TRAIL leads to a synergistic increase in caspase activity and a decreased cell viability in human glioma cells *in vitro* and *in vivo* in xenograft experiments. Interestingly, Papagiannakopoulos *et al.*¹⁵ described that miR-21 targets multiple important components of the p53 tumor-suppressive pathways. They showed that downregulation of miR-21 in glioblastoma cells leads to repression of growth,

increased apoptosis and cell cycle arrest, through the regulation of target proteins such as HNRPK and TAp63. Our study describes for the first time the direct link between miR-21, TAp63 and TRAIL sensitivity. We demonstrated that miR-21 targets the 3'UTR sequence of TAp63, and that transfection of miR-21 is able to downregulate TAp63 at both mRNA and protein levels. More importantly, we demonstrated that miR-21, through TAp63, is able to modulate TRAIL sensitivity, as the co-transfection of miR-21 and TAp63 cDNA renders the cells again responsive to TRAIL. TAp63 is a transcription factor that regulates the expression levels of different apoptosis-regulating genes, such as TRAIL receptors, bcl211 and Apaf1.¹⁸ Thus, it is possible that those apoptosis-regulating molecules are regulated by miR-21 through TAp63.

Several studies link miR-30 to apoptosis and human cancer. Li *et al.*³⁷ demonstrated that miR-30 family members inhibited mitochondrial fission through the suppression of the expression of p53 and its downstream target Drp1, whereas, Joglekar *et al.*³⁸ demonstrated that miR-30 may have a role in epithelial-to-mesenchymal transition. Our recent data demonstrate that miR-30 targets the anti-apoptotic protein BIM, participating to gefitinib resistance in lung cancer.³⁹ MiR-30 has been also associated with stem cell properties. Yu *et al.*⁴⁰ described that miR-30 is reduced in breast tumor stem cells (BT-ICs), and demonstrated that enforced expression of miR-30 in BT-ICs inhibits their self-renewal capacity by reducing Ubc9, and induces apoptosis through silencing ITGB3. In our hands, miR-30 overexpression inhibits TRAIL-induced apoptosis in glioma cells by targeting caspase-3. In fact, modulating the expression of either miR-30 or caspase-3, we observed a modification of TRAIL sensitivity of glioma cells. The opposing results on the role of miR-30 on cell death may be ascribed either to different cell system (breast vs glioma), or to different type of cancer cell (stem vs differentiated cells). In favour of this hypothesis, many reports describe opposing role of miRs in a different cell context.²⁸ Recently, miR-30d has been described to target caspase-3 in breast cancer cells, and thus to regulate apoptosis.⁴¹ The seed sequence recognizing the 3'UTR of caspase-3 is highly homologous within the members of the miR-30 family (miR-30b/c/d) suggesting a more generalized role of miR-30 family members in the regulation of cell death and cancer progression.

In many experiments, we observed that there is a redundancy within miR-21 and miR-30 in the regulation of TRAIL sensitivity. Our data, either in primary or in established cell lines, demonstrates that it is sufficient that one of the two miRNAs is highly expressed in the cells, that apoptosis resistance will manifest. We have also observed that miR-30 has a predominant effect in contrasting TRAIL-induced apoptosis. This may be related to the effect of this miR in targeting one important component of the cell death machinery, that is, caspase-3.

In conclusion, our study analyzed microRNA expression pattern in TRAIL-resistant and TRAIL-sensitive glioma cells, and identified specific miRNAs and their targets involved in the regulation of the apoptotic programme. This may be of relevance for future cancer therapy improvement in glioma.

MATERIALS AND METHODS

Cell culture and transfection

U87MG, T98G, U251, TB10, CALU-1 and 293 cells were grown in Dulbecco's modified Eagle's medium (DMEM). H460 were grown in RPMI. Media were supplemented with 10% heat-inactivated fetal bovine serum, 2 mM L-glutamine and 100 U/ml penicillin/streptomycin. LN229 and LN18 were grown in Advanced DMEM (Invitrogen, Milan Italy) + 2 mM Glutamine + 5% fetal bovine serum. For miRNAs transient transfection, cells at 50% confluency were transfected using Oligofectamine (Invitrogen) with 100 nM of pre-miR-30c, -30b, -125b, -146b, -181a, -21, miR-scrambled or anti-miR- (Applied Biosystems, Milan, Italy). For caspase-3 and TAp63 transient transfection, cells were transfected using Lipofectamine and Plus Reagent with 4 µg of caspase-3 cDNA (Origene, Rockville, MD, USA) or TAp63 cDNA for 24 h. TAp63 cDNA was obtained from Professor Viola Calabrò (Naples). SuperKiller TRAIL for cell treatment was purchased from Enzo Biochem (New York, NY, USA).

Primary cell cultures

Glioblastoma specimens were collected at neurosurgical Unit of Cardarelli hospital (Naples). All the samples were collected according to a prior consent of the donor before the collection, acquisition or use of human tissue. To obtain the cells, samples were mechanically disaggregated, then the lysates were grown in DMEM-F12 medium supplemented with 10% fetal bovine serum 1% penicillin streptomycin and 20 ng/ml EGF (Sigma-Aldrich, Milan, Italy). To exclude a fibroblast contamination, cells were stained for GFAP, a protein found in glial cells.

Protein isolation and western blotting

Cells were washed twice in ice-cold phosphate-buffered saline, and lysed in JS buffer (50 mM HEPES pH 7.5 containing 150 mM NaCl, 1% Glycerol, 1% Triton X-100, 1.5 mM MgCl₂, 5 mM EGTA, 1 mM Na₃VO₄ and 1 × protease inhibitor cocktail). Protein concentration was determined by the Bradford assay (Bio-Rad, Milan, Italy) using bovine serum albumin as the standard, and equal amounts of proteins were analyzed by SDS-PAGE (12.5% acrylamide). Gels were electroblotted onto nitrocellulose membranes (Millipore, Bedford, MA, USA). For immunoblot experiments, membranes were blocked for 1 h with 5% non-fat dry milk in Tris-buffered saline containing 0.1% Tween-20, and incubated at 4 °C over night with primary antibody. Detection was performed by peroxidase-conjugated secondary antibodies using the enhanced chemiluminescence system (GE Healthcare, Milan, Italy). Primary antibodies used were: anti-βActin from Sigma-Aldrich; anti-caspase-8, 9 and 10 were from Cell Signalling Technology (Boston, MA, USA); anti-Caspase 3 and anti-TAp63 from Santa Cruz Biotechnologies (Santa Cruz, CA, USA).

miRNA microarray experiments

From each sample, 5 µg of total RNA (from T98G, LN18, TB10, LN229 cells) was reverse transcribed using biotin-end-labelled random-octamer oligonucleotide primer. Hybridization of biotin-labelled cDNA was performed on an Ohio State University custom miRNA microarray chip (OSU_CCC version 3.0), which contains 1150 miRNA probes, including 326 human and 249 mouse miRNA genes, spotted in duplicates. The hybridized chips were washed and processed to detect biotin-containing transcripts by streptavidin-Alexa647 conjugate and scanned on an Axon 4000B microarray scanner (Axon Instruments, Sunnyvale, CA, USA).

Raw data were normalized and analyzed with GENESPRING 7.2 software (zcomSilicon Genetics, Redwood City, CA, USA). Expression data were median-centered by using both the GENESPRING normalization option and the global median normalization of the BIOCONDUCTOR package (www.bioconductor.org) with similar results. Statistical comparisons were done by using the GENESPRING ANOVA tool, predictive analysis of microarray and the significance analysis of microarray software (<http://www-stat.stanford.edu/~tibs/SAM/index.html>).

RNA extraction and real-time PCR

Total RNAs (miRNA and mRNA) were extracted using Trizol (Invitrogen) according to the manufacturer's protocol. Reverse transcription of total miRNA was performed starting from equal amounts of total RNA per sample (1 µg) using miScript reverse Transcription Kit (Qiagen, Milan, Italy), for mRNAs SuperScript III Reverse Transcriptase (Invitrogen) was used. For cultured cells, quantitative analysis of Caspase-3, TAp63, β-Actin (as an internal reference), miR-30b/c, miR-21 and RNU5A (as an internal reference) were performed by real-time PCR using specific primers (Qiagen), miScript SYBR Green PCR Kit (Qiagen) and iQ SYBR Green Supermix (Bio-Rad), respectively. The reaction for detection of mRNAs was performed as follow: 95 °C for 15', 40 cycles of 94 °C for 15', 60 °C for 30' and 72 °C for 30'. The reaction for detection of miRNAs was performed as follow: 95 °C for 15', 40 cycles of 94 °C for 15', 55 °C for 30' and 70 °C for 30'. All reactions were run in triplicate. The threshold cycle (CT) is defined as the fractional cycle number at which the fluorescence passes the fixed threshold. For relative quantization, the 2^(-ΔCT) method was used as previously described.⁴² Experiments were carried out in triplicate for each data point, and data analysis was performed by using software (Bio-Rad).

Northern blot analysis

RNA samples (30 µg) were separated by electrophoresis on 15% acrylamide, 7 mol/l urea gels (Bio-Rad, Hercules, CA, USA) and transferred onto Hybond-N+ membrane (Amersham Biosciences, Piscataway, NJ, USA). Hybridization was performed at 37 °C in 7% SDS/0.2 mol/l Na₂PO₄ (pH 7.0) for 16 h. Membranes were washed at 42 °C, twice with 2 × standard saline phosphate (0.18 mol/l NaCl/10 mmol/l phosphate (pH 7.4)), 1 mmol/l EDTA (saline-sodium phosphate-EDTA; SSPE) and 0.1% SDS and twice with 0.5 × SSPE/0.1% SDS. The oligonucleotides (PRIMM, Milan, Italy) used, complementary to the sequences of the mature miRNAs, were: miR-21-probe 5'-TCAACATCAGTCTGATAAGCTA-3'; miR-30c-probe 5'-GCTGAG AGTGTAGGATGTTTACA-3'. An oligonucleotide complementary to the U6 RNA (5'-GCAGGGCCATGCTAATCTTCTCTGTATCG-3') was used to normalize the expression levels. Totally, 100 pmol of each probe were end labelled with 50 mCi [³²P]ATP using the poly-nucleotide kinase (Roche, Basel, Switzerland). Blots were stripped by boiling in 0.1% SDS for 10 min before re-hybridization.

Luciferase assay

The 3' UTR of the human Caspase-3 genes was PCR amplified using the following primers: Caspase-3 forward: 5'-TCTAGAAGGGCGCCATCGCCAAG TAAGAAA-3', Caspase-3 reverse: 5'-TCTAGACCCGTGAAATGTCACTGA CAG-3' and cloned downstream of the Renilla luciferase stop codon in pGL3 control vector (Promega, Milan, Italy). A deletion was introduced into the miRNA-binding sites by using the QuikChange Mutagenesis Kit (Stratagene, La Jolla, CA, USA) using the following primers: Caspase-3 mut forward 5'-GCAAAATCTTAAGTATGTTATTTCTGTTGAAATCAAAGGA AAATAGTAATGTTTATACT-3'. Caspase-3mut reverse 5'-AGTATAAAACAT TACTATTTTCCTTTGATTTCAACAGAAAATAACATACTTAAGAATTTTGC-3'.

The 3' UTR of the human TAp63 gene was PCR amplified using the following primers: TAp63 forward: 5'-TCTAGAGCAAGAGATAAGTCTTT CATGGCTGCTG-3', TAp63 reverse: 5'-TCTAGATGGAAATCCCACTATCCCA AG-3', and cloned downstream of the Renilla luciferase stop codon in pGL3 control vector (Promega). A deletion was introduced into the miRNA-binding sites by using the QuikChange Mutagenesis Kit (Stratagene) using the following primers: TAp63 mut forward 5'-CTGGTCAAGGGCTGTCATTG CACTCCATTTAATTT-3' TAp63 mut reverse 5'-AAATTAATGGAGTGCAT GACGCCCTTGACCAG-3'.

Hek-293 cells were cotransfected with 1.2 µg of generated plasmid and 400 µg of a Renilla luciferase expression construct pRL-TK (Promega) with Lipofectamine 2000 (Invitrogen). Cells were harvested 24 h post transfection and assayed with Dual Luciferase Assay (Promega) according to the

manufacturer's instructions. Three independent experiments were performed in triplicate.

Cell death quantification

Cells were plated in 96-well plates in triplicate, stimulated and incubated at 37 °C in a 5% CO₂ incubator. SuperKiller TRAIL was used at final concentration of 50 or 100 ng/ml for 24 h. Apoptosis was analyzed via propidium iodide incorporation in permeabilized cells by flow cytometry. The cells (2×10^5) were washed in phosphate-buffered saline and resuspended in 200 µl of a solution containing 0.1% sodium citrate, 0.1% Triton X-100 and 50 µg/ml propidium iodide (Sigma). Following incubation at 4 °C for 30 min in the dark, nuclei were analyzed with a Becton Dickinson FACScan flow cytometer (Becton Dickinson, Milan, Italy). Cellular debris was excluded from analyses by raising the forward scatter threshold, and the DNA content of the nuclei was registered on a logarithmic scale. The percentage of elements in the hypodiploid region was calculated. Cell viability was evaluated with the CellTiter 96 AQueous One Solution Cell Proliferation Assay (Promega) according to the manufacturer's protocol. Metabolically active cells were detected by adding 20 µl of MTS to each well. After 2 h of incubation, the plates were analyzed in a Multilabel Counter (BioTek, Milan, Italy).

Colony assay

Cells were transfected with miR-scrambled, miR-30b/c or miR-21 for 24 h, then were harvested and 2.4×10^4 cells were plated in six-well plates. After 24 h, cells were treated with 50 or 100 ng/ml of superKiller TRAIL for 24 h, as indicated. Cells were transferred to 100 mm dishes and let grown for 6 days. Finally, the cells were coloured with 0.1% crystal violet dissolved in 25% methanol for 20 min at 4 °C. Dishes were washed with water and then let dry on the bench, and then photographs were taken.

ACKNOWLEDGEMENTS

This work was partially supported by funds from Associazione Italiana Ricerca sul Cancro, AIRC to GC (grant n.ro 10620), and MERIT (RBNE08E8CZ_002) to GC. CQ and MI are supported by the 'Federazione Italiana Ricerca sul Cancro' (FIRC) Post-Doctoral Research Fellowship. GR is supported by a MERIT project Fellowship.

REFERENCES

- 1 Tran B, Rosenthal MA. Survival comparison between glioblastoma multiforme and other incurable cancers. *J Clin Neurosci* 2010; **17**: 417–421.
- 2 Purow B, Schiff D. Advances in the genetics of glioblastoma: are we reaching critical mass? *Nat Rev Neurol* 2009; **5**: 419–426.
- 3 Schaefer U, Voloshanenko O, Willen D, Walczak H. TRAIL: a multifunctional cytokine. *Front Biosci* 2007; **12**: 3813–3824.
- 4 Falschlehner C, Emmerich CH, Gerlach B, Walczak H. TRAIL signalling: Decisions between life and death. *Int J Biochem Cell Biol* 2007; **39**: 1462–1475.
- 5 Younes A, Vose JM, Zelenetz AD, Smith MR, Burris HA, Ansell SM *et al*. A Phase 1b/2 trial of mapatumumab in patients with relapsed/refractory non-Hodgkin's lymphoma. *Br J Cancer* 2010; **103**: 1783–1787.
- 6 Trarbach T, Moehler M, Heinemann V, Kohne CH, Przyborek M, Schulz C *et al*. Phase II trial of mapatumumab, a fully human agonistic monoclonal antibody that targets and activates the tumour necrosis factor apoptosis-inducing ligand receptor-1 (TRAIL-R1), in patients with refractory colorectal cancer. *Br J Cancer* 2010; **102**: 506–512.
- 7 Garofalo M, Romano G, Quintavalle C, Romano MF, Chiurazzi F, Zanca C *et al*. Selective inhibition of PED protein expression sensitizes B-cell chronic lymphocytic leukaemia cells to TRAIL-induced apoptosis. *Int J Cancer* 2007; **120**: 1215–1222.
- 8 Zanca C, Garofalo M, Quintavalle C, Romano G, Acunzo M, Ragno P *et al*. PED is overexpressed and mediates TRAIL resistance in human non-small cell lung cancer. *J Cell Mol Med* 2008; **12**: 2416–2426.
- 9 Quintavalle C, Incoronato M, Puca L, Acunzo M, Zanca C, Romano G *et al*. c-FLIPL enhances anti-apoptotic Akt functions by modulation of Gsk3β activity. *Cell Death Differ* 2010; **17**: 1908–1916.
- 10 Calin GA, Croce CM. MicroRNA signatures in human cancers. *Nat Rev Cancer* 2006; **6**: 857–866.
- 11 Croce CM. Causes and consequences of microRNA dysregulation in cancer. *Nat Rev Genet* 2009; **10**: 704–714.
- 12 Garofalo M, Di Leva G, Romano G, Nuovo G, Suh SS, Ngankea A *et al*. miR-221 & 222 regulate TRAIL resistance and enhance tumorigenicity through PTEN and TIMP3 downregulation. *Cancer Cell* 2009; **16**: 498–509.

- 13 Garofalo M, Quintavalle C, Di Leva G, Zanca C, Romano G, Taccioli C *et al*. MicroRNA signatures of TRAIL resistance in human non-small cell lung cancer. *Oncogene* 2008; **27**: 3845–3855.
- 14 Incoronato M, Garofalo M, Urso L, Romano G, Quintavalle C, Zanca C *et al*. miR-212 increases tumor necrosis factor-related apoptosis-inducing ligand sensitivity in non-small cell lung cancer by targeting the antiapoptotic protein PED. *Cancer Res* 2010; **70**: 3638–3646.
- 15 Papagiannakopoulos T, Shapiro A, Kosik KS. MicroRNA-21 targets a network of key tumor-suppressive pathways in glioblastoma cells. *Cancer Res* 2008; **68**: 8164–8172.
- 16 Gaur AB, Holbeck SL, Colburn NH, Israel MA. Downregulation of Pdc4 by mir-21 facilitates glioblastoma proliferation *in vivo*. *Neuro-Oncology* 2011; **13**: 580–590.
- 17 Zhu S, Si M-L, Wu H, Mo Y-Y. MicroRNA-21 Targets the Tumor Suppressor Gene Tropomyosin 1 (TPM1). *J Biol Chem* 2007; **282**: 14328–14336.
- 18 Gressner O, Schilling T, Lorenz K, Schulze Schleithoff E, Koch A, Schulze-Bergkamen H *et al*. TAP63[α] induces apoptosis by activating signaling via death receptors and mitochondria. *EMBO J* 2005; **24**: 2458–2471.
- 19 Nagane M, Huang HJS, Cavenee WK. The potential of TRAIL for cancer chemotherapy. *Apoptosis* 2001; **6**: 191–197.
- 20 Gonzalez F, Ashkenazi A. New insights into apoptosis signaling by Apo2L/TRAIL. *Oncogene* 2010; **29**: 4752–4765.
- 21 Walczak H, Bouchon A, Stahl H, Krammer PH. Tumor necrosis factor-related apoptosis-inducing ligand retains its apoptosis-inducing capacity on Bcl-2- or Bcl-xL-overexpressing chemotherapy-resistant tumor cells. *Cancer Res* 2000; **60**: 3051–3057.
- 22 Balyasnikova IV, Ferguson SD, Han Y, Liu F, Lesniak MS. Therapeutic effect of neural stem cells expressing TRAIL and bortezomib in mice with glioma xenografts. *Cancer Lett* 2011; **310**: 148–159.
- 23 Unterkircher T, Cristofanon S, Vellanki SHK, Nonnenmacher L, Karpel-Massler G, Wirtz CR *et al*. Bortezomib primes glioblastoma, including glioblastoma stem cells, for TRAIL by increasing tBid stability and mitochondrial apoptosis. *Clin Cancer Res* 2011; **17**: 4019–4030.
- 24 Chuntharapai A, Dodge K, Grimmer K, Schroeder K, Marsters SA, Koepfen H *et al*. Isotype-dependent inhibition of tumor growth *in vivo* by monoclonal antibodies to death receptor 4. *J Immunol* 2001; **166**: 4891–4898.
- 25 Plummer R, Attard G, Pacey S, Li L, Razak A, Perrett R *et al*. Phase 1 and pharmacokinetic study of lexatumumab in patients with advanced cancers. *Clin Cancer Res* 2007; **13**: 6187–6194.
- 26 Ichikawa K, Liu W, Zhao L, Wang Z, Liu D, Ohtsuka T *et al*. Tumoricidal activity of a novel anti-human DR5 monoclonal antibody without hepatocyte cytotoxicity. *Nat Med* 2001; **7**: 954–960.
- 27 Garofalo M, Condorelli G, Croce CM. MicroRNAs in diseases and drug response. *Curr Opin Pharmacol* 2008; **8**: 661–667.
- 28 Garofalo M, Quintavalle C, Romano G, Croce CM, Condorelli G. miR221/222 in cancer: their role in tumor progression and response to therapy. *Curr Mol Med* 2012; **12**: 27–33.
- 29 Garofalo M, Condorelli GL, Croce CM, Condorelli G. MicroRNAs as regulators of death receptors signaling. *Cell Death Differ* 2010; **17**: 200–208.
- 30 Malzkorn B, Wolter M, Liesenberg F, Grzendowski M, Stühler K, Meyer HE *et al*. Identification and functional characterization of microRNAs involved in the malignant progression of gliomas. *Brain Pathol* 2009; **20**: 539–550.
- 31 Gabriely G, Wurdinger T, Kesari S, Esau CC, Burchard J, Linsley PS *et al*. MicroRNA 21 promotes glioma invasion by targeting matrix metalloproteinase regulators. *Mol Cell Biol* 2008; **28**: 5369–5380.
- 32 Kwak HJ, Kim YJ, Chun KR, Woo YM, Park SJ, Jeong JA *et al*. Downregulation of Spry2 by miR-21 triggers malignancy in human gliomas. *Oncogene* 2011; **30**: 2433–2442.
- 33 Moore LM, Zhang W. Targeting miR-21 in glioma: a small RNA with big potential. *Expert Opin Therap Targets* 2010; **14**: 1247–1257.
- 34 Lakomy R, Sana J, Hankeova S, Fadrus P, Kren L, Lzicarova E *et al*. miR-195, miR-196b, miR-181c, miR-21 expression levels and O-6-methylguanine-DNA methyltransferase methylation status are associated with clinical outcome in glioblastoma patients. *Cancer Sci* 2011; **102**: 2186–2190.
- 35 Chan JA, Krichevsky AM, Kosik KS. MicroRNA-21 is an antiapoptotic factor in human glioblastoma cells. *Cancer Res* 2005; **65**: 6029–6033.
- 36 Corsten MF, Miranda R, Kasmieh R, Krichevsky AM, Weissleder R, Shah K. MicroRNA-21 knockdown disrupts glioma growth *in vivo* and displays synergistic cytotoxicity with neural precursor cell delivered S-TRAIL in human gliomas. *Cancer Res* 2007; **67**: 8994–9000.
- 37 Li J, Donath S, Li Y, Qin D, Prabhakar BS, Li P. miR-30 regulates mitochondrial fission through targeting p53 and the dynamin-related protein-1 pathway. *PLoS Genet* 2010; **6**: e1000795.
- 38 Joglekar MV, Patil D, Joglekar VM, Rao GV, Reddy ND, Mitnala S *et al*. The miR-30 family microRNAs confer epithelial phenotype to human pancreatic cells. *Islets* 2009; **1**: 137–147.

- 39 Garofalo M, Romano G, Di Leva G, Nuovo G, Jeon Y-J, Ngankea A *et al*. EGFR and MET receptor tyrosine kinase-altered microRNA expression induces tumorigenesis and gefitinib resistance in lung cancers. *Nat Med* 2011; **18**: 74–82.
- 40 Yu F, Deng H, Yao H, Liu Q, Su F, Song E. Mir-30 reduction maintains self-renewal and inhibits apoptosis in breast tumor-initiating cells. *Oncogene* 2010; **29**: 4194–4204.
- 41 Li N, Kaur S, Greshock J, Lassus H, Zhong X, Wang Y *et al*. A combined array-based comparative genomic hybridization and functional library screening approach identifies mir-30d as an oncomir in cancer. *Cancer Res* 2011; **72**: 154–164.
- 42 Livak KJ, Schmittgen TD. Analysis of relative gene expression data using real-time quantitative PCR and the $2^{-\Delta\Delta C(T)}$ Method. *Methods* 2001; **25**: 402–408.

Supplementary Information accompanies the paper on the Oncogene website (<http://www.nature.com/onc>)